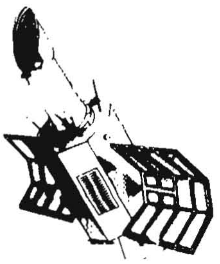

IUE esa

NEWSLETTER

TABLE OF CONTENTS

NO. 16 APRIL 1983

Observatory Controller's Message	2
New personnel at VILSPA	3
AIYOUEE at APOGEE	5
Acknowledgements: Atlas of IUE SN Spectra	6
IUE Spacecraft Status	8
Residual images from previous exposures	10
Photometric Calibration of IUE. X.: Quantification of High Dispersion Order Overlap problem for SWP Camera.	17
IUE Data Reduction XXXI. : Improved LWP Large-Aperture Offset	28
Note on the Wavelength Calibration of Alpha Ori	32
Bright spot detection on IUE images	38
IUE VILSPA Publications	42
Approved proposals 6th round	
(European Allocation)	45
(NASA Allocation)	55
Vilspa log of images (1 April-30 April 82) (1 October 82-1 February 83)	69
Conference Announcements; Various forms	89

IUE ESA Newsletter:

Editor: W. Wamsteker

Published by: The ESA IUE Observatory
Apartado 54065, Madrid, Spain
Telephone: +34-1-4019661
Telex: 42555 VILS E

Typing: C. Ramirez Palacios

Drawings: J. Garcia Palacios

OBSERVATORY CONTROLLER's MESSAGE

On the 26th of January we celebrated the fifth anniversary of the launch of IUE. Our satellite has now surpassed the design lifetime and in the absence of major failures we can expect three more years of operations.

Almost on the same day this year, IRAS (Infrared Astronomical Satellite) was launched: we wish every success to our IR colleagues involved in this project.

The selection of the European IUE proposals for the 6th period has been completed (see page 45) as well as their scheduling. Changes however are to be expected in the present schedule due to the launch of EXOSAT. We are now analyzing, in collaboration with the scientists of the EXOSAT Control Station, the scheduling of those proposals wich were approved for the 5th year, and which require coordinated IUE-EXOSAT observations. Depending on the success of this joint scheduling and on the final performance of EXOSAT, the IUE Allocation Committee will reconsider the IUE-EXOSAT proposals which were submitted for the present round and put on stand-by, awaiting a more definitive plan of the EXOSAT operations.

As announced in the last issue, a further change has taken place in the staff of the Observatory: André Heck, Deputy Observatory Controller, left VILSPA on March 31st for the Centre de Données Stellaires in Strasbourg. Andre is one of the founder- members of the IUE Observatory and his contribution to the project has been very important, especially during the most difficult periods: we wish him the best success in his new activity. The position of Deputy Observatory Controller has been taken over by Willem Wamsteker.

Replacements in the vacancies have already started with the arrival of A. Talavera, our first Spanish Resident Astronomer. In the next months more arrivals are expected.

NEW PERSONNEL AT VILSPA

Francisco Javier Olivera Poll (32) has joined the very important group of people, who quietly assure that the results of the observations are properly reduced (IGCS),as image processing specialist. He has an advanced Physics Degree specializing in Automatic Calculus. Previously he worked for a mining company and an idependent service institute. He is married and has 2 children. His favorite pastimes are reading and playing basketball.

Antonio Talavera Iniesta (29) has joined the Resident Astronomers staff at VILSPA. Born in Albacete (La Mancha) he is the first Spanish Resident Astronomer. He obtained his Astrophysical education at the Universidad Complutense in Madrid and did his Ph. D. at the University of Barcelona. After his studies he worked for four years at Meudon on high resolution spectroscopy of normal and peculiar A stars. He likes the outdoors life, especially mountain hiking is one of his favorite pastimes.

The UK Resident Scientist for IUE at the Rutherford Appleton Laboratory, Alan Harris (31) took up the position of UK Resident Astronomer in VILSPA in December. After his Ph. D. at The University of Leeds on balloon-borne far infrared astronomy, he spent 3 years at the M.P.I. for Astronomy in Heidelberg. His research concentrated on infrared observations of H II regions and molecular cloud complexes. Apart from infrared astronomy he also works actively on UV absorption line studies of the interstellar medium. His spare time is usually distributed among photography and, amateur dramatics. Some of the roles he has played include God and a ladies breast prothesis salesman, so we can be sure of his efficient work at VILSPA.

Lourdes Sanz Fernandez de Cordoba has been delegated to the IUE Observatory as Scientific member of the INTA support staff. Her main task within the Observatory will be to keep order in our small but precious Astronomical Library. She obtained her Masters Degree in Astronomy at the Universidad Complutense on the subject of UV spectra of Supernovae. When she is not worrying about books or remote explosions, she likes to do oil painting. Outdoors she passes her time preferably in the company of horses and dogs.

DEPARTURES

Luciana Bianchi:	Resident Astronomer (6-12-82)
Patrizio Patriarchi:	Resident Astronomer (1-1-83)
Javier Barbero:	Image Processing Specialist (1-3-83)
Andre Heck:	Deputy Observatory Controller (1-4-83)

AIYOUEE AT APOGEE (Five Years)

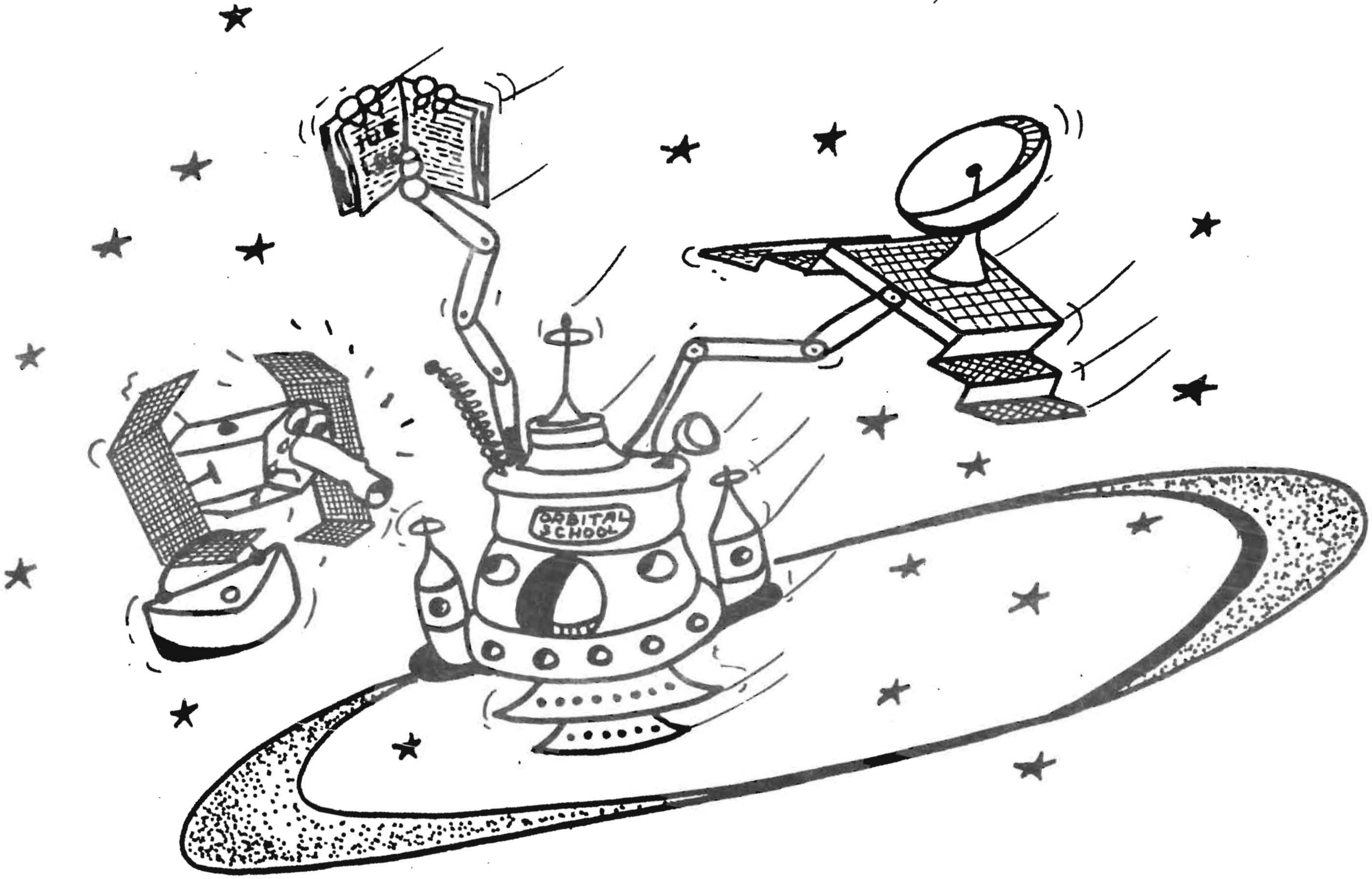

I do not want to go to school!!!

ATLAS OF IUE SPECTRA OF SUPERNOVAE

Due to the large number of Supernovae, which have gone off and been discovered during the past five years, and the uniqueness of the UV spectra obtained by IUE, it was deemed useful to collect all IUE observations of the 6 supernovae observed until March 82 in a special atlas. This atlas has recently appeared in the special Publications Series of the European Space Agency as ESA-SP 1046: An atlas of UV Spectra of Supernovae. The Atlas contains, apart from plots of the individual spectra in absolute units, color reproductions of the line by line spectra and the tabulated flux values. The spectra of 3 type II Supernovae and 3 type I Supernovae are collected (SN 1978g, 1979c, 1980k, 1980n, 1981b, 1982b). The data in the atlas (4th and 5th files) can also be obtained from the VILSPA IUE Data Bank as a special Archive Tape.

The atlas can be ordered (price : FF 140.- approx.) from:

Distribution Office
ESA Scientific and Technical
Publications Branch
ESTEC
Zwarteweg
2200 AG Noordwijk
HOLLAND

The tape can be requested (free of charge) from:

IUE Observatory Controller
ESA-VILSPA
P.O. Box 54065
Madrid
SPAIN

ACKNOWLEDGEMENT

Usually we all feel sad when Resident Astronomers leave VILSPA to return to their home institutes or similar locations. However Prab Gondhalekar has found a marvelous way to alleviate our saddness. Knowing (as you all do) the rather limited content of the VILSPA Astronomical library and realizing the difficulties that this generates for the Resident Astronomers, he has used the opportunity of his departure to make a gift to the VILSPA Astronomical Library. He has donated a large number of back issues of Monthly Notices and The Observatory. Also a number of basic physics and mathematics courses. The IUE-VILSPA Observatory staff (and, I am sure, also quite few Guest Observers) wish to express our thanks for this remarkable gesture!

THE EDITOR

IUE SPACECRAFT STATUS

IUE Spacecraft Operations are continuing normally and effectively, even though the satellite is well in its 6th year of in-orbit operations. It is recalled here that the design lifetime of the hardware is 3 years, with a goal, including the sizing of consumables and degradable hardware, of 5 years.

There are several areas where operational constraints are developing:

The Solar Array Panels are degrading due to radiation at a rate of about 6% per year, therefore operations at extreme Beta angles are limited in time, since the on-board batteries cannot deliver indefinite additional power to the S/C-bus. We believe that we will be able to observe between Beta greater than 20 and less than 120 throughout the 6th round of IUE observations.

The Hydrazine Subsystem temperatures continue to rise. The operating limits were increased in February 1983 to 85 C, except for the +Z Line temperature, which is set to 90 C. This adjustment was necessary to avoid impact on science operations and it is hoped that the new limits will give at least one more year of operations without significant impact on the scientific observations. At present the scheduling software will be reviewed for the 7th round of IUE observations in order to minimize the impact on science operations.

In IUE ESA Newsletter No. 15 we gave information about the Gyroscopes and the feasibility of a backup control system. The following paragraph will provide you with an updated status on this subject, which I received from Ivan Mason, IUE Project Operations Director, GSFC:

"The development of the 2-Gyro/Fine Sun Sensor (FSS) backup spacecraft control system, for use in the event of another gyro failure, is progressing satisfactorily. The new on-board computer (OBC) software control system has been assembled and all design tests have been successfully completed. The ground software modifications have also been completed. Operational simulations are now being performed to verify the interactive capability of all ground and spacecraft software, as best we can, using the ground spacecraft simulator. In June we plan to perform tests with the spacecraft. During these tests operational capabilities and limitations of the new control system will be evaluated".

The satellite emerged from the biannual eclipse season (No. 11) in March with no difficulties being noted. The maximum depth of discharge of the two on-board batteries was less than 56%. The battery data indicate that no further reduction of power will be necessary and that the present SI-Configuration during eclipse can be maintained until and prior to eclipse season No. 16, which commences August 25, 1985.

J. Faelker

RESIDUAL IMAGES FROM PREVIOUS EXPOSURES

1. INTRODUCTION

On quite a few IUE images with long exposure times faint residual spectra from previous (over)exposures have been noticed. There are two, entirely different sources of residual images: burnt-in signals in the SEC target and phosphorescence in the UV to optical converter. Virtually all practical problems for guest observers are due to phosphorescence during long exposures. In particular: how do you establish that the faint signal detected after a 7 hour exposure is due to the target studied and not to residual phosphoresence of a previous over-exposure? This problem has two aspects: how do you prevent it to happen and how do you assess the reliability of the images in the data bank.

2. SEC TARGET RESIDUALS

Spectra burnt-in in the SEC target are normally properly removed. The standard SPREP sequence cleans the SEC target satisfactorily after a normal exposure and executing XSPREP takes care of the burnt-in image after an over exposure. XSPREP has to be done immediately after an overexposure in excess of 8x. Residuals in the SEC target should then not present any serious problem.

Of course one should be aware that the high illumination level of the UVC in an XSPREP (300% + 200% + 50% vs. 200% + 50% for a normal SPREP) will give a higher background due to phosphoresence immediately following the PREP.

3. AFTERIMAGES DUE TO PHOSPHORESENCE

The P11 phosphor in the UV to optical converter (UVC) exhibits phosphorensence i.e. the conversion is not an instantaneous process and the integration capacity of the phosphor results in a decay slower then the incoming photon rate. A small fraction of the incident energy, typically 1%, is stored in the phosphor and later slowly released. The dynamic range of incoming flux accessed by IUE is ~10xx5, this is mainly obtained through differences in the integration time.Thus for integrations from 30min to 8hrs the cumulative effect of the phosphor decay can be important. From pre-launch measurements (Coleman et al., 1977) we know that during this period the phosphor decay signal, Fp(t), has a power-law dependance on the time interval, since the original excitation (Δt):

$$F_p(t) = k \times F_i \times (\Delta t)^{-n}$$

where k and n are camera dependant constants (table 1) and F(t) is the flux during the earlier exposure. An exposure between t1 and t2 of an object with signal strength, F_i , will result in a total incident flux on the camera of Fo $=F_i$ x(t2-t1) where we have assumed that F(t) is time independent. The resultant phosphor decay signal during a later exposure from t3 to t4 will be:

$$F = \int_{t_1}^{t_2} \int_{t_3}^{t_4} k \times F_i \times (t-t')^{-n} \, dt dt'$$

$$= \frac{k \times F_o}{(t_2-t_1) \times p \times (1-n)} \times \{(t_4-t_1)^p-(t_4-t_2)^p+(t_3-t_2)^p-(t_3-t_1)^p\}$$

where p=2-n.In most cases of practical interest the original exposure between t1 and t2 is virtually instanteneous with respect to (t3 - t4) in which case a simpler formula can be used

$$F = \frac{k \quad F_o}{(1-n)} \times \{(t_4-t_{12})^{(1-n)} - (t_3-t_{12})^{1-n}\}$$

Representative values for k and n are 2x10xx-4 and 0.75. Note that these formulae diverge for very large values of t4, eventually the phosphoresence should decrease faster than the t^{-n} power law predicts. The laboratory measurements by Coleman et al. were done over periods up to 8 hours. Practical experience with the cameras in orbit shows that for longer periods relations (2) and (3) overestimate the amount of phosphoresence. In fact I do not know of any example of noticable phosphor decay after 2 shifts (16 hours) have passed. If one calculates phosphor decay over periods longer then 8 hrs, the calculated decay is too large.

In table 1 we list the predicted phosphor decay signal during a 7 hour exposure, after a 10x overexposure 2 hours before the start of the 7 hour exposure. A 10x overexposure corresponds to a peak flux of 2000DN. 0.2% to 0.5% of the incident signal is emitted as a phosphorescent signal. The constants n and k are temperature sensitive (Coleman, 1978) the results in table 1 are valid for T = 20C. In orbit the phosphors operate in a slightly cooler environment: T = 6-17C; consequently n will be slightly lower and k slightly larger. The temperature dependence of the constants is not well known but over the temperature range of interest the changes are most likely less than 30%.

4. DISCUSSION

Phosphor decay is a problem because the IUE cameras are efficient at integrating weak signals over long periods. If a 6 min exposure to 200 DN is made 3 hrs after a 50x overexposure, the phosphor decay signal corresponds to 0.5 DN and can thus be ignored. However if you do a 7 hour exposure on a faint target which will result in a 25 DN signal, the equally large phosphor decay signal will be a major problem. A good example of such problems is SWP 14423 a low resolution 14h exposure of a faint object which has a high resolution decay signal, resulting from 4 images, 15x to 20x overexposed, superimposed on it (see figure 1). The decay and object signal have equal intensities and so far the unfortunate observers have not disentangled them succesfully.

Note that phosphorescence effects add up: a couple of small over exposures can be as bad as a single large one, in particular if they come from objects with the same type of spectra.

The precise level of an overexposure is often not known. Especially for early images retrieved from the data bank it is important to look for other images of the same star in the Merged Image Log and to obtain, if possible, reliable estimates of the overexposure level.

Camera operations without overexposures normally do not cause measurable phosphorescence. The only exception is an accumulation of optimum exposures in one shift (say a 200 DN exposure every hour) followed by a full shift exposure immediately afterwards. Provided the decay signals add up (same aperture, resolution and object types) a very faint 2.5 to 5 DN peak signal will be generated. I have seen two examples of this in the LWR camera (low resolution object spectrum and a high resolution decay signal). In both cases the decay signal was so faint that the observers simply ignored the high resolution remnant. Obviously the situation is very difficult if the previous overexpsures were made in the same spectrograph configuration as your long exposure. Then the observed signal can sometimes be completely due to the phosphor decay.

One trick, which has been tried by observers with a recently overexposed camera, is to do an XSPREP, expose the camera for half an hour during the slew to their target and read the camera after arrival. If this 30 min test image was completely blank they assumed that the effects of the overexposure could be ignored. This is incorrect: a 25x overexposure 3 hours before your 30 min test images gives rise to a ~1 DN phosphor decay signal, which is undetectable. If you follow this up with a 2 shift exposure a 10 to 15 DN decay signal is deposited by the phosphor and that is quite noticable. This test only shows that the XSPREP has effectively cleaned the SEC target. I was actually able to test this during a 2 shift LWR exposure. The SWP camera had been repeatedly overexposed during the previous shift on A and F stars. A 30 min and a 767 min SWP blank sky image were obtained during the 14 hour LWR exposure (SWP 8192 and SWP 8193). The 30 min exposure showed no detectable signal (a peak signal of about 1 DN was predicted to be present) but the 767 min blank sky image shows a 10 to 20 DN signal longward of 1700 A, a clear residual from the A and F type spectra.

Some practical points of interest should be noted: the 10 to 20 DN signal corresponded in this case to a flux level of 1 to 2x10xx-15 erg cm-2 s-1 A-1. This is a typical flux level (for phosphor decay) in the SWP camera after heavy overexposures followed by 7 to 14 hour integrations. The image log gives exposure levels in DN, but most guest observers think in physical fluxes. These numbers illustrate the phosphor decay in physical units. Typically one can measure fluxes down to 1x10xx-15 erg cm-2 s-1 A-1 during 7-14 hours exposures with the SWP camera for >1600 A without much problem. For fainter objects systematic errors (e.g.: background determination, phosphor decay and overlapping weak radiation hits) make measuring the signal or establishing its reality difficult (Hammerschlag- Hensberge et al. 1982, Snijders et al. 1982). For the LWR camera the corresponding numbers are: a minimum flux level of 5x10xx-16 erg cm-2 s-1 A-1 can be measured between 2600 A and 2900 A and a 10 DN peak phosphor decay signal in 7 hours corresponds to 7x10xx-16 erg cm-2 s-1 A-1.In summary: phosphor decay generates only a weak signal but during long exposures it can quite easily exceed the flux from a faint target. It might be good to point out at this stage that most of the problems with overexposed cameras are <u>not</u> due to errors in the calculated exposure time, but usually occur because an observer wants to study a very steep spectrum with a large dynamic range and is interested in the fainter parts of it (e.g. the 2200 A extinction maximum or F star continua below 1700 A). Such programs can be identified and it is therefore beneficial for the scheduling of IUE, when users notify the project of such conditions in their response to the scheduling questionnaires.

M.A.J. SNIJDERS

REFERENCES:

1. Coleman, C., Golton, E., Gondhalekar, P., Hall, J., Oliver, M., Sandford, M., Snijders, T., and Stewart, B., 1977, IUE technical note nr. 31, "Camera Users Guide".

2. Coleman, C.I., 1978, "The 7th symposium on Photo-Electronic Image Devices", ed. D. Mc Mullan and Morgan, B.L., p. 125.

3. Hammerschlag-Hensberge, G., McClintock, J.E. and van Paradijs, J., 1982, Ap. J. Lett., 254, L1.

4. Snijders, M.A.J., Penston, M.V., Boksenberg, A., and Sargent, W.L.W., 1982, M.N.R.A.S., 201, 801.

TABLE 1

Phosphor decay parameters for the IUE cameras

CAMERA	k(x10xx4)	n	DN PEAK
LWP	1.2	0.72	5.4
LWR	2.9	0.77	8.0
SWP	1.8	0.78	4.5
SWR	1.0	0.70	5.4

SOURCE

Coleman *et al*. (1977) for k and n (T ~ 20C); DN(peak) is the predicted decay signal during a 7 hour exposure which started 2 hours after a 10x overexposure. A 10x overexposure corresponds to peak fluxes which would give rise to 2000DN signal. k is the scale factor for phosphor decay; n is the exponent for the decay time dependence.

FIGURE 1:

The image SWP 14423 shows the target exposure (14hrs) of Neptune. Superposed one clearly distinguishes the high resolution spectra due to phosphorensence .

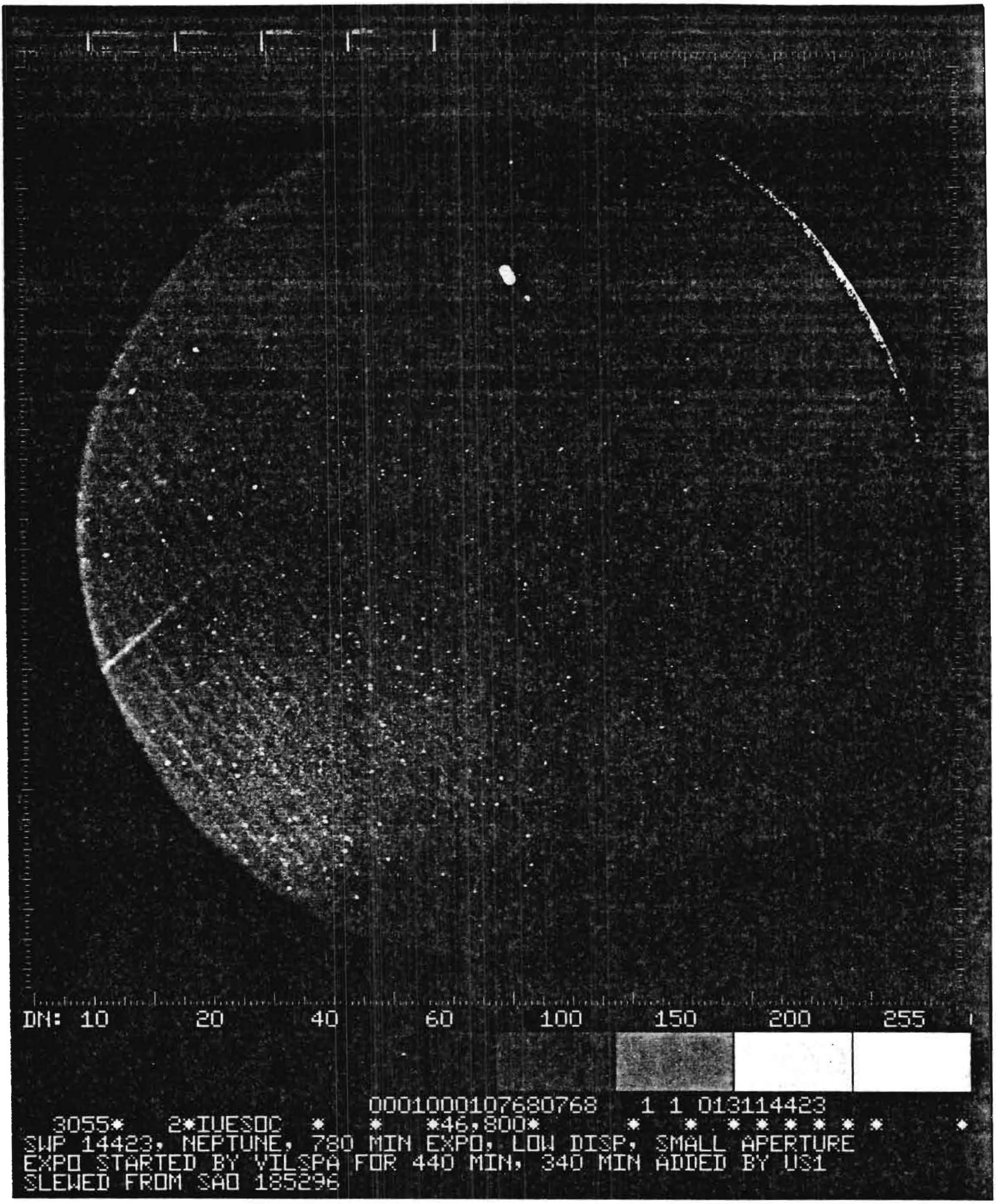
DN: 10 20 40 60 100 150 200 255
0001000107680768 1 1 013114423
3055* 2*IUESOC * * *46,800*
SWP 14423, NEPTUNE, 780 MIN EXPO, LOW DISP, SMALL APERTURE
EXPO STARTED BY VILSPA FOR 440 MIN, 340 MIN ADDED BY US1
SLEWED FROM SAO 185296

FIGURE 1

PHOTOMETRIC CALIBRATION OF THE IUE

X. Quantification of the High Dispersion Order Overlap Problem for SWP

L. Bianchi and R. Bohlin

I. INTRODUCTION

A long standing problem with IUE data is the determination of the true background level in the region of the spectral format where the high dispersion orders are closely spaced. Bianchi (1980) has outlined a technique for determining the net spectrum directly from the extracted gross data without reference to the extracted interorder background.The problem has been reduced, but not eliminated, by the introduction of the new software and automatic registration techniques (Bohlin and Turnrose 1982 and Thompson and Bohlin 1982.) These two production improvements have made high dispersion extractions consistent and stable, which is essential to the correction technique outlined here.

In order to evaluate any correction technique and to quantify the errors in IUE line profiles that are caused by the order overlap, we have compared line depths in IUE spectra to line depths observed by the *Copernicus* satellite. The excess line depth (i.e. order overlap) in IUE spectra can be expressed as a percent of the local net continuum level. The interpretation of these excesses suggest that the amount of order overlap for point sources is about 32% at 1150Å and decreases to zero at about 1400 Å. The transfer of a spectral feature from one order to the next is below the 5% level. The net is the most appropriate quantity to scale the order overlap, because the background and gross are affected by the radiation level and the variability of the camera null level.

II. COPERNICUS DATA

The resolution of *Copernicus* is 0.05Å for U1 spectra and 0.2Å for U2. Since the IUE resolution is 0.1Å, the absorption lines chosen for study are those that are broad enough so that the U1 and U2 line depths agree to within 5%. The choice of lines was further restricted to strong lines with central depths between 0 and 35% of the continuum. The spectra studied are those with complete U1 scans: zeta Oph(Morton 1975), zeta Pup(Morton and Underhill 1977), tau Sco(Rogerson and Upson 1977), and iota Her (Upson and Rogerson 1980). Except for iota Her (see section IV), all *Copernicus* U1 and U2 spectra were corrected for instrumental scattered light from the grating and for the U2 stray light by the method of Bohlin (1975). The *Copernicus* line depths should be accurate to about 3% of the continuum, although about half of the lines considered go to zero in both U1 and U2 and, therefore, have zero error.

III. IUE DATA

The four IUE spectra are listed in Table 1.

TABLE 1

HD	NAME	SWP NO.	APER.	EXP(s)
66811	zeta Pup	13726	L	4
149438	tau Sco	16222	L	6
149757	zeta Oph	14428	L	24
160762	iota Her	5720	S	80

All four spectra were reprocessed for this study with the production software in effect at GSFC in June 1982. The continua are drawn in the same way as for the Copernicus spectra, so that the main source of error is in the choice of the bottom of the line. Again, this error is estimated at 3%.

IV. RESULTS

The amount of order overlap in IUE spectra can be measured by the difference between the line depth in Copernicus and the line depth in IUE. The measured order overlap is shown in Fig. 1, as measured in % of the local net continuum. The first letter of the star's constellation is centered at each measured value. The vertical bars with the letter at the top of the bar represent the range of order overlap as determined by U1 and U2, independently. The straightline fit through the data of Fig. 1 is drawn without regard for the iota Her points which lie systematically low. Evidently, either the Copernicus scattered light corection is too large or this small aperture IUE spectrum has less order overlap. The former possibility is relevant, since Upson and Rogerson (1980) found that the normal scattered light correction is not applicable to the Copernicus U1 data for iota Her. Darius (1980) argued against any lower order overlap in the small aperture, but his large error bars permit the small ~5% difference found here. One error bar of ± 3% is illustrated, and all data (except iota Her) agree with the fit within their expected uncertainty.

Since the measured lines are all broad and deep, the contribution of the order itself to the excess background is generally small. Therefore, the actual order overlap appropriate to regions without strong lines in adjacent orders is significantly more than the amount shown in Fig. 1.(See Appendix 1.)

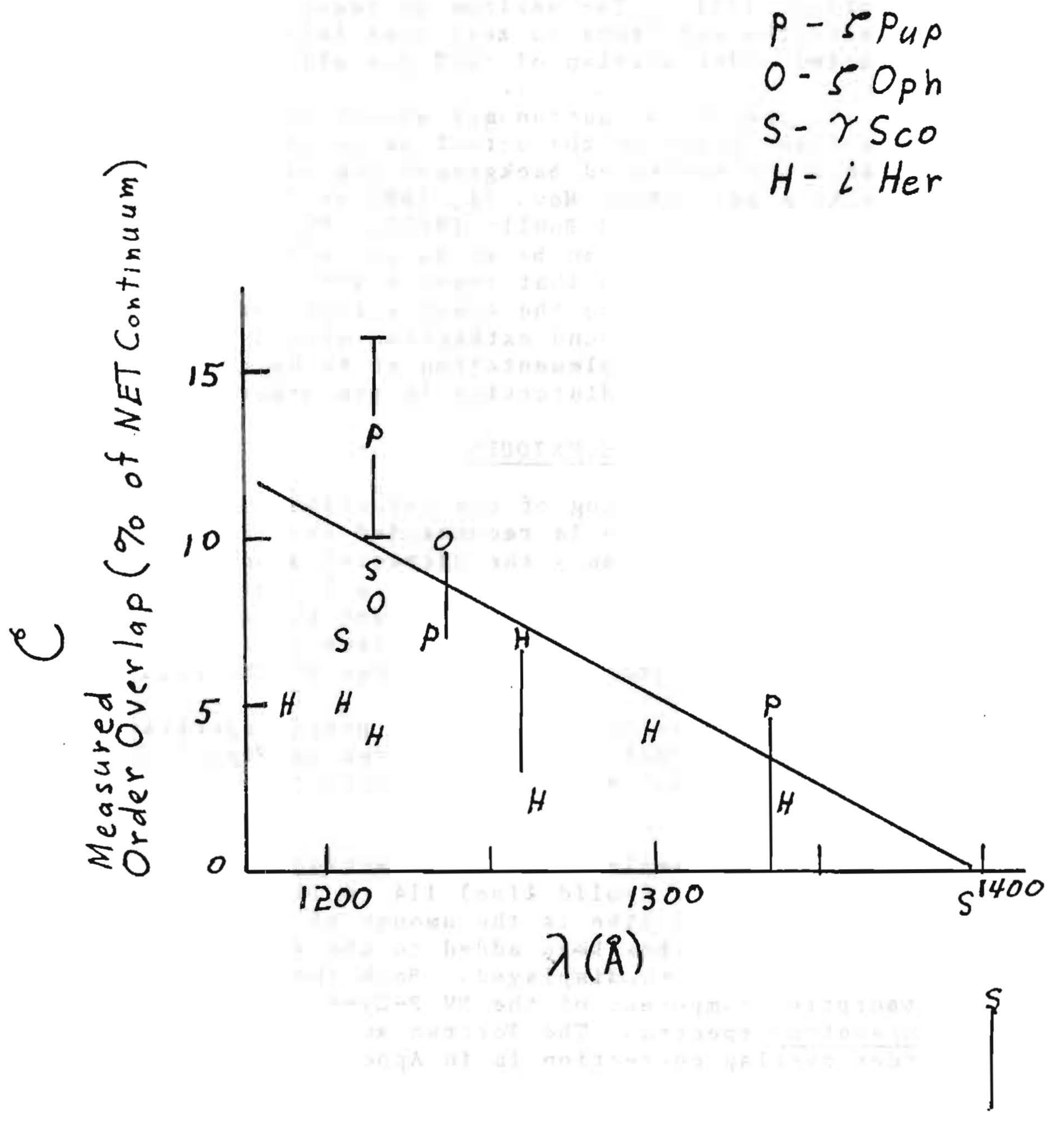
P - ζ Pup
O - ζ Oph
S - γ Sco
H - ι Her
Measured Order Overlap (% of NET Continuum)
C
15
10
5
0
1200
1300
1400
λ (Å)
P
O
S
H

Fig. 1

V. ORDER OVERLAP IN THE OLD SOFTWARE

Since the background was systematically higher with the old high dispersion software in use before Nov. 10, 1981 at GSFC and before March 11, 1982 at Vilspa, the order overlap was worse. The amount of added order overlap in old software is the ratio of NEW/OLD net spectra as shown in Fig. 4 of Bohlin and Turnrose (1982). The maximum increase is ~10% at the shortest wavelengths and drops to zero near 1400Å, giving a maximum expected order overlap of ~42% for old SWP spectra.

However, an astronomer should regard the 42% derived above as a lower limit to the actual uncertainty in old reductions, because the extracted background was not accurately registered in a routine way before Nov. 24, 1981 at GSFC and March 11, 1982 at Vilspa (Thompson and Bohlin 1982). The random photometric errors before these dates can be as large as 35% (Bohlin and Coulter 1982). For problems that require accurate backgrounds, an astronomer shold have the spectra reprocessed with the modern system. The background extraction should continue to improve with the planned implementation of techniques to remove the residual geometric distortion in the orders.

VI. CORRECTION TECHNIQUES

If reprocessing of old reductions is impractical, a correction technique is recommended such as that of Bianchi (1980), which uses only the extracted gross spectrum. This technique assumes a Gaussian plus a Lorentz function for the order profile and takes into account the correction for the neighboring two orders. The accuracy of the result depends on actual shape of the long range wings of the PSF.

For modern reductions with proper spectral registration, the amount of order overlap measured in Fig. 1 can be used to make a simple, but sufficiently accurate, correction as described in Appendix 1.

As an example of this correction technique, Fig. 2 shows corrected orders (solid line) 114 to 111 in the spectrum of zeta Pup. The dashed line is the amount of the order overlap correction that has been added to the standard extracted net to get the solid line displayed. Both the Lα line and the shifted absorption component of the NV P-Cygni line go to zero in the *Copernicus* spectra. The Fortran subroutine used to compute the order overlap correction is in Appendix 2.

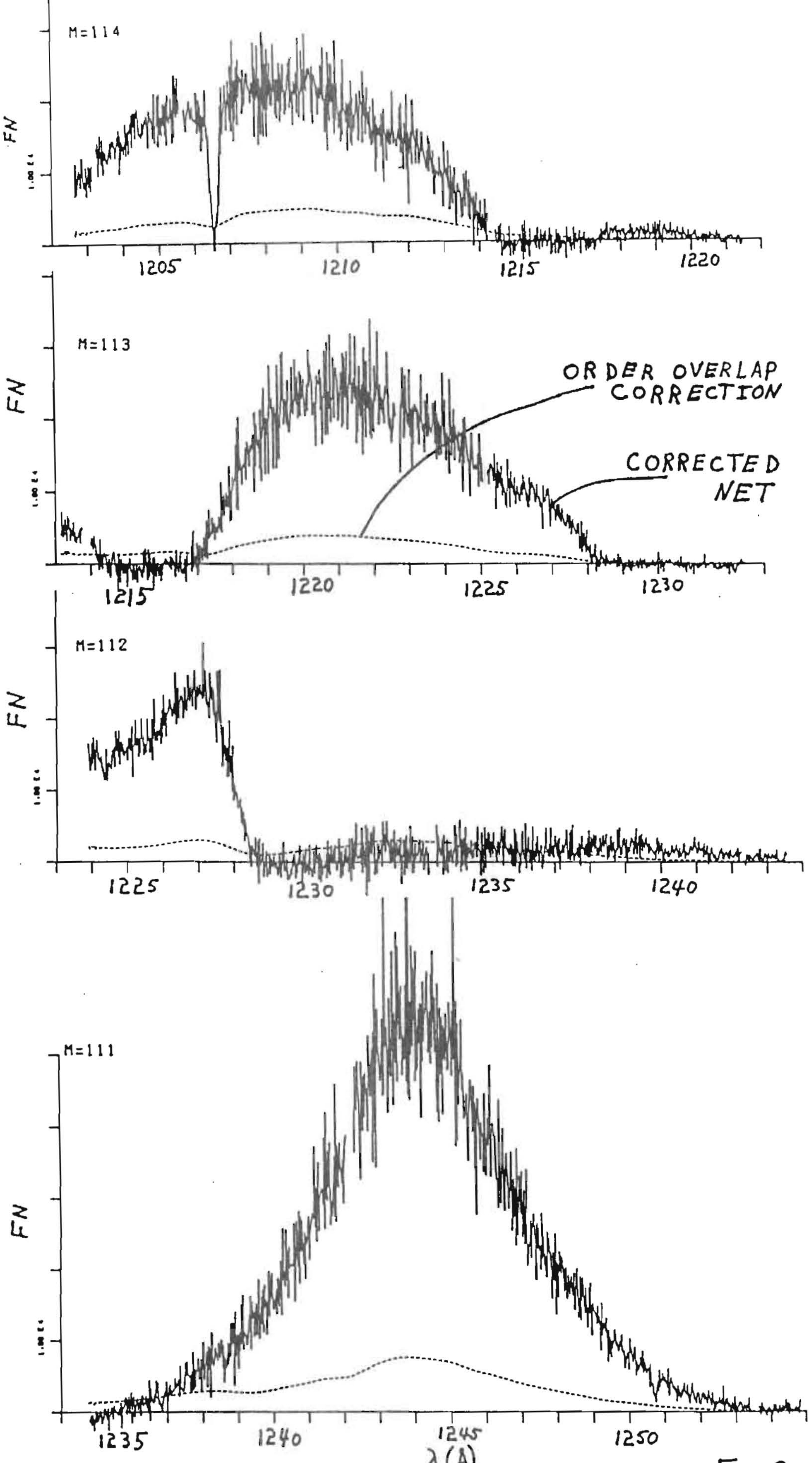
M=114
FN
1205
1210
1215
1220
M=113
FN
ORDER OVERLAP
CORRECTION
CORRECTED
NET
1215
1220
1225
1230
M=112
FN
1225
1230
1235
1240
M=111
FN
1235
1240
1245
1250
λ(Å)

Fig. 2

APPENDIX 1

The order overlap correction derived here deals with the order m itself and the neighboring two orders m-1 and m+1. The wings of all other orders should contribute nearly equal amounts to extracted gross and background spectra. The derivation here is for point sources in focus. Extended sources and out of focus high dispersion IUE spectra cannot be reduced properly with standard procedures at the short wavelengths where the orders are not well separated.

The corrected net N_o can be expressed in terms of the net n_o on the new software tapes as

$$N_o = n_o + \Delta B_o + \frac{\Delta B_- + \Delta B_+}{2} - \Delta N_- - \Delta N_+ . \qquad (1)$$

The subscripts -, o, and + refer to the orders m-1, m, and m+1, respectively throughout this discussion. The corrections ΔB are normalized to the extraction slit height and are due to the fact that the extracted background is too high which makes the net n_o too low. The corrections ΔN are the excess contributions to the gross from the wings of the adjacent orders. A correction ΔN_o is not needed for the few percent of the order m that lies outside the extraction slit, because a photometrically stable signal can be defined for any length slit as long as the extraction is precisely registered.

For the case of a deep line as measured by the correction C in Fig. 1, $\Delta B_o = 0$. On the average, the neighboring orders have approximately equal net continua n. With these assumptions and some knowledge of the order profile shape, a solution can be obtained. The precise PSF for IUE is not known, however, Bianchi (1980) has shown that the core of the profile is Gaussian with a longer range component in the wings. These wings produce the elevated background in the short wavelength orders and probably drop off as r^{-2}, where r is the distance from the peak of the order. De Boer, Preussner, and Grewing (1982) find IUE high dispersion profiles are purely Gaussian but suggest that their results are consistent with Bianchi, presumably because the faint Lorentz wings are difficult to detect.

Thus, if b is the background contribution due to one order, then this order contributes as an increase of b/4 to the neighboring net and as b/9 to the background on the other side of order m (See Fig. 3). In summary:

$$\Delta B_o = 0$$
$$\Delta B_- = \Delta B_+ = b + b/9$$
$$\Delta N_- = \Delta N_+ = b/4$$
$$n_- = n_+ = n$$

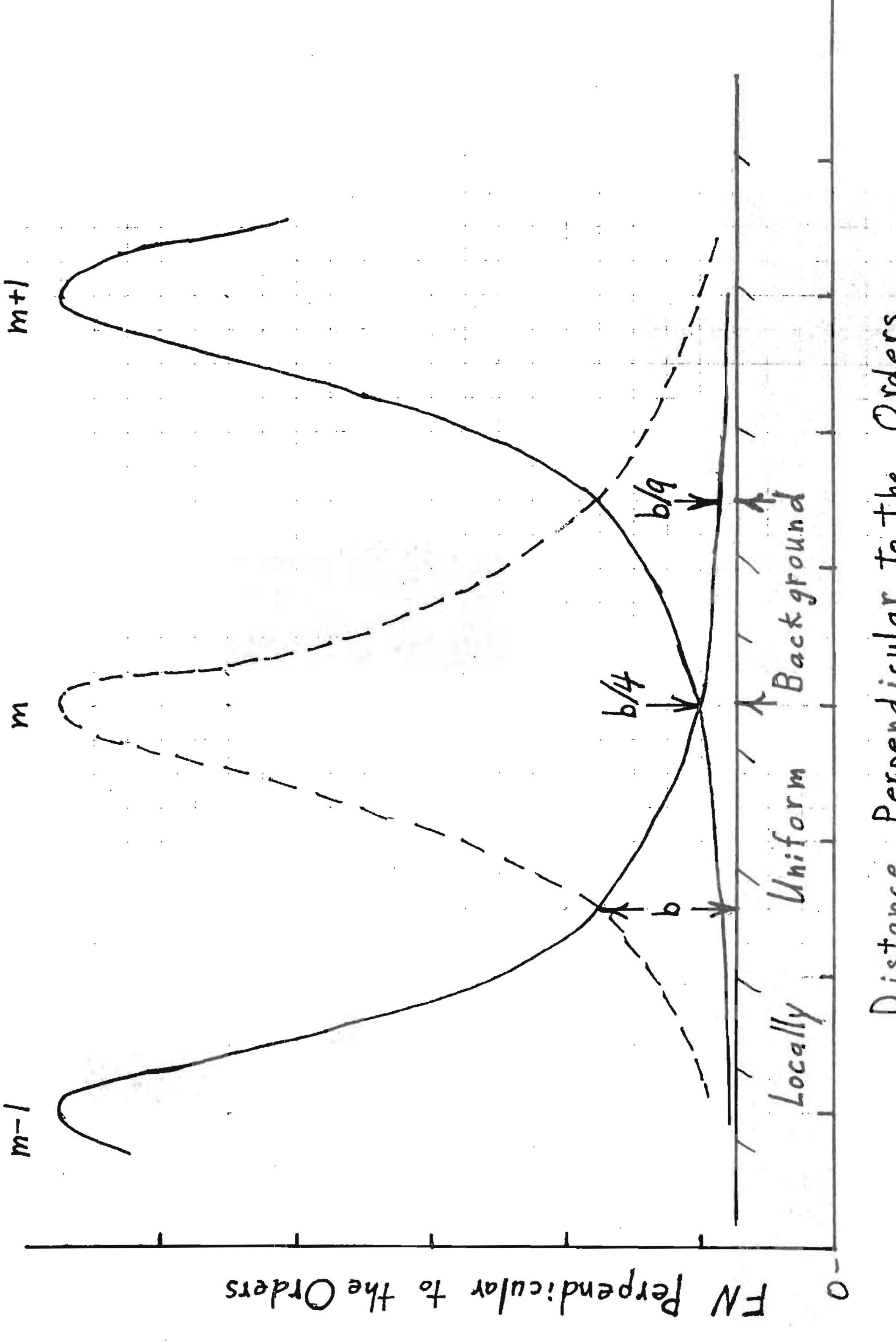
m-1
m
m+1
b
b/4
b/9
Locally Uniform Background
Distance Perpendicular to the Orders
FN Perpendicular to the Orders
0

Fig. 3

Eq. 1 becomes:

$$N_o - n_o = b+b/9 - b/4 - b/4 = \frac{11b}{18} \tag{2}$$

Since this difference $N_o - n_o$ is just what has been measured in Fig. 1, where C if the fractional correction in terms of n, Eq. 2 becomes:

$$b = \frac{18Cn}{11} \tag{3}$$

This suggests for arbitrary continua in the three orders that the contribution to the background from any order is:

$$b_- = \frac{18C}{11} n_-$$

$$b_o = \frac{18Cn_o}{11}$$

$$b_+ = \frac{18Cn_+}{11}$$

For the case of non-zero signal in the order m, the contribution

$$\Delta B_o = b_o$$

and the general solution to Eq. 1 becomes

$$N_o = n_o + \frac{18C}{11}[n_o] + \frac{10C}{11}[n_-] + \frac{10C}{11}[n_+] - \frac{9C}{22}[n_-] - \frac{9C}{22}[n_+]$$

$$N_o = n_o + 1.636C\,[n_o] + 0.5C\,[n_-] + 0.5C\,[n_+] \tag{4}$$

where the [ ] indicates the appropriately smoothed net spectrum. The appropriate smoothing is 31 points done twice, just the same as the background smoothing for the new software, since the correction is essentially for errors in the smooth background that is used to compute the net on the tape. The FORTRAN program to implement Eq. 4 appears in Appendix 2.

In the case where the 3 continua are all equal, Eq. 4 becomes:

$$\frac{N_o - n_o}{[n_o]} = 2.636C \quad , \tag{5}$$

which is used to estimate the maximum order overlap of 32% when C = 0.12 at 1150Å.

Order overlap is primarily an artificially raised background caused by the overlapping wings of the order profile in the higher echelle orders. A secondary effect of order overlap is the transfer of a spectral feature from one order to a neighboring order, since the wings of the point spread function (PSF) are not zero at the location of a close order. The depth of these "ghost lines" is the contribution ΔN_+ from a neighboring order. The smoothing of these ΔN terms was assumed to be the large interval of 31 points in deriving Eq. 4. The following arguments will set a low limit on the importance of ghost lines and therefore justify the large smoothing of these excess contributions to the extracted net: Suppose that a zero depth line in the continuum of m + 1 with $n_+ = n_o$ is present as a narrow ghost line in order m. The depth of the dip is

$$\frac{\Delta N_+}{n_o} = \frac{b}{4n_o} = 0.41C$$

This is a maximum of 5% at 1150Å and drops to the even more insignificant upper limit of 3% longward of 1260Å. The lack of any visible ghost lines from the strong emission lines in WAVECAL spectra is consistent with these limits.

```
      SUBROUTINE OVRLAP(NUMORD,MPTS,WLM,EPS,FNET,OOCOR)
C+
C     CORRECT THE SWP (ICAM=3) IUE HI-DISP SPECTRA FOR ORDER OVERLAP.
C
CU    USER INPUT IS THE NUMBER OF ORDERS (NUMORD), THE NUMBER OF POINTS
CU    IN EACH ORDER (MPTS), THE WAVELENGTHS OF EACH POINT IN THE ORDER
CU    (WLM), AND THE EPSILON VALUES (EPS).
CU    THE PROGRAM COMPUTES THE CORRECTION (OOCOR) AND ADDS
CU    IT TO FNET.  FNET IS FLAGGED AS A BAD POINT (-1.E-20) IF THE
CU    POINT IS A RESEAU, SATURATED, OR A PING. THE CORRECTED ORDERS
CU    ARE 2 THROUGH NUMORD-1.
C
CS    SUBROUTINE AV IS NEEDED TO SMOOTH WITH A BOX FILTER (31 POINTS
CS    WIDE) AND ARRAY LENGTH NPTS.
C
CH    AUTHOR: RALPH BOHLIN
CH            GSFC-CODE 681 AND ST SCI HOMEWOOD CAMPUS
CH    WRITTEN: 3 JULY 1982
C-
      COMMON/NPTS/NPTS
      COMMON/VICHDR/IL,IS,ICAM
      DIMENSION MPTS(NUMORD),WLM(1022,NUMORD),EPS(1022,NUMORD),
     C          FNET(1022,NUMORD),OOCOR(1022,NUMORD),AVG(1022,3),
     C          AVGT(1022),CORR(3)
      IF(ICAM.NE.3)RETURN
C
C     INITIALIZE THE 1ST 2 SMOOTHED ORDERS & CORRECTION FACTORS.
         DO 100 I=1,2
         NPTS=MPTS(I)
         CALL AV(FNET(1,I),AVGT,31)
         CALL AV(AVGT,AVG(1,I),31)
         WLCOR=WLM(NPTS/2,I)
100      CORR(I)=(1400.-WLCOR)*0.000533/2.
C
C     MAIN LOOP WHERE VARIABLE ENDING WITH: LO-PREVIOUS ORDER
C                                           AT-ORDER BEING CORRECTED
C                                           HI-NEXT ORDER
         LSTCOR=NUMORD-1
         DO 300 I=2,LSTCOR
         ILO=MOD(I-2,3)+1
         IAT=MOD(I-1,3)+1
         IHI=MOD(I  ,3)+1
         NPTS=MPTS(I+1)
         CALL AV(FNET(1,I+1),AVGT,31)
         CALL AV(AVGT,AVG(1,IHI),31)
         WLCOR=WLM(NPTS/2,I+1)
         CORR(IHI)=(1400.-WLCOR)*0.000533/2.
         MIDLO=MPTS(I-1)/2
         MIDAT=MPTS(I  )/2
         MIDHI=MPTS(I+1)/2
            NPTS=MPTS(I)
            DO 200 J=1,NPTS
            NPTLO=J-MIDAT+MIDLO
            NPTHI=J-MIDAT+MIDHI
            IF(NPTLO.LT.1)NPTLO=1
            IF(NPTHI.LT.1)NPTHI=1
            IF(NPTLO.GT.MPTS(I-1))NPTLO=MPTS(I-1)
            IF(NPTHI.GT.MPTS(I+1))NPTHI=MPTS(I+1)
COMPUTE CORRECTION DUE TO NEIGHBORING ORDERS
            OOCOR(J,I)=AVG(NPTLO,ILO)*CORR(ILO)
     C                +AVG(NPTHI,IHI)*CORR(IHI)
CORRECT FOR NEIGHBORING ORDERS. COMPUTE CORR. FOR ORDER ITSELF & ADD IT
          OOCOR(J,I)=OOCOR(J,I)+(AVG(J,IAT)+OOCOR(J,I))*3.273*CORR(IAT)
            FNET(J,I)=FNET(J,I)+OOCOR(J,I)
            IF(EPS(J,I).LE.-220.)FNET(J,I)=-1.E-20
200         CONTINUE
300      CONTINUE
      RETURN
      END
```

REFERENCES

Bianchi, L. 1980, in IUE Data Reduction, ed. W. W. Weiss *et al.*, Vienna: Austrian Solar and Space Agency, p. 161.

Bohlin, R. C. 1975, *Ap.J.*, 200, 402.

Bohlin, R. C. and Coulter, B. T. 1982, "Photometric Calibration of the IUE IX. Photometric Stability in High Dispersion," NASA IUE Newsletter No. 19, p. 48.

Bohlin, R. C., and Turnrose, B. E. 1982, "IUE data Reduction XXV. Implementation of Basic Improvements to Extraction of High Dispersion Spectra," NASA IUE Newsletter No. 18, p. 29.

Darius, J. 1980, "Spectral Resolution and Interorder Background," ESA IUE Newsletter No. 5, p. 28.

de Boer, K. S., Preussner, P.-R., and Grewing, M. 1982, *Astron. and Astrophys.*, in press.

Morton, D. C. 1975, *Ap.J.*, 197, 85.

Morton, D. C., and Underhill, A. B. 1977, *Ap.J. Suppl.*, 33, 83.

Rogerson, J. B., and Upson, W. L. 1977, *Ap.J. Suppl.*, 35, 37.

Thompson, R. W., and Bohlin, R. C. 1982, "IUE Data Reduction XXVI. Automatic Registration of the Extraction Slit with the Spectral Format," NASA IUE Newsletter No. 18, p.45.

Upson, W. L., and Rogerson, J. G. 1980, *Ap. J. Suppl.*, 42, 175.

IUE DATA REDUCTION

XXXI. Improved LWP Large-Aperture Offset

With the information available from the latest set of mean LWP dispersion constants (see IUE Data Reduction XXX), it is possible to calculate a refined value for the offset from the long wavelength small aperture (LWSA) to the long wavelength large aperture (LWLA) as seen in the long wavelength prime (LWP) camera. This offset value is needed to transplant the fundamental LWP small-aperture dispersion relations to the large aperture. For the short wavelength prime (SWP) and long wavelength redundant (LWR) cameras, small-to-large-aperture offsets were presented in IUE Data Reduction Memo V (NASA IUE Newsletter No. 6). The preliminary LWP offsets in use prior to the effective date of this memo represented a mirror-reflection of the LWR offsets.

If Z is the distance along the low-resolution order in pixels, the low resolution dispersion $d\lambda/dZ$ is defined by

$$\frac{d\lambda}{dZ} = \frac{1}{\frac{dZ}{d\lambda}} = \frac{1}{\sqrt{\left(\frac{ds}{d\lambda}\right)^2 + \left(\frac{d\ell}{d\lambda}\right)^2}} = \frac{1}{\sqrt{a_2^2 + b_2^2}} = \frac{1}{.3779060}$$

$$= 2.646 \pm 0.002 \text{ Å/pixel}$$

where $a_2 = -0.286471340$ and $b_2 = 0.246469336$ are the scale terms of the mean dispersion relations.

For comparison, in the long wavelength redundant (LWR) camera the dispersion scale is $d\lambda/dZ = 2.652 \pm 0.002$ Å/pixel. This implies that in the spectral image plane, 1 LWP pixel = 0.9977 ± 0.001* LWR pixel. Hence the separation of the LWSA and the LWLA, taken to be R = 26.9 pixels (with an estimated uncertainty of about 0.1 pixels) in LWR, may with little error be taken to be 26.9 pixels in LWP as well.

*Formal error if the LWR and LWP errors quoted above are considered to be independent. If they are non-independent, this formal error estimate increases to ±0.004 pixels.

Together with the knowledge of the angle which the low dispersion spectrum makes with the image scan lines, this information is used to calculate the offset to the LWLA from the LWSA, as follows. The angle Θ between the order and an image line is defined by

$$\Theta = \arctan\left(\frac{d\ell}{ds}\right) = \arctan\left(\frac{b_2}{a_2}\right) = -40.°7.$$

Since the angle ω_s between the dispersion line and the line joining the LWSA and the LWLA is known from LWR studies to be $83°\pm0.°5$, the angle α between an image line and the LWSA-LWLA connector is $42.°3\pm0.°5$; see Figure 1. Hence the line and sample components of the offset to the LWLA from the LWSA are

$$\Delta L = R \sin\,(42.°3\pm0.°5) = +18.1\pm0.2 \text{ pixels}$$

$$\Delta S = R \cos\,(42.°3\pm0.°5) = +19.9\pm0.2 \text{ pixels}$$

Effective September 21, 1982 these offsets have been used in defining the large-aperture dispersion relations for LWP, replacing the previously-used LWR mirror-reflection values of $\Delta L = 19.4$ and $\Delta S = 18.6$. Assuming that the new offsets correctly indicate the location at which objects are placed in the large aperture, Figure 2 shows that the use of the former offsets had introduced a wavelength error of -4.8Å in low dispersion and a velocity error of -1.0 kms^{-1} (i.e., -0.008Å in order 100) in high dispersion.

B.E. Turnrose

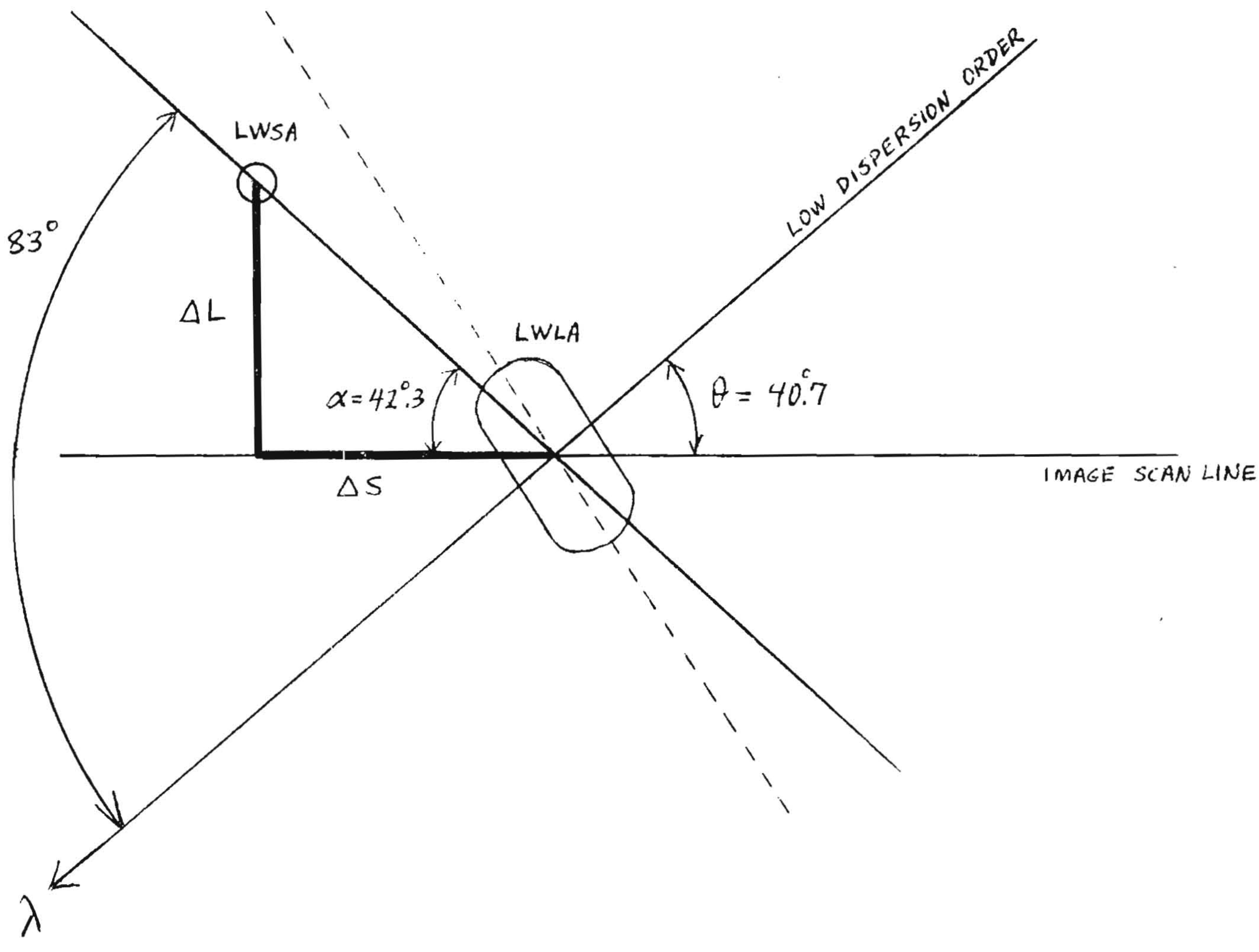

Figure 1. LWP Aperture Geometry.

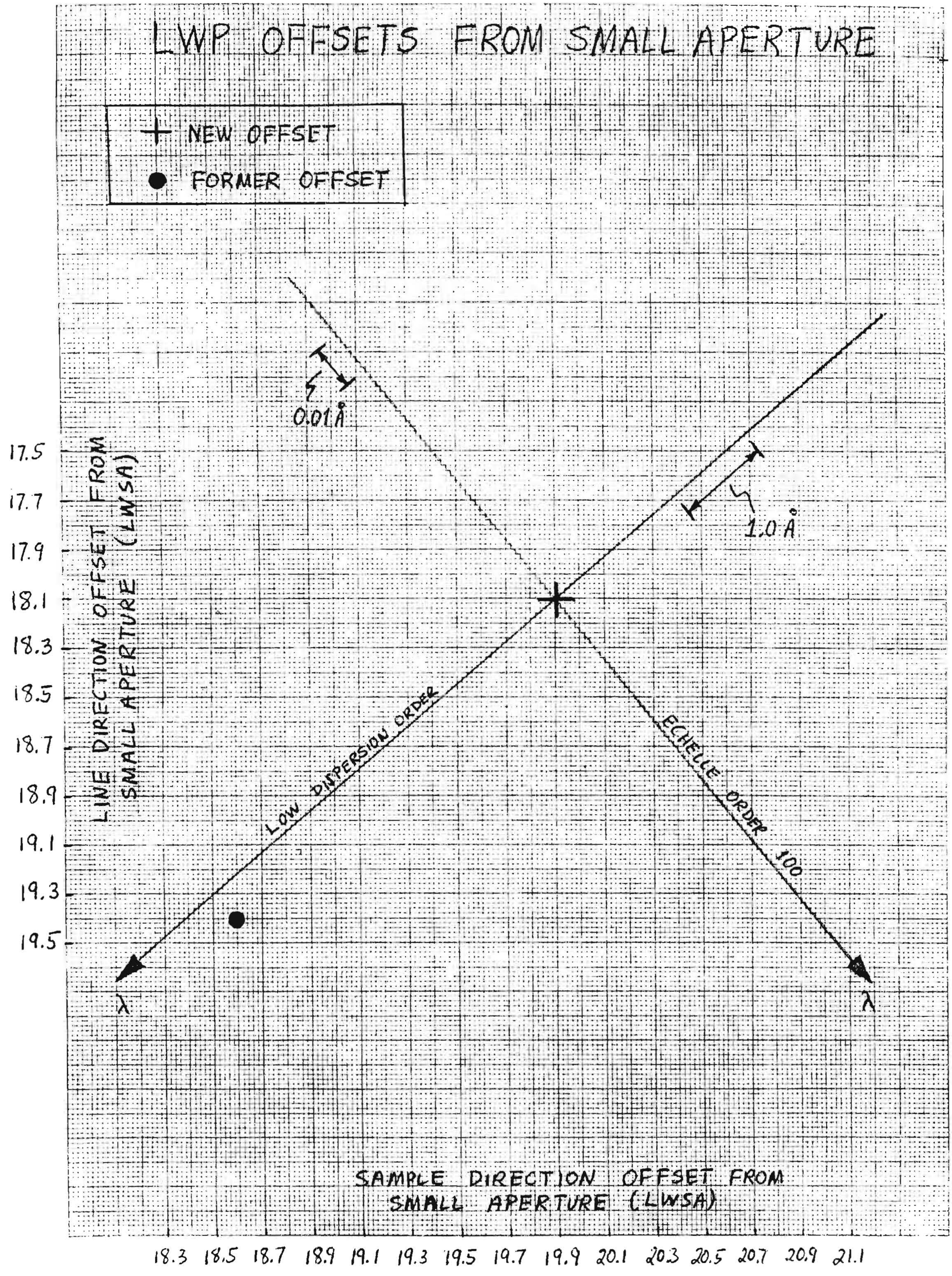
LWP OFFSETS FROM SMALL APERTURE
NEW OFFSET
FORMER OFFSET
0.01 Å
1.0 Å
LOW DISPERSION ORDER
ECHELLE ORDER 100
λ
λ
LINE DIRECTION OFFSET FROM SMALL APERTURE (LWSA)
17.5
17.7
17.9
18.1
18.3
18.5
18.7
18.9
19.1
19.3
19.5
SAMPLE DIRECTION OFFSET FROM SMALL APERTURE (LWSA)
18.3 18.5 18.7 18.9 19.1 19.3 19.5 19.7 19.9 20.1 20.3 20.5 20.7 20.9 21.1

Figure 2

ON THE ABSOLUTE WAVELENGTH CALIBRATION : α ORI.

The spectrum of α Ori was exposed for 930 min with the SWP/ HI mode of the IUE during joint NASA/ESA shifts on 19 August 1981 (SWP 14775). The spectrum was recorded through the large aperture of the spectrograph.

The resulting wavelengths of identified and well exposed lines (see Figure 1) are given in Table I. When the radial velocity of the star (+21 km/s) is taken into account the lines are found to be blue shifted by -0.131 ± 0.015A (-23.2 ± 27 km/s). This would imply an outflow velocity at chromospheric level of about 20 km/s for α Ori.

This was a remarkable and quite surprising result, and we looked for possible instrumental causes for the measured shift. It was noted that a slight positioning error of the star within the large aperture would give rise to an apparent shift of the spectrum relative to the wavelength standard derived with the Pt-Ne calibration lamp. A positional error of the star within large aperture by 1 arcsec may lead to an error of the SWP/HI wavelength scale by as much as 7 km/s.

A new spectrum of α Ori was obtained on 20 August 1982 (SWP 17725). This time we made the exposure through the small aperture of the spectrograph, and with an exposure time of 370 minutes. The stellar spectrum was followed immediately by a Ne-Pt lamp exposure.

The 20 August spectrum of α Ori is quite noisy as shown by Figure 2. Only five lines could be measured with confidence (Table 1). The average shift of the five lines was to the red and became $\lambda(\alpha \mathrm{Ori}) - \lambda(\mathrm{lab}) = 0.015 \pm 0.053$ A (2.4 ± 8.3 km/s).

We selected 28 well exposed lines of the Ne II and 28 lines of Pt II ($\lambda\lambda$ 1400 – 1950 A) of the Ne-Pt lamp spectrum to check the adopted wavelength scale. The laboratory wavelengths are taken from Kelly and Palumbo (1973) and Turnrose and Bohlin (1981) respectively. From the Ne II line spectrum we derived λ(Ne-Pt lamp, IUE) – λ(lab) = 0.005 ± 0.013 A (0.8 ± 2.1 km/s). In the case of Pt II we found corresponding relative shift 0.014 ± 0.012 A (2.4 ± 2.1 km/s).

We conclude that we observe no significant, relative wavelength displacement for the "chromospheric" lines of α Ori within the accuracy of the measurements.

The present observations of α Ori SWP/HI spectra have shown that when observing with the large aperture the wavelength scale may be off by as much as 25 km/s.

TABLE 1

Emission lines of Ori observed with the IUE SWP/HI mode
(1): Observations with large aperture on 19 August 1981
(2): Observations with small aperture on 20 August 1982

λ(lab)	Line Ident	λ(α Ori)-λ(lab) (1)	λ(α Ori)-λ(lab) (2)
1641.178A	O I	-0.127A	-
1785.272	Fe II	-0.147	-
1786.752	Fe II	-0.137	-
1787.996	Fe II	-0.142	-
1807.311	S I	-0.130	-
1820.342	S I	-0.123	+0.091
1826.245	S I	-0.109	-0.014
1900.286	S I	-0.159	-0.028
1914.698	S I	-0.113	-0.022
1993.620	C I	-0.125	+0.050

REFERENCES:

Kelly, R.L., Palumbo, L.J., 1973, "Atomic and Ionic Emission Lines below 2000 Angstrom", NRL Report 7599.

Turnrose, B.E., Bohlin, R.C., 1981, IUE NASA Newsletter No. 13.

++++++++++++++++++

O.Engvold, O. Kjeldseth Moe, E. Jensen, A. Brown, C. Jordan, R.A. Stencel, J. Linsky.

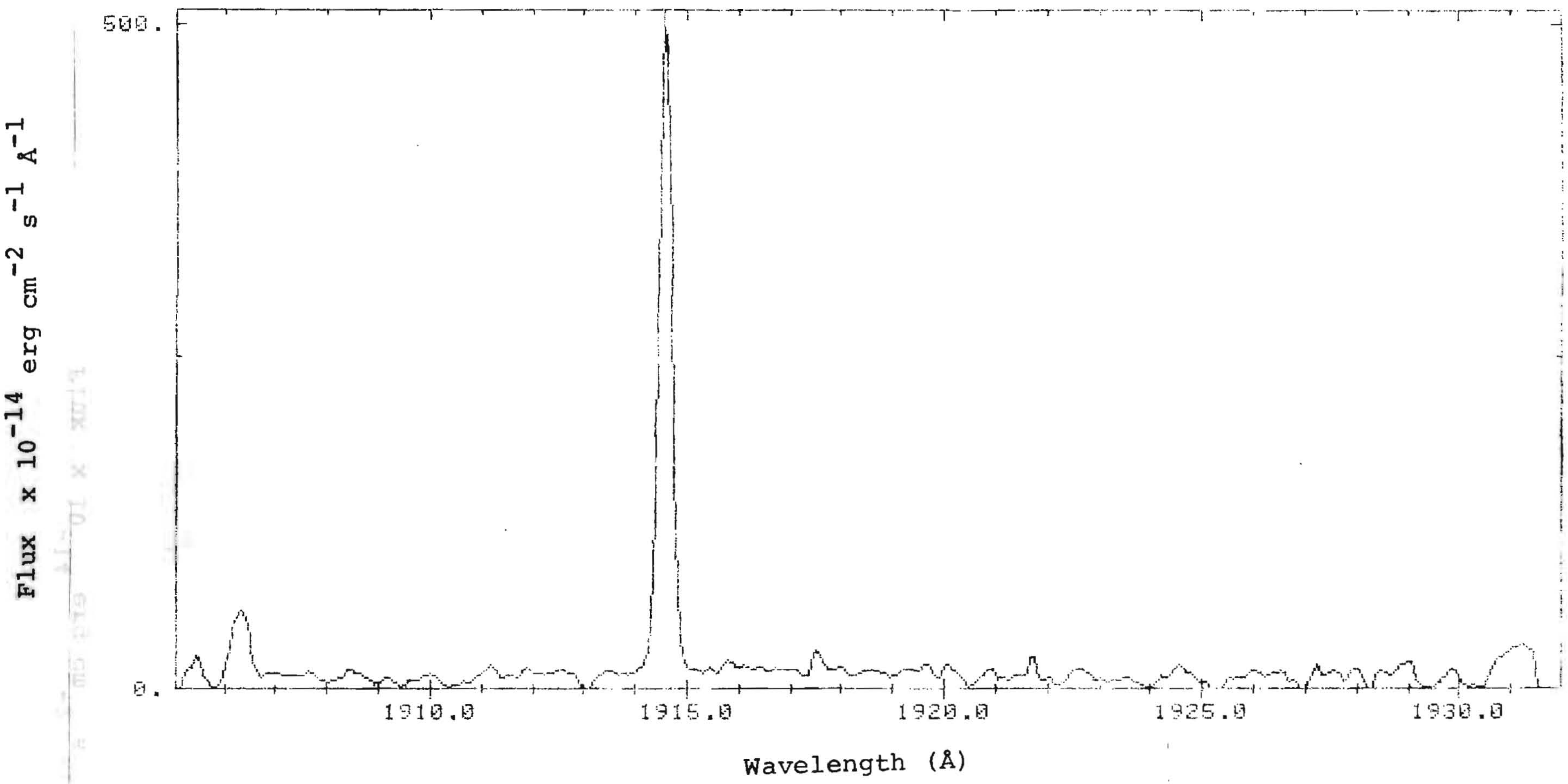

Figure 1 - α Ori observed with large aperture 19 August 1981 (SWP/HI order no. 72)

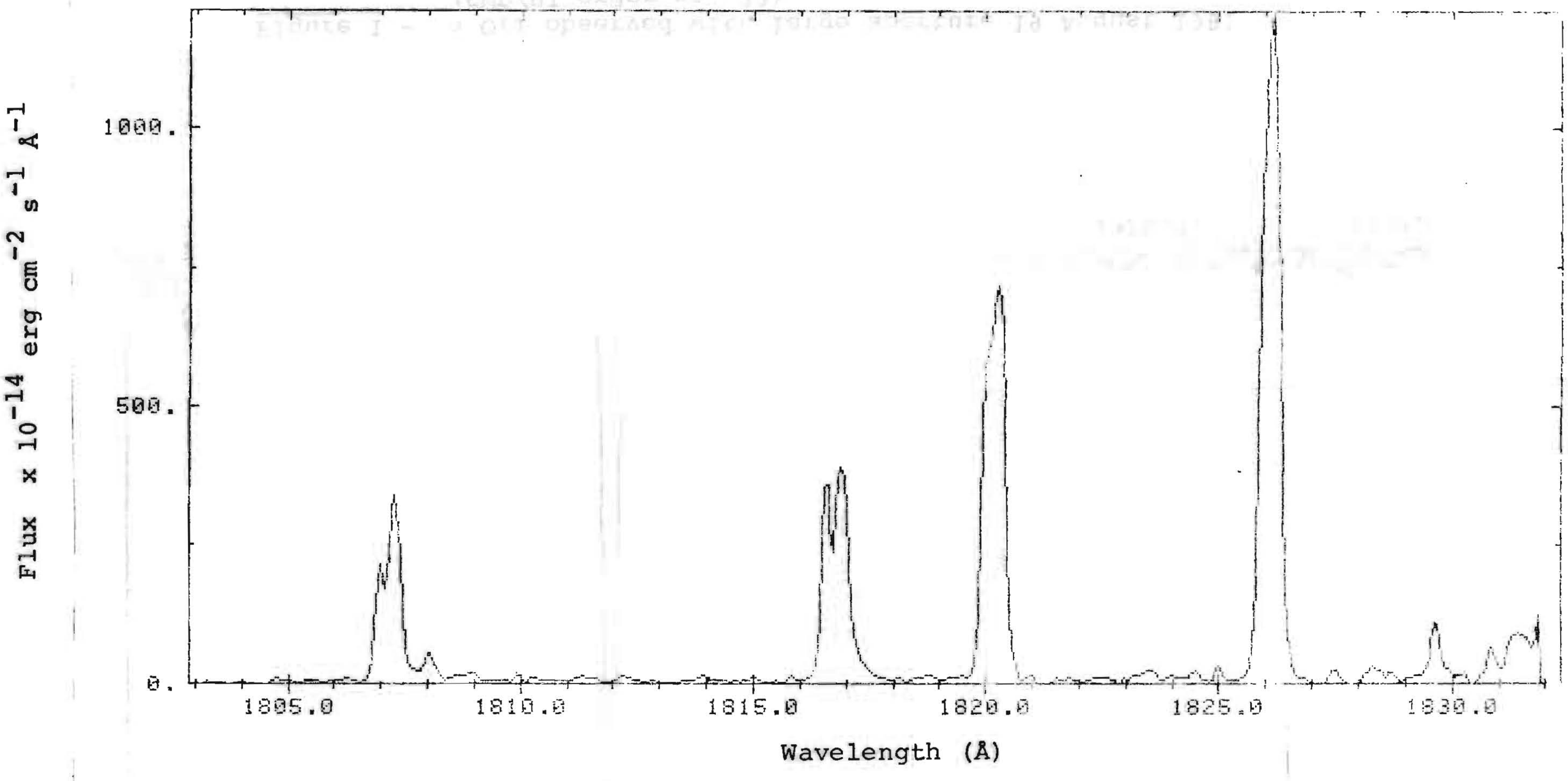

Figure 1 - α Ori observed with large aperture 19 August 1981
(SWP/HI order no. 76)

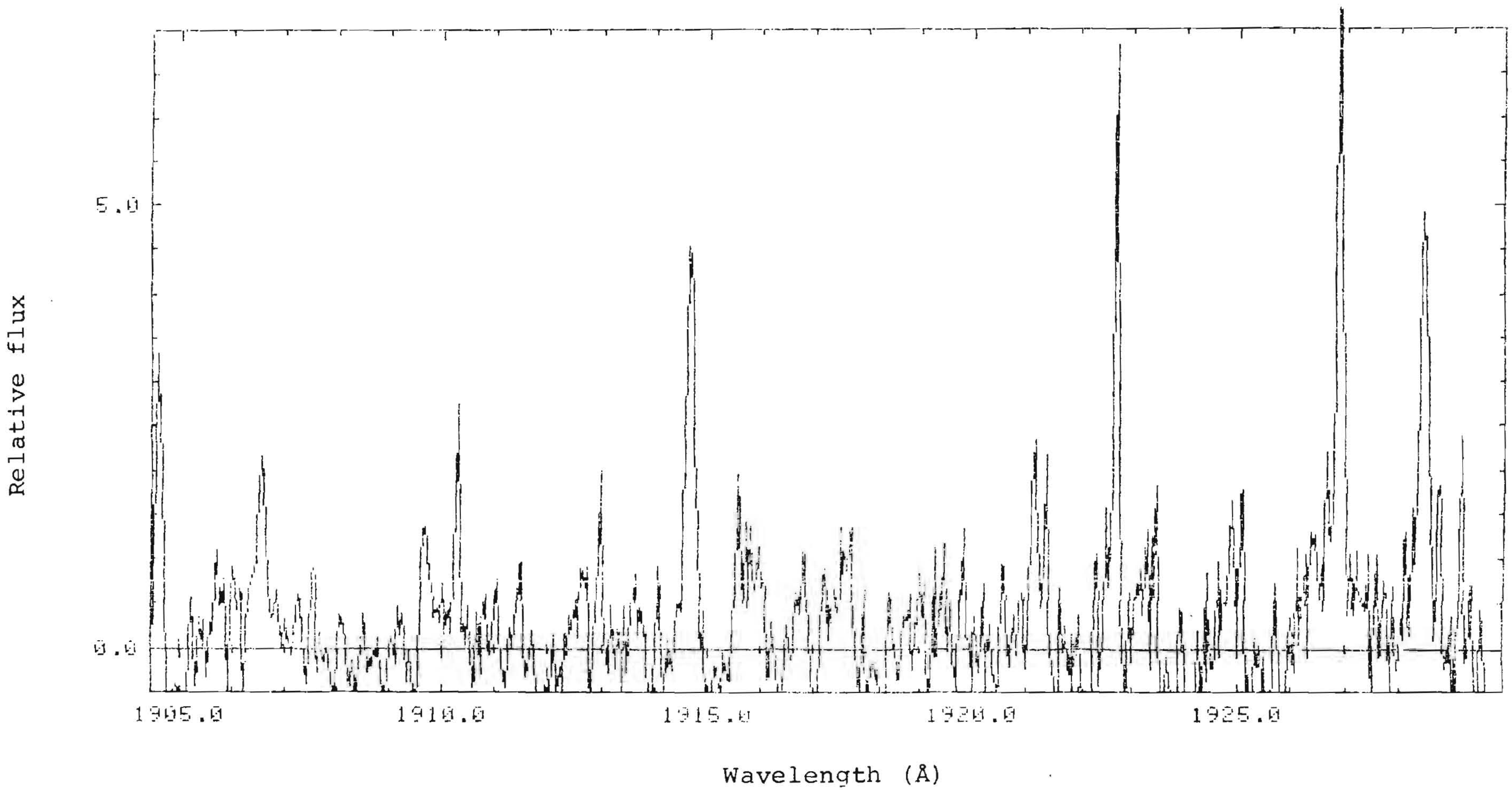

<u>Figure 2</u> - α Ori observed with small aperture 20 August 1982 (SWP/HI order no. 72)

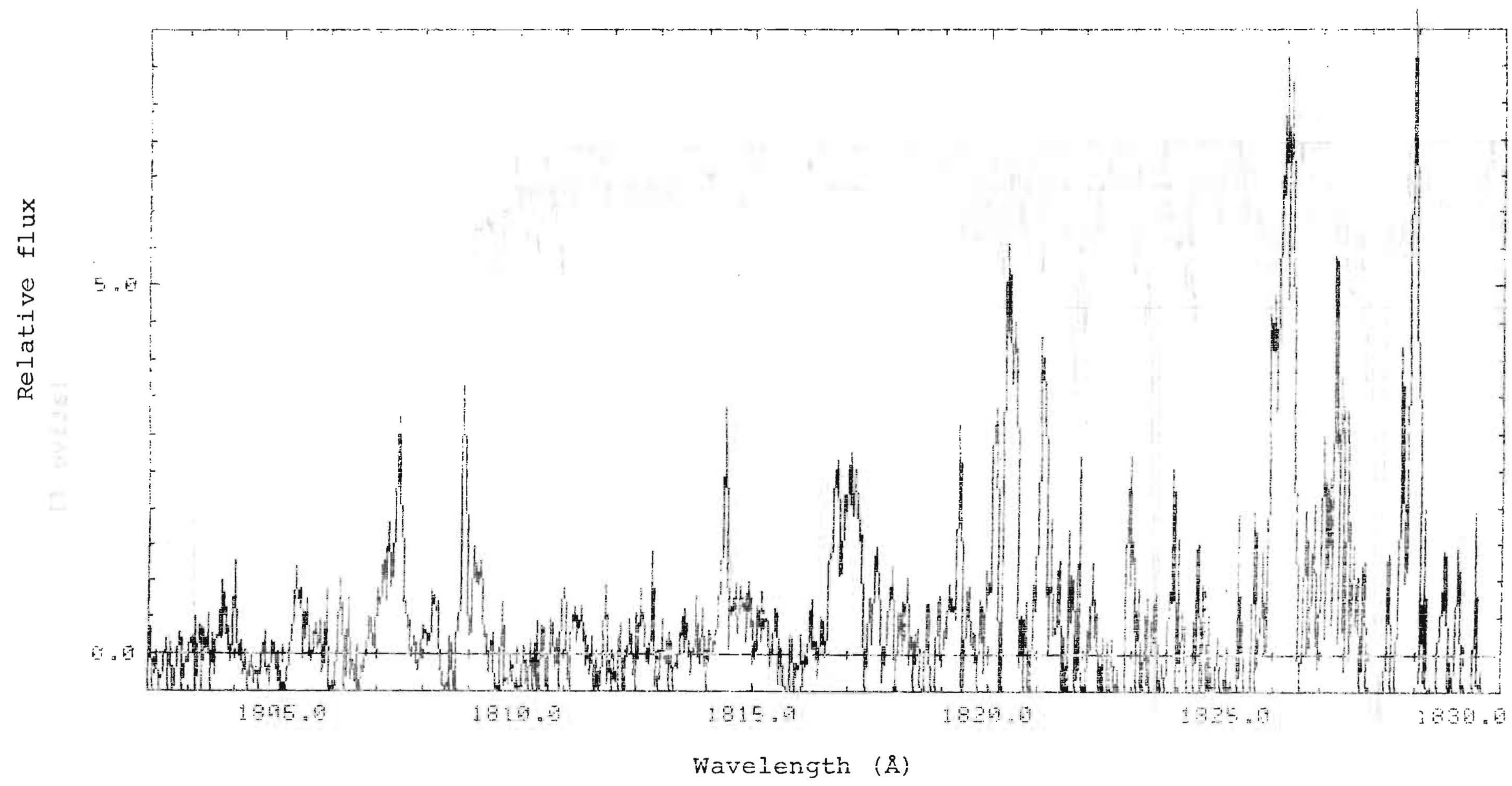

<u>Figure 2</u> - α Ori observed with small aperture 20 August 1982 (SWP/HI order no. 76)

BRIGHT SPOT DETECTION ON IUE IMAGES

INTRODUCTION

Long exposure IUE images show discrete impulse noise produced in the UV converter and in the SEC Vidicon tube. This noise is produced by random "hot" pixels (IUE Newsletter No 8, October 1980, pages 12-14) with a high probability of being excited or by particle events induced by the natural-radiation environment of the IUE orbit. The result is a set of "bright spots" in the IUE raw images.

The analysis of such bright spots will require to identify the affected pixels in the raw image photowrites. This tedious procedure was replaced by implementing under IUESIPS the BSPOT program.

The algorithm used is described in this note, along with the standard parameters used at both VILSPA and GODDARD (implementation: 19 October 1982 at both stations). A discussion about the suitability of the standard parameters is also given.

ALGORITHM

The algortihm used to detect discrete impulse noise on two dimensional IUE raw images, is a cascade (mean + median) filter.

Raw images are scanned in the following way:

Let R(i,j) be the portion of image to be scanned.

A pixel in line i, sample j is detected as a bright spot whenever the conditions (1) and (2) are fulfilled.

$$D(i,j) > \mathrm{Ave}\{D(k,l)\} + \Delta \qquad (1)$$

$$D(i,j) > \mathrm{Med}\{D(k,l)\} + \Delta \qquad (2)$$

with $(i,j) \in R(i,j)$ and
$(k,l) \in S(i,j)$

D(i,j) is the DN value of a pixel,
Δ is a threshold
S(i,j) is a seven pixel window running parallel to the orders centered in the pixel under test as shown in Figure 1.

Ave {.} is the weighted average operator:

$$\text{Ave} = \frac{\sum W(k,l) \quad D(k,l)}{\sum W(k,l)}$$

with $W(k,l)$ = weight of pixel $(k,l) \in S(i,j)$

Med {.} is the median operator.

The standard parameters used by BSPOT are:

Threshold: Δ = 90 DN
Weights : W = 0,0,1,0,1,0,0

Program BSPOT produces a list of detected pixels used later during the spectral extraction to flag bad quality fluxes (= -300). This list is also printed out along with the used parameters.

The region where the algorithm is applied, corresponds to the region where the photometrical correction will be performed. A detected pixel can be found in three different parts:

- Gross spectrum, its value is not modified, it will only be flagged.
- Background, the pixel will not be considered when calculating the smoothed background. It will be flagged.
- Out of the spectral extraction zone, no action is taken. It will only appear in the printout.

DISCUSSION

The suitability of the standard bright spot parameters is not completely determined. Many tests have been performed on several images, indicating that the parameters are related with the background level.

This implies that a variable threshold is necessary to flag bright pixels efectively.

The value of 90 is mainly intended for high background level images and those are the images for which bright spot flagging is more important. In Table 1 a sample of BSPOT printout is shown. Underlined are those bright spots corresponding to "hot" pixels.

J.R. Munoz Peiro

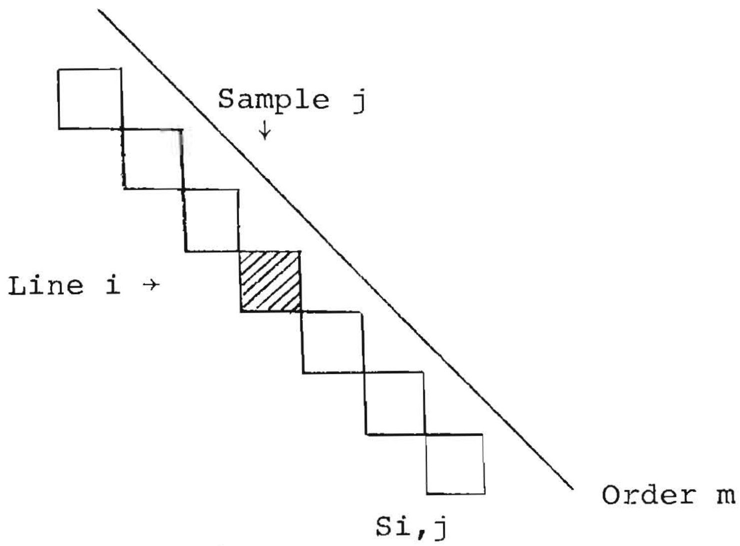

Figure 1 - BSPOT detecting slit. For each camera the slit runs parallel to the orders.

TABLE 1

```
*** OPERATING PARAMETERS FOR BSPOT ***

CAMERA  3   HIGH DISPERSION
  FLAG      MODE
THRESHOLD  90      NPIXEL  7
 WEIGHTS  0  0  1  0  1  0  0
  N. INPUT FILES =  1     N. OUTPUT FILES =  1


BSPOT POSITIONS AS  LINE-SAMPLE
```

107-550	119-355	132-265	188-494	200-399	202-552	206-551	224-497	256-436	256-469
259-452	260-267	261-266	296-682	326-452	334-394	343-296	344-475	348-525	369-427
376-371	399-522	399-523	440-186	442-239	449-474	456-232	457-231	460-128	474-312
475-414	495-495	516-496	523-463	532-450	532-451	577-350	612-387	613-387	615-512
703-337									

```
TOTAL N. OF SPOTS =  41
```

SWP 17147   EXP. TIME = 25800 sec.


```
*** OPERATING PARAMETERS FOR BSPOT ***

CAMERA  2   HIGH DISPERSION
  FLAG      MODE
THRESHOLD  90      NPIXEL  7
 WEIGHTS  0  0  1  0  1  0  0
  N. INPUT FILES =  1     N. OUTPUT FILES =  1


BSPOT POSITIONS AS  LINE-SAMPLE
```

169-499	170-200	175-369	177-610	178-610	207-391	208-392	215-326	256-323	256-324
408-529	412-385	424-549	426-516	433-479	468-555	473-446	518-545		

```
TOTAL N. OF SPOTS =  18
```

LWR 15436   EXP. TIME = 1320 sec.

IUE VILSPA PUBLICATIONS

Mass Loss from Extreme Helium Stars, Hamann, W.R., Schonberner, D., Heber, U., 1982, Astron. Astrophys. 116, 273-285.

Interpretation of Line Profiles of the Symbiotic Star V 1016 Cyg, Kindl, C., Marxer, N., Nussbaumer, H., 1982, Astron. Astrophys. 116, 265-272.

Atmospheric Parameters and Carbon Abundance of White Dwarfs of Spectral Types C2 and DC, Koester, D., Weidemann, V., Zeidler-K.T., E.M., 1982, Astron. Astrophys. 116, 147-157.

The Far-UV Spectrum of the Low-excitation Planetary Nebula HD 138403, Surdej, J., Heck, A., 1982, Astron. Astrophys. 116, 80-88.

Shell and Photosphere of Sigma Ori E:New Observations and Improved Model, Groote, D., Hunger, K., 1982, Astron. Astrophys. 116, 64-74.

The Galactic Abundance Gradient from Supernova Remnant Observations, Binette, L., Dopita, M.A., D'Odorico, S., Benvenuti, P., 1982, Astron. Astrophys. 115, 315-320.

Chromospheric Mg II Emission in A5 to K5 Main Sequence Stars from High Resolution IUE Spectra, Blanco, C., Bruca, L., Catalano, S., Marilli, E., Astron. Astrophys. 115, 280-292.

Electron Densities from the OIV 1401 Multiplet, Nussbaumer, H., Storey, P.J., 1982, Astron. Astrophys. 115, 205-206.

A study of Ultraviolet Spectra of Aur/VV Cep Systems, Hempe, K., 1982, Astron. Astrophys. 115, 133-137.

The Width of Echelle Orders in IUE Images as Derived with the Astronomical Image Display and Analysis (AIDA) System in Tubingen, de Boer, K.S., Preussner, P.R., Grewing, M., 1982, Astron. Astrophys. 115, 128-132

The Visible and Ultraviolet Continuum from a Herbig-Haro Object in the Core of M16 (NGC 6611), Meaburn, J., 1982, Astron. Astrophys. 114, 367-372.

The UV Spectrum of the Old Nova HR Del at Different Orbital Phases, Friedjung, M., Andrillat, Y., Puget, P., 1982, Astron. Astrophys. 114, 351-356.

An SMC Star with a Galactic-type Ultraviolet Interstellar Extinction, Lequeux, J., Maurice, E., Prevot-Burnichon, M.L., Prevot, L., Rocca- Volmerange, B., 1982, Astron. Astrophys. 113, L15- L17.

Discovery of CaII Absorption at 1840 A in IUE Spectra of Two Helium-rich White Dwarfs, Koester, D., Vauclair, G., Weidemann, V., Zeidler-K.T., E.M., 1982, Astron. Astrophs. 113, L13-L14.

The Outer Atmosphere Structure of Three Late Type Stars, de Castro, E., Fernandez-Figueroa, M.J., Rego, M., 1982, Astron. Astrophys. 113, 94-98.

IUE Observations of Dwarf Novae During Active Phases, Klare, G., Krautter, J., Wolf, B., Stahl, O., Vogt, N., Wargau, W., Rahe, J., 1982, Astron. Astrophys. 113, 76-84.

Forbidden Emission Lines of Fe VII, Nussbaumer, H., Storey, P.J., 1982, Astron. Astrophys. 113, 21-26.

First Ultraviolet Observations of Two New Cataclysmic Variables 1E0643-1648 and 4U1849-31 Bonnet-Bidaud, J.M., Mouchet, M., Motch, C., 1982, Astron. Astrophys. 112, 355-360.

On the Linearity of the SWP Camera of the International Ultraviolet Explorer (IUE): A Correction Algorithm, Holm, A., Bohlin, R.C., Cassatella, A., Ponz, D.P., Schiffer, F.H., 1982, Astron. Astrophys. 112, 341-349.

The OB Subdwarf Feige 66, a Chemical-composition Twin to HD 149382, Baschek, B., Hoflich, P., Scholz, M., 1982, Astron. Astrophys. 112, 76-82.

The ultraviolet continuous and emission-line spectra of the Herbig- Haro objects HH 2 and HH 1, Bohm-Vitense, E., Bohm, K.H., Cardelli, J.A., Nemec, J.M., 1982, Astrophys. J., 262: 224-233.

Optical and ultraviolet observations of the X-ray globular cluster Bo 158 in M31, Cacciari, C., Cassatella, A., Bianchi, L., Fusi Pecci, F., Kron, R.G., Astrophys. J., 261: 77-84.

A study of interstellar absorption at high galactic latitudes I. Highly ionized gas, Pettini, M., West, K.A., 1982, Astrophys. J., 260: 561-578.

The violent interstellar medium associated with the Carina Nebula. I. The line of sight toward HD 93205, Laurent, C., Paul, J.A., Pettini, M., 1982, Astrophys. J., 260: 163-182.

Very extended ionized gas in radio galaxies - I. A radio, optical and ultraviolet study of PKS 2158 - 380, 1982, Fosbury, R.A.E., Boksenberg, A., Snijders, M.A.J., Danziger, I.J., Disney, M.J., Goss, W.M., Penston, M.V., Wamsteker, W., Wellington, K.J., Wilson, A.S., Mon. Not. R. Astr. S., 201, 991-1008.

IUE observations of the BL Lac object AO 0235+164, 1982, Snijders, M.A.J., Boksenberg, A., Penston, M.V., Sargent, W.L.W., Mon. Not. R. A. S., 201, 801-805.

Ultraviolet spectra of planetary nebulae - IX. High-dispersion observations of NGC 7662, 1982, Flower, D.R., Penn, C.J., Seaton, M.J., Mon. Not. R. A. S., 201, 39P-43P.

The carbon and nitrogen abundances in WN and WC Wolf-Rayet stars, 1982, Smith, L.J., Willis, A.J., Mon. Not. R. A. S., 201, 451-472.

Interstellar extinction in the Small Magellanic Cloud, 1982, Nandy, K., McLachlan, Thompson, G.I., Morgan, D.H., Willis, A.J., Wilson, R., Gondhalekar, P.M., Houziaux, L., Mon. Not. R. A. S., 201, 1P-6P.

The evolution of viscous discs - III. Giant discs in symbiotic stars, 1982, Bath, G.T., Pringle, J.E., Mon. Not. R. A. S., 201, 345-355.

The ultraviolet spectra of the nuclei of spiral galaxies - I. NGC 4594, 3031, 5194 and 4258, 1982, Ellis, R.S., Gondhalekar, P.M., Efstathiou, G., Mon. Not. R. A. S., 201, 223-251.

GUEST OBSERVER PROPOSALS APPROVED BY THE EUROPEAN ALLOCATION COMM.

Program Title	Authors	Institute	NUMBER
The integrated spectra of globular clusters in M31 and the Fornax dwarf galaxy.	Fusi-Pecci	Bologna	FE002
Interstellar studies of the gas in galactic giant HII regions	Welsh	UCL	FM004
UV observations of blue stragglers	Fracassini	Milano	FA009
High resolution spectroscopy of Blue Halo Stars	Baschek	Heidelberg	FA010
High dispersion observations of Planetary Nebulae	Koppen	Heidelberg	FA011
Star formation in NGC 5367	Reipurth	Copenhagen	FA013
Investigations of motions in the gaseous Galactic Halo	de Boer	Tubingen	FM014
UV Variability of FK Comae	Rucinski	Munchen	FC015
Stellar activity cycle in Beta Hydri	Fredga	Stockholm	FC016
A 'Star Burst' Galactic Nucleus?	Meaburn	Manchester	FE019
UV spectroscopy of blue dwarf galaxies	Gondhalekar	RAL	FE021
UV observations of supernovae	Panagia	Bologna	FE022
Effective temperatures and gravities of subdwarf B-stars	Heber	Kiel	FA027
The atmospheric eclipsing binary Epsilon Aurigae	Hack	Trieste	FC029
The symbiotic star CH Cygni	Hack	Trieste	FC030
The protoplanetary nebula V 1016 Cyg	Nussbaumer	Zurich	FI031

Massive Post-Main-Sequence Envelope objects of the LMC	Wolf	Heidelberg	FA032
Interstellar extinction and a study of early type supergiants in the SMC	Nandy	Edinburgh	FM034
Very low excitation (VLE) compact Nebulae in the Magellanic Clouds	Nandy	Edinburgh	FA035
Composition of dust and gas in the Perseus Arm	Nandy	Edinburgh	FM036
Expanding shells of interstellar gas around OB associations	Phillips	UCL	FM038
High dispersion spectroscopy of interacting binaries	Drechsel	Nuernberg	FI041
Atmospheric abundances of white dwarfs in binary and suspected binary systems	Bues	Bamberg	FA042
Detection of a gas stream in algol	Molaro	Trieste	FI043
UV Observations of inhomogeneous Red Dwarfs atmospheres	Moe	Oslo	FC044
IUE Observations of strong X-ray sources embedded in otherwise "normal" galactic nuclei	Clavel	Meudon	FE045
UV Spectroscopy of White Dwarfs	Koester	Kiel	FC046
Lambda Bootis Stars	Baschek	Heidelberg	FA050
Observations of Variable Seyfert Nuclei	Ulrich	Munchen	FE052
UV FeII fluorescence in cool giant and supergiant stars	Engvold	Oslo	FC053
The symbiotic star HBV 475	Nussbaumer	Zurich	FI054
Coronae and chromospheres of cool giants and supergiants dependence on spectral type	Jordan	Oxford	FC055
Study of the emission line profile and continuum in very blue quasars of low redshift	Bergeron	Paris	FE056
Spectroscopy of high excitation narrow emission line galaxies with radiative Balmer decrement	Durret	Paris	FE059

Mass loss from central stars of planetary nebulae	Perinotto	Arcetri	FA060
A study of two, young, solar-type stars	Jordan	Oxford	FC061
High dispersion observations of alpha Boo	Jordan	Oxford	FC062
Simultaneous UV, X-ray and optical observations of NGC 4593	Clavel	Meudon	FE063
High resolution and time resolved spectroscopy of cataclysmic variables	Jameson	Leicester	FI065
UV observations of Nova-Like Cataclysmic Variables	Hill	St Andrews	FI066
Absorption from companions to quasars or from the quasar itself ?	Bergeron	Paris	FE067
High resolution spectra of two FK Comae-type stars	Rucinski	Munchen	FC068
Investigation of the High-velocity components in the Great Carina Nebula	Laurent	Verrieres	FM069
Observations of the Seyfert Galaxy NGC 5548	Ulrich	Munchen	FE070
Stellar populations in Lenticular Galaxies	Ellis	Durham	FE073
The enigmatic Hypergiant P Cygni	Waters	Utrecht	FA074
High resolution spectroscopy of White Dwarf accreting systems	Cassatella	Vilspa	FI075
The UV activity phase of the recurrent nova T CrB	Cassatella	Vilspa	FI076
Interstellar molecular lines	Somerville	London	FM079
Anomalous interstellar extinction	Somerville	London	FM080
UV spectrophotometry of compact southern planetary nebulae and their central stars	Clegg	London	FA081
Lines from nebular envelopes of importance for spectroscopic diagnostics and abundance determinations	Seaton	London	FA082

Ultraviolet spectrophotometry of planetary nebulae in the Magellanic Clouds	Barlow	London	FA083
Observations of two heavily reddened planetary nebulae	Barlow	UCL	FA084
Evolution of Blue Horizontal Branch and Subdwarf B Stars	Lynas-Gray	London	FA085
Rapid fluctuations in low-luminosity Seyfert I galaxies	Wilson	London	FE086
Ultraviolet variations in in selected Seyfert galaxies	Wilson	London	FE087
A study of the UV variations of the double quasar	Wilson	London	FE088
An attempt to apply the Gun Peterson Test to intergalactic Helium	Wilson	London	FE089
High dispersion spectroscopy of HZ Her: the nature and origin of the emission lines	Wilson	London	FI090
Spectrophotometry of HZ Her: the accretion disk	Wilson	London	FI091
UV spectral variations of HD 50896 (WN5+?) - Do WR+Collapsar systems exists ?	Willis	London	FI094
Fundamental parameters of the super Eddington X-ray transient source A0538-66	Willis	London	FI095
Stellar wind variations in the enigmatic subluminous star HD 45166 (qWR+B8V)	Willis	London	FA096
Physical properties of the accretion disk in RZ Oph	Willis	London	FC097
Diagnosis of physical conditions in the North Polar Spur	Hartquist	London	FM098
UV Observations of epsilon Aurigae	Stickland	RGO	FI101
Galactic coronal gas investigations by I2.0observations of young globula clusters of the LMC	Geyer	Daun	FM104

UV-observations of bright, compact open cluster and neighbouring young globular cluster of the LMC	Cassatella	Vilspa	FE105
UV observations of hot hydrogen-deficient variables	Hill	St Andrews	FA107
Studies of nuclear regions of Sersic-Pastoriza galaxies - II	Thompson	Edinburgh	FE108
Winds and Coronae in Red Giants	Reimers	Hamburg	FC109
Mass-loss of Red Giants with Hot Companions	Reimers	Hamburg	FC110
Lyman-Alpha emission from X-ray Clusters with Cooling Cores	Norgaard	Copenhagen	FE112
UV energy distribution in CD galaxie	Bertola	Padova	FE113
Non-LTE analysis of Central Stars of Planetary Nebula	Kudritzki	Munchen	FA114
Non-LTE analysis of Subdwarf O-stars	Kudritzki	Munchen	FA115
Deep exposures on the Cygnus Loop	Danziger	Munchen	FM117
The long-term variability of the Lyman alpha emission from Jupiter, Saturn, and Uranus	Fricke	Bonn	FS118
Study of interstellar gas adjacent to two spiral arms	Harris	RAL	FM122
Study of M-Dwarf Flares	Bromage	RAL	FC123
A high resolution study of the Jet of R Aquarii	Charles	Oxford	FC124
Periodic & new comets	Wallis	Cardiff	FS125
Studies of High Galactic Latitude Ga	Harris	RAL	FM126
Best possible UV line list from RR Tel	Penston	RGO	FI128
Completion of UV observations of an all-sky sample of X-ray active galaxies	Lawrence	RGO	FE130
Abundances and excitation mechanisms in peculiar emission-line nuclei of galaxies	Pagel	RGO	FE131
Continued monitoring of NGC 4151	Penston	RGO	FE132

The extent of the gaseous galactic halo	Pettini	RGO	FM133
IUE observations of QSOs and BL Lac Objects	Snijders	RGO	FE135
A study of ultraviolet variability of Seyfert 2 galaxies	Snijders	RGO	FE137
Short wavelength line profiles in T Tauri stars	Penston	RGO	FC138
Long exposure observations of extragalactic sources	Penston	RGO	FE139
Distances of 21 centimeter high velocity (OORT) clouds	Pettini	RGO	FM140
UV observations of stars rotating very close to theoretical breakup velocity	Molaro	Trieste	FA141
Chromospheric and coronal activity in regular-period RS CVn-like stars	Fernandez	Madrid	FC142
Structure of the envelope of Be star	Hubert-D.	Paris	FA144
UV observations of the interacting Binary CX Dra	Koubsky	Ondrejov	FI146
Observations of a BL Lac object	Ulrich	Munchen	FE148
The UV variability and rotational modulation of T Tauri stars	Jordan	Oxford	FC150
Observational basis for an empirical theoretical modeling of Be stars	Doazan	Paris	FA152
Investigation of mass-loss and chromospheric effects in a A-shell stars	Doazan	Paris	FA153
High resolution observations of Mercury-Manganese stars	Dworetsky	London	FA154
Evolved globular cluster stars	Caloi	Frascati	FA155
Integrated spectra of globular clusters	Caloi	Frascati	FE156
Contemporaneous studies of active galactic nuclei	Coe	Southampton	FE157
Periodicities in X-ray sources	Coe	Southampton	FI158
Variability of Akn 120	Kollatschny	Gottingen	FE162

Barred spirals with X-ray nuclei	Fricke	Gottingen	FE164
The outburst of AG Draconis	Altamore	Roma	FI166
Study of matter ejected by superluminous stars	Giangrande	Frascati	FM167
Coordinated UV and optical observations of BL Lac objects	Tanzi	Milano	FE176
Star formation in irregular galaxies	Casini	Milano	FE177
A search for UV variability in the clumpy irregular galaxy Markarian 297 (=NGC 6052)	Benvenuti	Vilspa	FE178
The UV stellar classification programme	Heck	Vilspa	FA179
Ultraviolet observations of V348 Sgr during ascending and descending phases	Heck	Vilspa	FA180
Ultraviolet studies of the shells of Herbig Ae and Be stars	Tjin	Amsterdam	FA181
Near ultraviolet observations of the high-redshift BL Lac object 0215+015	Blades	Vilspa	FE182
Absolute spectrophotometry of blue stars for calibration of space instruments, including space telescope	Blades	Vilspa	FA183
Observations of Lyman alpha haloes of galaxies, using QSOs as back-ground probes	Blades	Vilspa	FE184
Absorption measures of gas in haloes of galaxy	Blades	Vilspa	FM185
Far UV study of an X-ray selected sample of active galactic nuclei	Grewing	Tubingen	FE191
Probing the HI holes in the direction of HZ 43 and HR 1099	Grewing	Tubingen	FM192
Study of blue stars in the LMC emission nebula N 144	Grewing	Tubingen	FA193
The shell structure of the Herbig Ae star HD 250550	Talavera	Meudon	FA194

Emission, mass loss and envelopes in Herbig Ae stars	Praderie	Paris	FA195
A far UV study of the interstellar matter in the Small Magellanic Cloud	Prevot	Marseille	FM197
Simultaneous ground-based and UV observations of the star V 4046 Sgr	de la Reza	Brazil	FC199
IUE observations of FK Comae stars with coordinated ground-based photometry	Bianchi	Torino	FC201
Observations of Orion nebulary variables emitting soft X-rays	Bianchi	Torino	FC203
Dust envelopes of Herbig Ae stars	Catala	Meudon	FA208
Modelling of the T Tauri star RU Lupi	Gahm	Stockholm	FC210
UV observations of star-forming cooling flows	Fabian	Cambridge	FE212
UV, optical and IR observations of T Tauri type stars	Giovannelli	Frascati	FC215
Mass loss rate from a 0535+26/ HDE 245770 system in quiescence and in outburst	Giovannelli	Frascati	FI217
UV spectra of Gygnus OB2 association	Giovannelli	Frascati	FA218
UV observations of the secondary component of Algol-type binaries	Catalano	Catania	FC220
Mg II emission of MS stars in open clusters	Catalano	Catania	FC221
Coordinated ultraviolet-X ray observations of Seyfert galaxies	di Cocco	Bologna	FE223
Determination of absolute velocities for emission lines in late type stars	Engvold	Oslo	FC225
Wolf rayet stars in dwarf emission line galaxies	Joubert	Marseille	FE227
Emission lines in the halo of edge-on galaxies	Joubert	Marseille	FE228
Lyman continuum observations of broad absorption line QSOs	McMahon	Cambridge	FE229

Masses of cepheids	Eichendorf	Munchen	FC231
Classical cepheids and their blue companions	Eichendorf	Munchen	FC232
H II regions and star formation bursts in NGC 1510	Eichendorf	Munchen	FM233
Star formation and chemical enrichment in two blue compact galaxies	Bergvall	Uppsala	FE235
Nuclear region of the galaxy NGC 1365	Jorsater	Sweden	FE237
Ultraviolet observations of newly discovered X-ray sources	Bonnet B	Saclay	FI240
High resolution ultraviolet spectra of the carbon star TW Hor	Querci F	Toulouse	FC241
UV energy distribution of the dwarf elliptical galaxy NGC 205	Bertola	Padova	FE243
Carbon abundance in M 33 and M 31 from supernova remnants	D'odorico	Munchen	FE248
IUE observations of surface structure of eclipsing and non-eclipsing RS CVN systems	Rodono	Catania	FC249
High dispersion study of luminous cool stars	Gustafsson	Uppsala	FC251
Search for chromospheres in A-type stars	Freire	Strasbourg	FA252
Time scales of M dwarf flares	Butler	Armagh	FC254
Short time variations in the mass-loss rate of early type stars	Henrichs	Amsterdam	FA255
Probing Seyfert I nuclei through observations over a large wavelength interval	Wamsteker	Vilspa	FE257
High resolution UV spectra of M 83 (=NGC 5236)	Wamsteker	Vilspa	FE258
2000-5000 A observations of weak Fe II line Seyferts	Netzer	Tel Aviv	FE260
Carbon stars sequence: R to N stars	Querci M	Toulouse	FC265

IUE observations of POP II standard stars	Cacciari	Vilspa	FC268
Spatial coverage of Jupiter and Saturn	Combes	Meudon	FS269
Accretion in twin degenerate systems	Solheim	Tromso	FI270
Star forming activity in interacting galaxies	Alloin	Meudon	FE272
Study of the interstellar medium in the Scorpius-Ophiuchus region	Pottasch	Groningen	FM273
Spatial variation of the plasma electron temperature in the IO Torus	Bertaux	Verrieres	FS275

####################

NASA APPROVED IUE PROGRAMS FOR THE SIXTH YEAR

NAME		INSTITUTION	COUNTRY	PROG ID
TITLE				
A'HEARN	MICHAEL F.	MARYLAND	U. S.	STFMA
SOLAR ANALOGS FOR CALIBRATION OF REFLECTIVITIES OF BODIES IN THE SOLAR SYSTEM				
A'HEARN	MICHAEL F.	MARYLAND	U. S.	SCFMA
COMETS AS TARGETS OF OPPORTUNITY				
ADELMAN	SAUL J.	CITADEL	U. S.	HSFSA
ELEMENTAL ABUNDANCES IN SHARP-LINED LATE B AND EARLY A STARS				
AGRAWAL	PRAHLAD C.	TATA INST.	INDIA	CVFPA
ULTRAVIOLET OBSERVATIONS OF NEWLY DISCOVERED AM HERCULIS-LIKE X-RAY BINARY H0139-68				
AHMAD	IMAD A.	IMAD-AD-DEAN	U. S.	VVFIA
SECONDARY MINIMA OF ZETA AURIGAE BINARIES				
AKE	THOMAS B.,III	CSC	U. S.	VVFTA
FURTHER ECLIPSE OBSERVATIONS OF EPSILON AURIGAE				
ALLER	LAWRENCE H.	CAL LA	U. S.	NPFLA
STRUCTURE OF AND ABUNDANCES IN HIGH-EXCITATION PLANETARIES				
AYRES	THOMAS R.	COLORADO-LASP	U. S.	LGFTA
HIGH-DISPERSION OBSERVATIONS OF ALPHA BOOTIS				
AYRES	THOMAS R.	COLORADO-LASP	U. S.	STFTA
SME AND IUE: THE SOLAR-STELLAR CONNECTION				
AYRES	THOMAS R.	COLORADO-LASP	U. S.	LDFTA
CAPELLA HL				
AYRES	THOMAS R.	COLORADO-LASP	U. S.	CCFTA
THE HYDROGEN EMISSION OF ACTIVE RED DWARFS				
AYRES	THOMAS R.	COLORADO-LASP	U. S.	CSFTA
DETERMINATION OF ABSOLUTE VELOCITIES FOR EMISSION LINES OF LATE-TYPE STARS				
BALIUNAS	SALLIE L.	CFA - SAO	U. S.	LGFSB
VERTICAL STRUCTURE OF THE ATMOSPHERES OF ACTIVE G-GIANT STARS				
BARKER	PAUL K.	W. ONTARIO	CANADA	BEFPB
ENVELOPE EJECTION BY ACTIVE BE STARS				
BARKER	PAUL K.	W. ONTARIO	CANADA	MLFPB
SUPERIONIZED WINDS AND H ALPHA EMISSION IN QUIESCENT BE STARS				

NASA APPROVED IUE PROGRAMS FOR THE SIXTH YEAR

NAME		INSTITUTION	COUNTRY	PROG ID	TITLE
BARKER	TIMOTHY	WHEATON	U. S.	NPFTB	THE IONIZATION STRUCTURE OF PLANETARY NEBULAE
BASRI	GIBOR S.	CAL BERKELEY	U. S.	IGFGB	AN ABSORPTION LINE STUDY OF HIGH LATITUDE DIFFUSE CLOUDS
BLAIR	WILLIAM P.	CFA - SAO	U. S.	NSFWB	CARBON ABUNDANCE IN M33 AND M31 FROM SUPERNOVA REMNANTS
BOGGESS	ALBERT	GSFC	U. S.	QSFAB	UV OBSERVATIONS OF SEYFERT GALAXIES
BOGGESS	ALBERT	GSFC	U. S.	HZFAB	AN ATTEMPT TO DETECT INTERGALACTIC HELIUM IN A HIGH-Z QUASAR SPECTRUM
BOHM	KARL-HEINZ	WASH.	U. S.	CSFKB	THE ENVIRONMENT OF THE COHEN-SCHWARTZ STAR
BOHM	KARL-HEINZ	WASH.	U. S.	IMFKB	INTERSTELLAR ABSORPTION AND EXTINCTION
BOHM-VITENSE	ERIKA	WASH.	U. S.	CCFEB	CHROMOSPHERIC EMISSION OF CLOSE BINARIES WITH NONSYNCHRONIZED ORBITAL & ROTATIONAL PERIODS
BOHM-VITENSE	ERIKA	WASH.	U. S.	HCFEB	CEPHEID COMPANIONS AND MASSES
BOHM-VITENSE	ERIKA	WASH.	U. S.	LGFEB	WHITE DWARF COMPANIONS AND CHROMOSPHERES OF STARS WITH PECULIAR ELEMENT ABUNDANCES
BOND	HOWARD E.	LOUISIANA ST.	U. S.	NPFHB	ULTRAVIOLET OBSERVATIONS OF CLOSE-BINARY AND PULSATING NUCLEI OF PLANETARY NEBULAE
BOND	HOWARD E.	LOUISIANA ST.	U. S.	HCFHB	A SEARCH FOR WHITE-DWARF COMPANIONS OF SUBGIANT CH STARS
BOWYER	C. STUART	CAL BERKELEY	U. S.	WDFCB	CONTINUING STUDIES OF HOT WHITE DWARFS AND THE LOCAL ISM
BOWYER	C. STUART	CAL BERKELEY	U. S.	SPFCB	OBSERVATIONS OF H LY ALPHA EMISSION FROM NEPTUNE
BOWYER	C. STUART	CAL BERKELEY	U. S.	SUFCB	OBSERVATIONS OF H LY ALPHA EMISSION FROM URANUS

NASA APPROVED IUE PROGRAMS FOR THE SIXTH YEAR

NAME		INSTITUTION	COUNTRY	PROG ID
TITLE				
BOWYER	C. STUART	CAL BERKELEY	U. S.	XGFCB
FAR UV SPECTROSCOPY OF X-RAY ACTIVE GALACTIC NUCLEI				
BOWYER	C. STUART	CAL BERKELEY	U. S.	EHFCB
SEARCH FOR EMISSION LINES IN THE GASEOUS HALO OF EDGE-ON GALAXIES				
BOWYER	C. STUART	CAL BERKELEY	U. S.	NJFCB
FAR UV SPECTROSOCOPY OF THE OPTICAL EMISSION KNOTS IN THE INNER JET OF CEN A				
BROWN	DOUGLAS N.	WASH.	U. S.	HEFDB
MASS LOSS AND PHOTOSPHERIC STRUCTURE IN EARLY-TYPE SPECTRUM VARIABLES				
BRUGEL	EDWARD W.	COLORADO-LASP	U. S.	IBFEB
ANALYSIS OF THE SYMBIOTIC STARS V1016 CYG, HM SGE AND V1329 CYG				
BRUHWEILER	FREDERICK C.	CSC	U. S.	GHFFB
AN ULTRAVIOLET SEARCH FOR HIGH VELOCITY GAS AT HIGH GALACTIC LATITUDES				
BRUHWEILER	FREDERICK C.	CSC	U. S.	WDFFB
MASS LOSS AND RADIATIVE LEVITATION IN HOT WHITE DWARFS				
BRUHWEILER	FREDERICK C.	CSC	U. S.	EHFFB
THE LYMAN ALPHA ABSORPTION FOREST IN QSOS OF INTERMEDIATE REDSHIFT				
CALDWELL	JOHN	STONY BROOK	U. S.	SPFJC
IUE SOLAR SYSTEM OBSERVATIONS, I. URANUS AND NEPTUNE BELOW 2000 ANGSTROMS				
CALDWELL	JOHN	STONY BROOK	U. S.	SSFJC
IUE SOLAR SYSTEM OBSERVATIONS, II. SATURN'S RINGS				
CALDWELL	JOHN	STONY BROOK	U. S.	SJFJC
IUE SOLAR SYSTEM OBSERVATIONS ,IV. CHEMICAL COMPOSITION AT JUPITER'S POLES				
CHAPMAN	ROBERT D.	GSFC	U. S.	VVFRC
PHYSICS OF THE CIRCUMSTELLAR ENVELOPE, ACCRETION DISK & SECONDARY COMPANION IN EPSILON AUR				
CODE	ARTHUR D.	WISCONSIN	U. S.	IEFAC
A STUDY OF REDDENING IN GALACTIC SYMBIOTIC STARS				
COHEN	ROSS D.	CAL SAN DIEGO	U. S.	QSFRC
HYDROGEN LINE RATIOS IN THE NARROW-LINE REGIONS OF ACTIVE GALAXIES				
CONTI	PETER S.	COLORADO	U. S.	MLFPC
STELLAR WINDS IN THE MAGELLANIC CLOUDS				

NASA APPROVED IUE PROGRAMS FOR THE SIXTH YEAR

NAME		INSTITUTION	COUNTRY	PROG ID
TITLE				
CONTI	PETER S.	COLORADO	U. S.	WRFPC
UV SPECTRAL VARIATIONS OF HD 50896 (WN 5+?)				
COWLEY	CHARLES R.	MICHIGAN	U. S.	HSFCC
SUPERFICIALLY NORMAL EARLY B STARS WITH SHARP SPECTRAL LINES				
DAVIDSON	KRIS	MINNESOTA	U. S.	EGFKD
UV SPECTROSCOPY OF TWO SPECIAL EXTRAGALACTIC OBJECTS				
DEAN	CHARLES A.	S M SYSTEMS	U. S.	MLFCD
SHARP LINE DISPLACED FEATURES IN O SUBDWARFS: A SECOND MASS LOSS MECHANISM?				
DOSCHEK	GEORGE A.	NRL	U. S.	HSFGD
THE BEST POSSIBLE UV LINE LIST FROM RR TEL				
DRILLING	JOHN S.	LOUISIANA ST.	U. S.	HSFJD
ULTRAVIOLET SPECTROSCOPY OF SUBLUMINOUS O STARS				
DUFOUR	REGINALD J.	RICE	U. S.	NDFRD
HIGH DISPERSION IUE OBSERVATIONS OF METAL-POOR H II REGIONS - II				
DUPREE	ANDREA K.	CFA - SAO	U. S.	QSFAD
ULTRAVIOLET VARIABILITY OF THE DOUBLE QSO 00957+561				
DUPREE	ANDREA K.	CFA - SAO	U. S.	CCFAD
CHROMOSPHERES IN METAL DEFICIENT GIANTS				
FANG	LI ZHI	CFA-S&T CHINA	CHINA	QSFLF
UV OBSERVATIONS OF CIV EMISSION LINES FOR LOW REDSHIFT QSOS				
FEIBELMAN	WALTER A.	GSFC	U. S.	NPFWF
OBSERVATIONS OF THE BIPOLAR PLANETARY NEBULA NGC 2346				
FEKEL	FRANCIS C.,JR.	GSFC	U. S.	CCFFF
ULTRAVIOLET OBSERVATIONS OF UNUSUAL CHROMOSPHERICALLY ACTIVE GIANT STARS				
FELDMAN	PAUL D.	JOHNS HOPKINS	U. S.	SCFPF
OBSERVATIONS OF COMETS WITH THE INTERNATIONAL ULTRAVIOLET EXPLORER				
FERLAND	GARY J.	KENTUCKY	U. S.	QSFGF
ULTRAVIOLET AND OPTICAL OBSERVATIONS OF 3C 120				
FESEN	ROBERT A.	GSFC	U. S.	NSFRF
UV STUDIES OF TYPE I SNRS IN THE LARGE MAGELLANIC CLOUD				

NASA APPROVED IUE PROGRAMS FOR THE SIXTH YEAR

NAME		INSTITUTION	COUNTRY	PROG ID
TITLE				
GALLAGHER	JOHN S. III	ILLINOIS	U. S.	EPFJG
HIGH STAR FORMATION RATE IRREGULAR GALAXIES AND THE IMF OF MASSIVE STARS				
GARMANY	CATHARINE D.	COLORADO	U. S.	MLFCG
NARROW COMPONENTS IN HOT STAR WINDS				
GIAMPAPA	MARK S.	AURA - SAC PK	U. S.	FSFMG
OBSERVATIONS OF FLARE ACTIVITY ON SELECTED DME FLARE STARS				
GLASSGOLD	A. E.	NEW YORK U.	U. S.	QSFAG
QUASAR EMISSION LINES AND IONIZING RADIATION				
GLASSGOLD	A. E.	NEW YORK U.	U. S.	BLFAG
MULTIFREQUENCY OBSERVATIONS OF BL LAC OBJECTS AND VIOLENTLY VARIABLE QUASARS				
GREEN	RICHARD F.	ARIZONA	U. S.	QSFRG
HIGH DISPERSION QUASAR ABSORPTION SPECTRA				
GREEN	RICHARD F.	ARIZONA	U. S.	HZFRG
HIGH REDSHIFT QUASARS				
GREEN	RICHARD F.	ARIZONA	U. S.	XQFRG
BRIGHT OPTICALLY SELECTED QUASARS WITH HIGH X-RAY FLUX				
GUINAN	EDWARD F.	VILLANOVA	U. S.	CCFEG
COORDINATED ULTRAVIOLET SPECTROSCOPY AND OPTICAL PHOTOMETRY OF FK COMAE				
HAISCH	BERNHARD M.	LOCKHEED	U. S.	CBFBH
IDENTIFICATION OF ACTIVE REGIONS ON THE ECLIPSING BINARY FLARE STAR PAIR YY GEM				
HAISCH	BERNHARD M.	LOCKHEED	U. S.	FSFBH
TEMPORAL EVOLUTION OF UV EMISSION LINES DURING FLARES ON DME STARS				
HAISCH	BERNHARD M.	LOCKHEED	U. S.	LDFBH
A COMPARATIVE STUDY OF DM AND DME STARS				
HALLAM	KENNETH L.	GSFC	U. S.	LDFKH
STELLAR ROTATION AND CHROMOSPHERIC SURFACE DISTRIBUTION				
HARTMANN	LEE W.	CFA - SAO	U. S.	MGFLH
A STUDY OF THE RELATIONSHIP BETWEEN MG II EMISSIAND AND ROTATION				
HARTMANN	LEE W.	CFA - SAO	U. S.	CCFLH
A STUDY OF CHROMOSPHERIC EMISSION DECAY IN OLD STARS				

NASA APPROVED IUE PROGRAMS FOR THE SIXTH YEAR

NAME		INSTITUTION	COUNTRY	PROG ID	TITLE
HECHT	JAMES H.	AEROSPACE COR	U. S.	CDFJH	DUST EXTINCTION IN HR 5999
HECKATHORN	JOY NICHOLS	CSC	U. S.	IGFJH	HIGH VELOCITY COMPONENTS OF UV INTERSTELLAR LINES IN THE CARINA NEBULA
HOBBS	LOU M.	CHICAGO-YRKS	U. S.	GHFLH	THE DISTRIBUTION OF INTERSTELLAR GAS IN THE GALACTIC HALO
HOBBS	LOU M.	CHICAGO-YRKS	U. S.	IGFLH	IUE OBSERVATIONS OF INTERSTELLAR CARBON
HODGE	PAUL W.	WASH.	U. S.	EGFPH	UV OBSERVATIONS OF OB STARS IN NGC 185 AND NGC 205
HODGE	PAUL W.	WASH.	U. S.	MLFPH	EVOLUTION OF MASS LOSS IN STARS OF MAGELLANIC CLOUD CLUSTERS
HOLBERG	JAY B.	USC - ARIZONA	U. S.	HSFJH	COMBINED VOYAGER AND IUE ENERGY DISTRIBUTIONS FOR HOT DEGENERATE STARS
HOLBERG	JAY B.	USC - ARIZONA	U. S.	WDFJH	HIGH RESOLUTION OBSERVATIONS OF HOT WHITE DWARFS
HOLM	ALBERT V.	CSC	U. S.	RCFAH	EXTINCTION IN R CRB VARIABLES
HOLM	ALBERT V.	CSC	U. S.	CBFAH	HIGH RESOLUTION SPECTROSCOPY OF WHITE DWARF ACCRETING SYSTEMS
HOLM	ALBERT V.	CSC	U. S.	CVFAH	THE 1978 OUTBURST OF WZ SAGITTAE
HONEYCUTT	R. KENT	INDIANA	U. S.	LGFRH	CHROMOSPHERIC ACTIVITY, TIO STRENGTH AND SPECTRAL TYPES IN M GIANTS
HUCHRA	JOHN P.	CFA - SAO	U. S.	EGFJH	ULTRAVIOLET SPECTROPHOTOMETRY OF HOT GALAXIES
IMHOFF	CATHERINE L.	CSC	U. S.	STFCI	ULTRAVIOLET DATA ON YOUNG STARS RELEVANT TO THE EARTH'S EARLY ATMOSPHERE
IMHOFF	CATHERINE L.	CSC	U. S.	PMFCI	ULTRAVIOLET OBSERVATIONS OF THE ERUPTIVE PRE-MAIN SEQUENCE STAR FU ORIONIS

NASA APPROVED IUE PROGRAMS FOR THE SIXTH YEAR

NAME		INSTITUTION	COUNTRY	PROG ID
TITLE				
JENKINS	EDWARD B.	PRINCETON	U. S.	EHFEJ
LYMAN-ALPHA HALOS OF GALAXIES				
JOHNSON	HOLLIS R.	INDIANA	U. S.	CSFHJ
STUDIES OF THE ULTRAVIOLET SPECTRA OF CARBON STARS				
KAFATOS	MINAS	GEORGE MASON	U. S.	NJFMK
A HIGH RESOLUTION STUDY OF THE JET IN R AQUARII				
KAFATOS	MINAS	GEORGE MASON	U. S.	CDFMK
ULTRAVIOLET EXTINCTION IN SYMBIOTICS STARS				
KAFATOS	MINAS	GEORGE MASON	U. S.	ZAFMK
OBSERVATIONS OF PECULIAR UV EMISSION IN RX PUPPIS				
KALER	JAMES B.	ILLINOIS	U. S.	NPFJK
CENTRAL STARS OF LARGE PLANETARY NEBULAE				
KEEL	WILLIAM C.	AURA - KPNO	U. S.	WRFWK
WOLF-RAYET STARS IN NGC 5430				
KIRSHNER	ROBERT P.	MICHIGAN	U. S.	SNFRK
SUPERNOVA SPECTROSCOPY				
KONDO	YOJI	GSFC	U. S.	BLFYK
COORDINATED OBSERVATIONS OF BL LACERTAE OBJECTS IN SERVERAL WAVELENGTH REGIONS				
KRISS	GERARD A.	MICHIGAN	U. S.	QSFGK
HYDROGEN LINE RATIOS IN SEYFERT GALAXIES AND LOW REDSHIFT QUASARS				
LAMBERT	DAVID L.	TEXAS	U. S.	VVFDL
EPSILON AURIGAE IN ECLIPSE				
LIEBERT	JAMES W.	ARIZONA	U. S.	WDFJL
TWO COOL WHITE DWARFS WITH METALLIC LINES				
LINSKY	JEFFREY L.	COLORADO-JILA	U. S.	MLFJL
MASS LOSS RATES FOR K-M GIANTS AND SUPERGIANTS				
LINSKY	JEFFREY L.	COLORADO-JILA	U. S.	FKFJL
HIGH RESOLUTION SPECTROSCOPY OF TWO FK COMAE STARS				
LINSKY	JEFFREY L.	COLORADO-JILA	U. S.	TTFJL
HIGH DISPERSION STUDY OF TWO T TAURI STARS: RU LUPI AND COD-34 7151				

NASA APPROVED IUE PROGRAMS FOR THE SIXTH YEAR

NAME		INSTITUTION	COUNTRY	PROG ID	TITLE
LINSKY	JEFFREY L.	COLORADO-JILA	U. S.	AFFJL	THE ROTATION-ACTIVITY CORRELATIONS FOR EARLY F DWARFS
LINSKY	JEFFREY L.	COLORADO-JILA	U. S.	CSFJL	UV VARIABILITY AND ROTATIONAL MODULATION OF T TAURI STARS
LINSKY	JEFFREY L.	COLORADO-JILA	U. S.	RSFJL	SURFACE STRUCTURE OF ECLIPSING AND NON-ECLIPSING RS CVN SYSTEMS
LINSKY	JEFFREY L.	COLORADO-JILA	U. S.	LGFJL	HIGH DISPERSION STUDY OF LUMINOUS COOL STARS
LINSKY	JEFFREY L.	COLORADO-JILA	U. S.	CCFJL	AN EMISSION MEASURE ANALYSIS OF STARS NEAR THE TRANSITION REGION DIVIDING LINE
LINSKY	JEFFREY L.	COLORADO-JILA	U. S.	LDFJL	LYMAN ALPHA EMISSION FROM COOL DWARF STARS
MARAN	STEPHEN P.	GSFC	U. S.	NVFSM	TIME VARIATIONS IN YOUNG PLANTARY NEBULAE OF THE MAGELLANIC CLOUDS
MARGON	BRUCE	WASH.	U. S.	EHFBM	A SENSITIVE PROBE FOR AN EXTENDED GALAXIAN HALO
MARGON	BRUCE	WASH.	U. S.	HSFBM	THE NATURE OF THE UV EXCESS OBJECTS WITH MISSING H-ALPHA
MASSEY	PHILIP L.	DAO	CANADA	MLFPM	STELLAR WINDS IN M31 AND M33
MCCLUSKEY	GEORGE E.	LEHIGH	U. S.	IBFGM	IUE SPECTROSCOPY OF THE INTERACTING BINARY U SAGITTAE
MICHALITSIANOS	ANDREW G.	GSFC	U. S.	NJFAM	LOW DISPERSION UV OBSERVATIONS OF THE R AQUARII JET
MILLER	H. RICHARD	GEORGIA ST.	U. S.	QSFHM	IUE OBSERVATIONS OF ACTIVE GALACTIC NUCLEI
MILLER	JOSEPH S.	CAL S CRUZ	U. S.	EGFJM	ULTRAVIOLET SPECTROPHOTOMETRY OF "NORMAL" SPIRAL GALAXIES
MOORE	RICHARD L.	CIT	U. S.	QSFRM	UV/OPTICAL/IR SPECTROPOLARIMETRY OF LOW AND HIGH POLARIZATION QUASARS

NASA APPROVED IUE PROGRAMS FOR THE SIXTH YEAR

NAME		INSTITUTION	COUNTRY	PROG ID
TITLE				
MOORE	RICHARD L.	CIT	U. S.	EQFRM
UV/OPTICAL/IR SPECTROPOLARIMETRY OF LOW POLARIZATION QUASARS				
MOOS	H. WARREN	JOHNS HOPKINS	U. S.	SPFHM
STUDY OF ULTRAVIOLET EMISSIONS FROM SATURN, URANUS AND NEPTUNE				
MOOS	H. WARREN	JOHNS HOPKINS	U. S.	SJFHM
STUDY OF SPATIAL AND TEMPORAL VARIATIONS IN JOVIAN ULTRAVIOLET EMISSIONS				
MOOS	H. WARREN	JOHNS HOPKINS	U. S.	SIFHM
STUDY OF THE TORUS OF IO USING THE IUE				
MORRISON	NANCY D.	TOLEDO	U. S.	CSFNM
THE ULTRAVIOLET ENERGY DISTRIBUTION OF PHI CASSIOPEIAE				
MORRISON	NANCY D.	TOLEDO	U. S.	AFFNM
A-TYPE SUPERGIANTS: THREE UNIQUE SPECTRA				
MULLAN	DERMOTT J.	DELAWARE	U. S.	LGFDM
STATISTICS OF MASS LOSS FLUCTUATIONS IN COOL GIANTS				
NELSON	ROBERT M.	JPL	U. S.	SPFRN
UV SPECTROPHOTOMETRY OF THE GALILEAN SATELLITES, SATURNIAN SATELLITES & SELECTED ASTEROIDS				
NOUSEK	JOHN A.	PENN ST.	U. S.	WDFJN
BLUE SOFT X-RAY CANDIDATES				
NOUSEK	JOHN A.	PENN ST.	U. S.	CVFJN
NEWLY DISCOVERED AM HER SYSTEMS: E2003 + 223 AND E1405-451				
OKE	JOHN BEVERLY	CIT	U. S.	QSFJO
IUE OBSERVATIONS OF VARIABLE TYPE 1 SEYFERT GALAXIES				
OLIVERSEN	NANCY A.	CSC	U. S.	ZAFNO
THE GEOMETRIC STRUCTURE OF ECLIPSING SYMBIOTIC BINARIES				
PANEK	ROBERT J.	CSC	U. S.	IMFRP
UV STUDY OF GAS AND DUST IN ORION				
PANEK	ROBERT J.	CSC	U. S.	APFRP
VARIABILITY OF THE AP SI STARS				
PANEK	ROBERT J.	CSC	U. S.	CVFRP
OUTBURST RISE OF DWARF NOVAE				

NASA APPROVED IUE PROGRAMS FOR THE SIXTH YEAR

NAME		INSTITUTION	COUNTRY	PROG ID	TITLE
PARSONS	SIDNEY B.	GSFC	U. S.	HCFSP	MASS RATIOS OF BINARY STARS WITH LUMINOUS COOL PRIMARIES AND HOT SECONDARIES
PARSONS	SIDNEY B.	GSFC	U. S.	DCFSP	CHROMOSPHERES OF TYPE I AND TYPE II CEPHEIDS OF LONG PERIOD
PARSONS	SIDNEY B.	GSFC	U. S.	IBFSP	HD 207739 AND OTHER STRANGE F + B BINARY STARS
PATTERSON	JOSEPH	CFA - SAO	U. S.	CVFJP	ACCRETION DISK PARAMETERS IN CATACLYSMIC VARIABLES
PLAVEC	MIREK J.	CAL LA	U. S.	CBFMP	INTERACTING BINARY STARS OF THE W SERPENTIS TYPE
RAYMOND	JOHN C.	CFA - SAO	U. S.	NSFJR	DEEP EXPOSURES ON THE CYGNUS LOOP
RAYMOND	JOHN C.	CFA - SAO	U. S.	NFFJR	THE TRANSITION TO RADIATIVE SHOCKS IN THE CYGNUS LOOP
RAYMOND	JOHN C.	CFA - SAO	U. S.	IGFJR	WHITE DWARFS AND THE INTERSTELLAR MEDIUM
RAYMOND	JOHN C.	CFA - SAO	U. S.	XBFJR	HIGH DISPERSION STUDY OF HZ HECULIS
RAYMOND	JOHN C.	CFA - SAO	U. S.	CVFJR	DEVELOPMENT OF P CYGNI PROFILES IN DWARF NOVA OUTBURST
REICHERT	GAIL A.	GSFC	U. S.	XGFGR	ULTRAVIOLET STUDIES OF X-RAY SELECTED ACTIVE GALACTIC NUCLEI
RUDY	RICHARD J.	ARIZONA	U. S.	QSFRR	LYMAN ALPHA OBSERVATIONS OF SEYFERT 1.8 AND 1.9 GALAXIES
RUDY	RICHARD J.	ARIZONA	U. S.	RGFRR	HYDROGEN LINES AND FEII EMISSION IN BROAD-LINE RADIO GALAXIES
RUMPL	WILLIAM M.	CSC	U. S.	WRFWR	AN INVESTIGATION OF THE BINARY NATURE OF THE WOLF-RAYET STAR HD 50896
SARGENT	WALLACE L. W.	CIT	U. S.	QSFWS	COORDINATED OBSERVATIONS OF VARIABILITY IN BRIGHT SEYFERT 1 GALAXIES

NASA APPROVED IUE PROGRAMS FOR THE SIXTH YEAR

NAME		INSTITUTION	COUNTRY	PROG ID
TITLE				
SARGENT	WALLACE L. W.	CIT	U. S.	ESFWS
ULTRAVIOLET AND OPTICAL VARIABILITY IN BRIGHT SEYFERT 1 GALAXIES				
SARGENT	WALLACE L. W.	CIT	U. S.	EHFWS
LONG EXPOSURE OBSERVATIONS OF EXTRAGALACTIC OBJECTS				
SAVAGE	BLAIR D.	WISCONSIN	U. S.	EHFBS
CONTINUED STUDIES OF MAGELLANIC CLOUD HALO GAS				
SAVAGE	BLAIR D.	WISCONSIN	U. S.	HSFBS
AN INVESTIGATION OF GLOBAL SPECTRAL PECULIARITIES IN THE NGC 6231 MAIN SEQUENCE B STARS				
SAVAGE	BLAIR D.	WISCONSIN	U. S.	IGFBS
THE GALACTIC DISTRIBUTION OF HIGHLY IONIZED GAS				
SAVAGE	BLAIR D.	WISCONSIN	U. S.	GHFBS
INVESTIGATION OF MOTIONS IN THE GASEOUS GALACTIC HALO				
SAVAGE	BLAIR D.	WISCONSIN	U. S.	IEFBS
A STUDY OF EXTINCTION IN THE LARGE MAGELLANIC CLOUD				
SAVAGE	BLAIR D.	WISCONSIN	U. S.	OBFBS
CONTINUA AND EXTINCTION OF OB STARS IN CLUSTERS				
SCHWARTZ	RICHARD D.	MISSOURI-ST.L	U. S.	HHFRS
ULTRAVIOLET OBSERVATIONS OF LOW EXCITATION HERBIG-HARO OBJECTS				
SHAW	J. SCOTT	GEORGIA	U. S.	WDFJS
IUE OBSERVATIONS OF THE RS CVN - WHITE DWARF BINARY DH LEO				
SHIPMAN	HARRY L.	DELAWARE	U. S.	WDFHS
CARBON AND SILICON IN THE HELIUM WHITE DWARF GD 40				
SHORE	STEVEN N.	CASE W.R.	U. S.	HEFSS
SPECTROPHOTOMETRY OF HELIUM PECULIAR STARS				
SHULL	J. MICHAEL	COLORADO-JILA	U. S.	IGFJS
IUE INTERSTELLAR OBSERVATIONS				
SHULL	J. MICHAEL	COLORADO-JILA	U. S.	IMFJS
STELLAR AND INTERSTELLAR STUDIES WITH IUE ARCHIVES				
SHULL	J. MICHAEL	COLORADO-JILA	U. S.	HHFJS
IUE OBSERVATIONS OF HERBIG-HARO OBJECTS				

NASA APPROVED IUE PROGRAMS FOR THE SIXTH YEAR

NAME		INSTITUTION	COUNTRY	PROG ID
TITLE				
SIMON	THEODORE	HAWAII	U. S.	CCFTS
A STUDY OF YELLOW GIANTS IN THE HERTZSPRUNG GAP				
SIMON	THEODORE	HAWAII	U. S.	RSFTS
CHROMOSPHERIC ATIVITY AND BINARY INTERACTION IN 39 CETI				
SIMON	THEODORE	HAWAII	U. S.	STFTS
A STUDY OF TWO, YOUNG, SOLAR - TYPE STARS				
SION	EDWARD M.	VILLANOVA	U. S.	HSFES
HIGH RESOLUTION ULTRAVIOLET OBSERVATIONS OF HOT SUBDWARF B STARS				
SION	EDWARD M.	VILLANOVA	U. S.	HEFES
ULTRAVIOLET STUDIES OF THE VERY HOT, PULSATING HELIUM-RICH "PG1159" DEGENERATE STARS				
SION	EDWARD M.	VILLANOVA	U. S.	CVFES
CONTINUED ULTRAVIOLET STUDIES OF UX URSA MAJORIS STARS				
SITKO	MICHAEL L.	MINNESOTA	U. S.	QSFMS
MULTIFREQUENCY OBSERVATIONS OF STRONG 1-MM SOURCES				
SLETTEBAK	ARNE	OHIO ST.	U. S.	LBFAS
ULTRAVIOLET OBSERVATIONS OF BRIGHT LAMBDA BOOTIS STARS				
SNOW	THEODORE P.,JR	COLORADO-LASP	U. S.	BEFTS
A SURVEY OF VARIABILITY IN BE STARS				
SNOW	THEODORE P.,JR	COLORADO-LASP	U. S.	HSFTS
A STUDY OF MODERATE IONIZATION IN BE STAR WINDS				
SNOW	THEODORE P.,JR	COLORADO-LASP	U. S.	IMFTS
INTERSTELLAR LINES AND ULTRAVIOLET EXTINCTION IN DARK CLOUDS				
SNOW	THEODORE P.,JR	COLORADO-LASP	U. S.	OBFTS
STELLAR WINDS IN B AND BE STARS				
SODERBLOM	DAVID R.	CFA - SAO	U. S.	CCFDS
ULTRAVIOLET STUDIES OF STARS IN A PLEIADES MOVING GROUP				
SODERBLOM	DAVID R.	CFA - SAO	U. S.	LDFDS
ROTATIONAL PERIODS OF ALPHA CENTAURI A AND B				
SONNEBORN	GEORGE	CSC	U. S.	OBFGS
ROTATIONAL BROADENING OF PHOTOSPHERIC LINES IN MAIN-SEQUENCE B STARS				

NASA APPROVED IUE PROGRAMS FOR THE SIXTH YEAR

NAME / TITLE		INSTITUTION	COUNTRY	PROG ID
STARRFIELD	SUMNER G.	ARIZONA ST.	U. S.	CVFSS
ULTRAVIOLET OBSERVATIONS OF GALACTIC NOVAE IN OUTBURST				
STONER	RONALD E.	BOWLING GREEN	U. S.	QSFRS
ANALYSIS OF TIME VARIABILITY OF EMISSION LINES IN SEYFERT 1 GALAXIES AS FOUND IN IUE DATA				
STURCH	CONRAD R.	CSC	U. S.	DCFCS
ULTRAVIOLET OBSERVATIONS OF THREE DWARF CEPHEIDS				
SZKODY	PAULA	WASH.	U. S.	CBFPS
A STUDY OF 4 NEW AM HER VARIABLES				
SZKODY	PAULA	WASH.	U. S.	CVFPS
EXTENDED OUTBURST/HIGH EXCITATION CATACLYSMIC VARIABLES				
SZKODY	PAULA	WASH.	U. S.	ZAFPS
A STUDY OF THE ORBITAL VARIABILITY OF Z CAM				
TORRES-PEIMBERT	SILVIA	U.N.A. DE MEX	MEXICO	NPFST
HIGH DISPERSION UV SPECTROSCOPY OF THE PLANETARY NEBULA NGC 3918				
TREMAINE	SCOTT D.	MIT	U. S.	GHFST
THE EXTENT OF A HOT GASEOUS GALACTIC HALO				
TURNSHEK	DAVID A.	PITTSBURGH	U. S.	QSFDT
LYMAN CONTINUUM OBSERVATIONS OF BROAD ABSORPTION LINE QSOS				
UNDERHILL	ANNE B.	GSFC	U. S.	SGFAU
SPOTTED SURFACES ON LUMINOUS EARLY-TYPE STARS				
WALDRON	WAYNE	DELAWARE	U. S.	CCFWW
CORONAL EFFECTS ON THE WINDS OF EARLY TYPE STARS				
WEEDMAN	DANIEL W.	PENN ST.	U. S.	QSFDW
STAR FORMATION IN NGC 1068				
WEGNER	GARY A.	DARTMOUTH	U. S.	WDFGW
A SEARCH FOR METAL LINES IN THE ULTRAVIOLET SPECTRA OF WHITE DWARFS				
WILLS	BEVERLEY J.	TEXAS	U. S.	QSFBW
THE CONTINUUM ENERGY DISTRIBUTIONS OF INTERMEDIATE REDSHIFT QUASARS				
WING	ROBERT F.	OHIO ST.	U. S.	CSFRW
A SEARCH FOR MOLECULAR ABSORPTION FEATURES IN THE PHOTOSPHERIC SPECTRA OF COOL STARS				

NASA APPROVED IUE PROGRAMS FOR THE SIXTH YEAR

NAME		INSTITUTION	COUNTRY	PROG ID
TITLE				
WOOTTEN	H. ALWYN	NRAD	U. S.	NPFHW
INVESTIGATION OF NEUTRAL CIRCUMNEBULAR MATERIAL IN PLANETARY NEBULAE				
WORDEN	SIMON P.	AIR FORCE SP.	U. S.	CCFSW
COORDINATED MAGNETIC AND CHROMOSPHERIC/CORONAL SYNOPTIC OBSERVATIONS				
WORRALL	DIANA M.	CAL SAN DIEGO	U. S.	BLFDW
COORDINATED MULTIFREQUENCY OBSERVATIONS OF VARIABLE AGNS				
WU	CHI-CHAO	CSC	U. S.	NSFCW
ULTRAVIOLET OBSERVATIONS OF THE BLUE STAR PROJECTED IN THE REMNANT OF SUPERNOVA AD1006				
WU	CHI-CHAO	CSC	U. S.	CVFCW
TARGET OF OPPORTUNITY OBSERVATIONS OF NOVA AND X-RAY NOVA				
WU	CHI-CHAO	CSC	U. S.	HSFCW
PHOTOMETRIC STANDARDS FOR SPACE TELESCOPE INSTRUMENTS				
WU	CHI-CHAO	CSC	U. S.	MLFCW
SHORT TIME VARIATIONS IN THE MASS-LOSS RATE OF EARLY TYPE STARS				
WU	CHI-CHAO	CSC	U. S.	QSFCW
UV OBSERVATIONS OF LOW REDSHIFT QUASARS				
YORK	DONALD G.	CHICAGO	U. S.	IGFDY
DISTANCES OF 21 CM HIGH VELOCITY (OORT) CLOUDS				
YORK	DONALD G.	CHICAGO	U. S.	EHFDY
ABSORPTION MEASURE OF GAS IN GALACTIC HALOS				
ZINN	ROBERT	YALE	U. S.	GCFRZ
INTEGRATED SPECTRA OF GLOBULAR CLUSTERS IN M31 AND THE FORNAX DWARF GALAXY				
ZOLCINSKI	MARIE-CHRISTIN	W CONNECTICUT	U. S.	CCFMZ
IUE SURVEY OF HYADES STARS, PART IV: THE K AND M DWARFS				

VILSPA Log of Images

01 Apr 82 - 30 Apr 82

and

01 Oct 82 - 01 Feb 83

PROGRAMME REFERENCE NUMBERS FOR THE PROGRAMME IDENTIFICATION IN THIS LISTING CAN BE FOUND IN I U E E S A NEWSLETTER NO. 13 (JUNE 1982), PAGE 43.

CLASSIFICATION OF OBJECTS USED IN THE JOINT ESA/SRC LOG OF IUE OBSERVATIONS
****

00 SUN
01 EARTH
02 MOON
03 PLANET
04 PLANETARY SATELLITE
05 MINOR PLANET
06 COMET
07 INTERPLANETARY MEDIUM
08
09

10 W C
11 W N
12 MAIN SEQUENCE O
13 SUPERGIANT O
14 OE
15 OF
16 SD O
17 WD O
18
19 UV-STRONG

20 B0-B2 V-IV
21 B3-B5 V-IV
22 B6-B9.5 V-IV
23 B0-B2 III-I
24 B3-B5 III-I
25 B6-B9.5 III-I
26 BE
27 BP
28 SDB
29 WDB

30 A0-A3 V-IV
31 A4-A9 V-IV
32 A0-A3 III-I
33 A4-A9 III-I
34 AE
35 AM
36 AP
37 WDA
38
39 COMPOSITE

40 F0-F2
41 F3-F9
42 FP
43 LATE TYPE DEGENERATE STARS
44 G (TO 1FEB79); GIV-VI (FROM 1FEB79)
45 G I-II (FROM 1FEB79)
46 K (TO 1FEB79); K IV-VI (FROM 1FEB79)
47 K I-III (FROM 1FEB79)
48 M (TO 1FEB79); M DWARFS (FM 1FEB79)
49 M I-III (FROM 1FEB79)

50 R,N OR S TYPES
51 LONG PERIOD VARIABLE STARS
52 IRREGULAR VARIABLES
53 REGULAR VARIABLES
54 DWARF NOVAE
55 CLASSICAL NOVAE
56 SUPERNOVAE
57 SYMBIOTIC STARS
58 T TAURI
59 X-RAY

60 SHELL STAR
61 ETA CARINAE
62 PULSAR
63 NOVA-LIKE
64 STELLAR OBJECT NOT INCLUDED ABOVE
65
66
67
68
69

70 PLANETARY NEBULA + CENTRAL STAR
71 PLANETARY NEBULA - CENTRAL STAR
72 H II REGION
73 REFLECTION NEBULA
74 DARK CLOUD (ABSORTION SPECTRUM)
75 SUPERNOVA REMNANT
76 RING NEBULA (SHOCK IONISED)
77
78
79

80 SPIRAL GALAXY
81 ELLIPTICAL GALAXY
82 IRREGULAR GALAXY
83 GLOBULAR CLUSTER
84 SEYFERT GALAXY
85 QUASAR
86 RADIO GALAXY
87 BL LACERTAE OBJECT
88 EMISSION LINE GALAXY (NON-SEYFERT)
89

90 INTERGALACTIC MEDIUM
91
92
93
94
95
96
97
98 WAVELENGTH CALIBRATION (NASA LOG)
99 NULLS AND FLAT FIELDS (NASA LOG)

THE CLASSIFICATION IS SUPPLIED BY D STICKLAND FOR USE ONLY WITHIN THE PROJECT

EXPOSURE CLASSIFICATION CODES
****

SINCE 1 AUG 78 A TWO-DIGIT CODE HAS BEEN USED TO DESCRIBE EXPOSURE LEVELS. THIS CODE OCCUPIES THE FIRST TWO CHARACTER POSITIONS OF THE COMMENT FIELD.

DIGIT 1: EXPOSURE LEVEL OF CONTINUUM
DIGIT 2: EXPOSURE LEVEL OF EMISSION LINES

THE CLASSIFICATIONS BELOW APPLY TO BOTH:

0: NOT APPLICABLE
1: NO SPECTRUM VISIBLE
2: FAINT SPECTRUM; MAX DN < 20 ABOVE BACKGROUND
3: UNDEREXPOSED: MAX DN < 100 ABOVE BACKGROUND
4: WEAK: MAX DN BETWEEN 100 AND 150 ABOVE BACKGROUND
5: GOOD: NO SATURATION BUT MAX DN OVER 150 ABOVE BACKGROUND
6: A BIT STRONG: A FEW PIXELS SATURATED
7: SATURATED FOR LESS THAN HALF THE SPECTRUM
8: MOSTLY SATURATED BUT SOME PARTS USABLE
9: COMPLETELY SATURATED

ON 1 SEP 79 A FURTHER DIGIT WAS ADDED TO DESCRIBE THE LEVEL OF THE BACKGROUND. THE MEAN DN GIVEN BY A SUBSET HISTOGRAM OF WIDTH 2 PIXELS BETWEEN:

SWP 550,130 AND 685,310
AND LWR 160,195 AND 90,300

HAS BEEN CODED AS FOLLOWS: (LIMITS INCLUSIVE)

0 DN<20
1 21<DN<30
2 31<DN<40
3 41<DN<50
4 50<DN<60
5 60<DN70
6 71<DN<80
7 80<DN<90
8 91<DN<100
9 DN>101
X SATURATED

OBJECT	CL	MAG	R.A.	DEC	D	C	IMAGE	A	DATE	EXPOSURE TIME	PRO	ECC
47 TUC	16	10.30	00 21 54	-72 21	L	3	16855	L 0	82APR29	07:29:00 0016:00	EA170	402
47 TUC	16	10.30	00 21 54	-72 21	L	2	13101	L 0	82APR29	06:39:00 0016:00	EA170	502
0045-735	22	13.10	00 45 05	-73 25	L	3	16699	L 0	82APR06	07:12:00 0075:00	EM210	400
0045-735	22	13.10	00 45 05	-73 25	L	2	12964	L 0	82APR06	06:09:00 0060:00	EM210	503
0046-735	22	14.40	00 46 24	-73 27	L	2	12965	L 0	82APR06	08:57:00 0046:00	EM210	202
0046-735	22	14.40	00 46 24	-73 27	L	2	12972	L 0	82APR07	03:05:00 0150:00	EM210	305
0048-737	21	11.10	00 48 49	-73 44	L	2	12973	L 0	82APR07	06:29:00 0008:00	EM210	602
0048-737	21	11.10	00 48 49	-73 44	L	3	16707	L 0	82APR07	06:16:00 0010:00	EM210	500
0052-730	22	12.25	00 52 20	-73 02	L	2	12963	L 0	82APR06	03:50:00 0040:00	EM210	603
0052-730	22	12.30	00 52 20	-73 02	L	3	16698	L 0	82APR06	04:35:00 0050:00	EM210	500
HD 5394	20	02.60	00 53 40	+60 27	H	3	16694	S 0	82APR05	06:36:00 0000:11	EA080	501
NGC 416	83	11.40	01 06 38	-72 37	L	3	16747	L 0	82APR11	02:58:00 0408:00	GLOBC	304
HD 18352	20	07.00	02 55 49	+61 05	H	3	16708	L 0	82APR07	08:06:00 0100:00	EM210	701
0312-770	85	15.90	03 12 56	-77 03	L	3	16816	L 0	82APR23	02:41:00 0425:00	UK427	343
NGC 1466	83	11.60	03 44 48	-71 50	L	3	16686	L 0	82APR03	02:35:00 0432:00	GLOBC	203
SK-70 36	59	13.20	05 01 39	-70 38	L	3	16740	L 0	82APR10	03:33:00 0065:00	EI108	501
SK-70 36	59	13.20	05 01 39	-70 38	L	2	12998	L 0	82APR10	02:33:00 0055:00	EI108	504
SK-70 36	59	13.20	05 01 39	-70 38	L	2	12981	L 0	82APR08	04:50:00 0055:00	EI108	503
SK-70 36	59	13.20	05 01 39	-70 38	L	3	16718	L 0	82APR08	03:23:00 0065:00	EI108	501
HD 32630	21	03.30	05 03 00	+41 10	L	1	01514	L 0	82APR05	05:53:00 0000:01	PHCAL	502
HD 34816	20	04.30	05 17 16	-13 14	L	1	01512	L 0	82APR05	04:30:00 0000:01	PHCAL	502
HD38666	00	00.00	05 17 16	-13 13	H	1	01511	L 0	82APR05	03:20:32 0000:41	PHCAL	503
HD34816	00	00.00	05 17 16	-13 13	H	1	01513	L 0	82APR05	05:04:35 0000:20	PHCAL	502
0537-441	85	14.00	05 37 21	-44 07	L	3	16829	L 0	82APR25	03:05:00 0402:00	UK370	203
LMC X-1	59	14.50	05 40 05	-69 46	L	2	12999	L 0	82APR10	05:02:00 0135:00	EI108	405
LMC X-1	59	14.50	05 40 05	-69 46	L	3	16741	L 0	82APR10	07:21:00 0145:00	EI108	301
LMC X-1	59	14.50	05 40 05	-69 46	L	3	16719	L 0	82APR08	06:36:00 0191:00	EI108	402
HD 38666	12	05.20	05 44 08	-32 19	L	1	01510	L 0	82APR05	02:47:00 0002:32	PHCAL	502
LWP1509	00	00.00	05 44 08	-32 19	H	1	01509		82APR01		PHCAL	
R MON	44	00.90	06 36 26	+08 47	L	2	13006	L 0	82APR12	02:31:00 0140:00	EC223	342
R MON	44	00.90	06 36 26	+08 47	L	3	16749	L 0	82APR12	04:54:00 0180:00	EC223	201
NGC 2261	73	00.00	06 36 26	+08 47	L	2	13007	L 0	82APR12	08:06:00 0087:00	EC223	202
HD 63032	47	03.60	07 43 28	-37 51	L	2	12925	L 0	82APR01	02:34:00 0015:00	EC140	702
HD 63032	47	03.60	07 43 28	-37 51	L	3	16675	S 0	82APR01	03:19:14 0015:00	EC140	401
HD 63032	47	03.60	07 43 28	-37 51	L	3	16675	L 0	82APR01	02:57:09 0015:00	EC140	601
04.40129	47	01.90	08 21 29	-59 21	H	2	12926	L 0	82APR01	04:32:00 0001:00	EC140	552
HD 71129	47	01.90	08 21 29	-59 21	H	3	16676	L 0	82APR01	04:36:00 0001:00	EC140	551
1004+130	85	14.00	10 04 45	+13 04	L	3	16824	L 0	82APR24	03:36:00 0371:00	UK427	333
NGC 4125	81	12.00	12 05 42	+65 27	L	2	13025	L 0	82APR15	02:42:00 0420:00	EE184	308
MK 198	84	14.50	12 06 43	+47 20	L	3	16842	L 0	82APR27	02:57:00 0410:00	UK370	224

OBJECT	CL	MAG	R.A.	DEC	D	C	IMAGE	A	DATE	EXPOSURE	TIME	PRO	ECC
3C 273	85	12.90	12 26 33	+02 20	H	3	16786	L 0	82APR18	02:04:00	0792:00	UK447	339
3C 273	85	12.90	12 26 33	+02 20	H	3	16791	L 0	82APR19	01:25:00	0825:00	UK447	339
HD109551	47	04.90	12 32 38	+70 18	H	2	12928	L 0	82APR01	09:20:00	0023:00	EC140	331
HD109551	47	04.90	12 32 38	+70 18	H	2	12927	L 0	82APR01	06:41:00	0030:00	EC140	332
HD109551	47	04.90	12 32 38	+70 18	L	3	16678	L 0	82APR01	07:17:00	0120:00	EC140	701
NGC 4889	81	14.00	12 57 44	+28 15	L	1	01524	L 0	82APR16	03:18:00	0368:00	EE184	203
ETA UMA	21	01.80	13 45 34	+49 34	H	1	01531	L 0	82APR20	07:55:00	0000:06	PHCAL	603
HD124448	21	10.00	14 11 47	-46 03	H	3	16782	L 0	82APR17	03:07:00	0270:00	EA015	512
HD124448	21	10.00	14 11 47	-46 03	H	2	13036	L 0	82APR17	07:41:00	0124:00	EA015	413
HD135345	45	05.20	15 12 46	-41 18	H	3	16677	L 0	82APR01	05:20:00	0030:00	EC140	501
+33 2642	20	10.80	15 50 01	+33 05	L	1	01525	L 0	82APR20	03:15:00	0003:00	PHCAL	503
+33 2642	20	10.80	15 50 01	+33 05	L	1	01526	L 0	82APR20	03:46:00	0004:00	PHCAL	603
HD143454	57	09.80	15 57 25	+26 04	H	1	01536	L 0	82APR30	03:18:00	0307:00	PHCAL	036
NGC 6254	16	13.40	16 54 30	-04 02	L	2	13100	L 0	82APR29	03:09:00	0090:00	EA170	603
NGC 6254	16	13.40	16 54 30	-04 02	L	3	16854	L 0	82APR29	04:44:00	0060:00	EA170	502
HD155763	25	03.50	17 08 38	+65 47	H	1	01533	L 0	82APR20	09:00:00	0000:25	PHCAL	402
HD155763	25	03.50	17 08 38	+65 47	H	1	01532	L 0	82APR20	08:33:00	0000:25	PHCAL	400
HD157451	10	10.60	17 21 47	-43 27	H	3	16835	L 0	82APR26	03:18:00	0389:00	EA093	243
ROB 162	16	13.30	17 36 48	-53 39	L	2	13092	L 0	82APR28	03:01:00	0008:00	EA170	302
ROB 162	16	13.30	17 36 48	-53 39	L	3	16846	L 0	82APR28	03:13:00	0393:00	EA170	303
HD164284	20	04.80	17 57 47	+04 22	H	3	16697	S 0	82APR05	09:30:00	0004:30	EA080	701
NGC 6626	16	14.00	18 33 18	-23 58	L	2	13102	L 0	82APR29	09:08:00	0028:00	EA170	002
NVA AQUI	55	13.00	19 20 50	-02 24	L	3	16730	L 0	82APR09	08:13:00	0094:00	VILSP	231
NVA AQUI	55	13.00	19 20 50	-02 24	L	3	16729	L 0	82APR09	02:52:00	0180:00	VILSP	242
NVA AQUI	55	13.00	19 20 50	-02 24	L	2	12990	L 0	82APR09	06:10:00	0120:00	VILSP	340
NVA AQUI	55	13.00	19 20 50	-02 24	L	2	13063	L 0	82APR22	06:56:00	0167:00	VILSP	105
NVA AQUI	55	13.00	19 20 50	-02 24	L	3	16811	L 0	82APR22	02:44:00	0240:00	VILSP	151
HM SGE	57	11.00	19 39 41	+16 38	H	3	16754	L 0	82APR13	06:25:00	0050:00	EI127	130
HM SGE	57	11.00	19 39 41	+16 38	H	2	13014	L 0	82APR13	07:35:00	0128:00	EI127	264
HM SGE	57	11.00	19 39 41	+16 38	L	2	13013	L 0	82APR13	05:19:00	0060:00	EI127	483
HM SGE	57	11.00	19 39 41	+16 38	L	3	16753	L 0	82APR13	04:01:00	0075:00	EI127	380
HM SGE	57	11.00	19 39 41	+16 38	L	3	16752	L 0	82APR13	03:01:00	0015:00	EI127	260
HM SGE	57	11.00	19 39 41	+16 38	L	2	13012	S 0	82APR13			EI127	363
HM SGE	57	11.00	19 39 41	+16 38	L	2	13012	L 0	82APR13			EI127	233
HBV 475	57	13.00	20 49 03	+35 24	L	3	16760	L 0	82APR14	02:49:00	0050:00	EI167	140
HBV 475	57	13.00	20 49 03	+35 24	L	2	13020	L 0	82APR14	03:43:00	0065:00	EI167	353
HBV 475	57	13.00	20 49 03	+35 24	H	3	16761	L 0	82APR14	08:48:30	0000:02	EI167	132
HD200120	20	04.70	20 58 07	+47 20	L	3	16696	S 0	82APR05	08:45:13	0000:01	EA080	501
HD200120	20	04.70	20 58 07	+47 20	L	3	16696	L 0	82APR05	08:48:30	0000:02	EA080	501

OBJECT	CL	MAG	R.A.	DEC	D	C	IMAGE	A	DATE	EXPOSURE TIME	PRO	ECC
HD200120	20	04.70	20 58 07	+47 20	L	2	12952	S 0	82APR05	08:51:33 0000:01	EA080	402
HD200120	20	04.70	20 58 07	+47 20	L	2	12952	L 0	82APR05	08:54:35 0000:02	EA080	502
HD200120	20	04.70	20 58 07	+47 20	H	3	16695	L 0	82APR05	07:46:00 0001:30	EA080	501
HD200120	20	04.70	20 58 07	+47 20	H	2	12951	L 0	82APR05	07:42:00 0001:30	EA080	502
+28 4211	16	10.50	21 48 56	+28 38	L	1	01530	L 0	82APR20	06:48:00 0003:01	PHCAL	403
+28 4211	16	10.50	21 48 56	+28 38	L	1	01529	S 0	82APR20		PHCAL	503
+28 4211	16	10.50	21 48 56	+28 38	L	1	01529	L 0	82APR20		PHCAL	703
HD214680	13	04.90	22 37 01	+38 47	H	1	01528	L 0	82APR20	05:09:00 0000:36	PHCAL	402
HD214680	13	04.90	22 37 01	+38 47	L	1	01527	L 0	82APR20	04:37:00 0000:02	PHCAL	503

++

CALUV60%	00	00.00	00 00 00	+00 00	L	1	01724		82NOV15	16:46:47 0002:04	PHCAL	
NULL	00	00.00	00 00 00	+00 00	L	1	01728		82NOV15		PHCAL	
CALUV120%	00	00.00	00 00 00	+00 00	L	1	01723		82NOV15	16:09:54 0004:08	PHCAL	
NULL	00	00.00	00 00 00	+00 00	L	1	01729		82NOV15		PHCAL	
NULL	00	00.00	00 00 00	+00 00	L	2	14636		82NOV15		PHCAL	
NULLIMAGE	00	00.00	00 00 00	+00 00	L	2	14802		82DEC07		EE049	
ULL2NDREA	00	00.00	00 00 00	+00 00	L	1	01727		82NOV15		PHCAL	
CALUV20%	00	00.00	00 00 00	+00 00	L	1	01722		82NOV15	15:36:13 0000:41	PHCAL	
NULL	00	00.00	00 00 00	+00 00	H	2	14888	L 0	82DEC24		PHCAL	
CALUV60%	00	00.00	00 00 00	+00 00	L	1	01721		82NOV15	15:01:16 0002:04	PHCAL	
NULL	00	00.00	00 00 00	+00 00		1	01707		82NOV08		EE255	
NULL	00	00.00	00 00 00	+00 00	L	1	01720		82NOV15		PHCAL	
CALVU160%	00	00.00	00 00 00	+00 00	L	1	01726		82NOV15	18:00:29 0005:31	PHCAL	
FLOOD1005	00	00.00	00 00 00	+00 00	L	1	01725		82NOV15	17:18:28 0001:40	PHCAL	
NULLREAD	00	00.00	00 00 00	+00 00		2	14632		82NOV15		PHCAL	
NULL	00	00.00	00 00 00	+00 00	L	2	14635		82NOV15		PHCAL	
FLOOD100%	00	00.00	00 00 00	+00 00	L	2	14634		82NOV15	13:19:59 0000:22	PHCAL	
60%CALUV	00	00.00	00 00 00	+00 00	L	2	14633		82NOV15	12:54:51 0001:51	PHCAL	
MRK335	84	13.80	00 03 45	+19 55	L	3	18463	L 0	82NOV03	16:37:53 0040:00	EE231	351
MRK335	84	13.80	00 03 45	+19 55	L	3	18462	L 0	82NOV03	13:13:58 0045:00	EE231	351
MRK335	84	13.80	00 03 45	+19 55	L	2	14555	L 0	82NOV03	17:23:00 0100:00	EE231	554
MRK335	84	13.80	00 03 45	+19 55	L	2	14554	L 0	82NOV03	14:04:57 0160:00	EE231	664
MRK335	84	13.80	00 03 45	+19 55	L	3	18464	L 0	82NOV03	19:14:12 0030:00	EE231	351
NGC40	70	11.00	00 10 16	+72 14	H	3	19081	L 0	83JAN25	12:11:46 0180:00	EA165	331
NGC40	70	11.00	00 10 16	+72 14	L	2	15104	S 0	83JAN25	15:18:55 0016:00	EA165	222
NGC40	70	11.00	00 10 16	+72 14	L	2	15104	L 0	83JAN25	15:39:47 0008:00	EA165	342
AKN120	84	09.93	00 13 37	-00 12	L	2	15056	L 0	83JAN15	12:13:38 0095:00	SEYFE	551
S00014+81	85	16.50	00 14 04	+81 18	L	3	18728	L 0	82DEC04	10:49:28 0418:00	EE159	002
HD2151	44	02.69	00 23 09	-77 32	H	2	14929	L 0	82DEC27	10:33:29 0015:00	EC004	752
HD2151	44	02.66	00 23 09	-77 32	H	2	14930	L 0	82DEC27	11:13:07 0015:00	EC004	752

OBJECT	CL	MAG	R.A.	DEC	D	C	IMAGE	A		DATE	EXPOSURE TIME		PRO	ECC
HD2151	44	02.68	00 23 09	-77 32	H	2	14931	L	0	82DEC27	11:56:32	0015:00	EC004	752
HD2151	44	02.69	00 23 09	-77 32	H	2	14933	L	0	82DEC27	13:15:06	0015:00	EC004	752
HD2151	44	02.69	00 23 09	-77 32	H	2	14932	L	0	82DEC27	12:35:48	0015:00	EC004	752
HD2665	45	07.60	00 27 58	+56 47	L	2	14879	S	0	82DEC23	11:42:25	0012:00	EC067	402
HD2665	45	07.60	00 27 58	+56 47	L	2	14879	L	0	82DEC23	11:59:35	0015:00	EC067	602
HD2665	45	07.60	00 27 58	+56 47	L	3	18871	L	0	82DEC23	10:23:58	0075:00	EC067	201
RTSCL	66	10.50	00 33 59	-25 56	L	3	18331	L	0	82OCT19	18:08:25	0024:00	EI073	301
RTSCL	66	10.50	00 33 59	-25 56	L	2	14443	L	0	82OCT19	19:26:53	0038:00	EI073	
SB290	20	10.30	00 40 30	-38 24	H	2	14450	L	0	82OCT20	18:22:23	0101:00	EA115	500
SB290	20	10.30	00 40 30	-38 24	H	3	18341	L	0	82OCT20	20:06:29	0101:00	EA115	401
SB290	28	10.30	00 40 30	-38 24	H	2	14464	L	0	82OCT22	18:47:51	0082:00	EA115	403
AF-AND	52	14.50	00 40 48	+40 55	L	2	14756	L	0	82NOV30	13:53:44	0316:00	EA007	203
M31	52	14.50	00 40 48	+40 55	L	3	18689	L	0	82NOV29	13:15:58	0391:00	EA007	303
SK7	24	12.66	00 44 00	-73 56	L	2	14964	L	0	82DEC30	16:58:26	0035:00	EM129	503
AV-126	23	13.50	00 50 46	-72 55	L	2	14947	L	0	82DEC29	11:38:28	0060:00	EM129	501
AV-126	23	13.50	00 50 46	-72 55	L	3	18908	L	0	82DEC29	12:42:33	0100:00	EM129	501
HD5394	26	02.20	00 53 40	+60 26	H	3	19097	L	0	83JAN27	12:17:15	0000:08	EA080	511
HD5448	30	04.00	00 53 58	+38 13	H	3	18569	L	0	82NOV16	13:35:31	0010:00	EA115	500
HD5448	40	04.00	00 53 58	+38 13	H	2	14644	L	0	82NOV16	13:07:34	0005:00	EA115	502
HD5448	30	04.00	00 53 58	+38 13	L	2	14643	S	0	82NOV16	12:31:54	0000:07	EA115	402
HD5448	30	04.00	00 53 58	+38 13	L	2	14643	L	0	82NOV16	12:29:10	0000:07	EA115	602
HD5448	30	04.00	00 53 58	+28 13	H	3	18568	S	0	82NOV16	12:37:49	0000:30	EA115	500
HD5448	30	04.00	00 53 58	+28 13	H	3	18568	L	0	82NOV16	12:34:55	0000:09	EA115	500
SK76	23	12.80	00 57 16	-72 48	L	3	18910	L	0	82DEC29	17:10:24	0040:00	EM129	501
SK76	23	12.80	00 57 16	-72 48	L	2	14949	L	0	82DEC29	16:39:35	0020:00	EM129	501
AV398	23	13.85	01 04 35	-72 12	L	2	14963	L	0	82DEC30	11:00:49	0110:00	EM129	505
AV398	23	13.85	01 04 35	-72 12	L	3	18911	L	0	82DEC30	12:53:19	0220:00	EM129	401
HD6582	44	05.90	01 04 55	+54 40	L	2	15138	S	0	83JAN28	12:43:48	0001:00	STAND	552
HD6582	44	05.90	01 04 55	+54 40	L	2	15138	L	0	83JAN28	12:40:18	0001:00	STAND	562
HD6961	31	04.50	01 08 02	+54 53	L	3	18684	L	0	82NOV28		0000:20	STAND	500
OL0109-38	84	14.40	01 09 09	-38 20	L	3	18374	L	0	82OCT23	15:31:36	0375:00	EE258	232
OL0109-38	84	00.00	01 09 09	-38 20	L	2	14469	L	0	82OCT23	15:31:36	0375:00	EE258	118
SK142	23	13.50	01 09 15	-72 58	L	3	18909	L	0	82DEC29	15:16:56	0060:00	EM129	501
SK142	23	13.70	01 09 15	-72 58	L	2	14948	L	0	82DEC29	14:42:28	0025:00	EM129	401
MKN1152	84	15.00	01 11 21	-15 06	L	3	18956	L	0	83JAN06	12:48:27	0174:00	EE266	231
FAIRAL9	84	13.20	01 21 51	-59 03	L	3	18506	L	0	82NOV08	13:57:52	0050:00	EE255	361
FAIRAL9	84	13.20	01 21 51	-59 03	L	2	14585	L	0	82NOV08	13:04:24	0050:00	EE255	442
NULL	00	00.00	01 30 33	+30 41		1	01717			82NOV11			EA007	
NULL	00	00.00	01 31 21	+30 19	L	2	14604			82NOV11			EA007	

OBJECT	CL	MAG	R.A.	DEC	D	C	IMAGE	A		DATE	EXPOSURE TIME	PRO	ECC
M33VAR83	53	14.30	01 31 21	+30 19	L	1	01718	L	0	82NOV11	13:28:34 0365:00	EA007	402
				+									
HD13267	24	05.79	02 07 58	+57 24	L	3	18887	S	0	82DEC25	14:53:47 0005:00	STAN1	700
HD13267	24	05.79	02 07 58	+57 24	L	3	18887	L	0	82DEC25	15:04:34 0005:33	STAN1	600
HD13267	24	05.87	02 07 58	+57 24	L	2	14906	S	0	82DEC25	15:20:58 0001:00	STAN1	502
HD13267	24	05.87	02 07 58	+57 24	L	2	14906	L	0	82DEC25	15:25:09 0001:25	STAN1	
													502
HD13841	23	07.39	02 13 15	+56 47	H	3	18512	L	0	82NOV09	15:12:20 0125:00	EM236	501
HD13866	23	07.49	02 13 27	+56 29	H	3	18513	L	0	82NOV09	17:55:02 0112:00	EM236	501
HD14422	29	08.50	02 18 17	+57 09	L	2	14769	L	0	82DEC02	17:22:09 0006:20	EI189	602
HD14443A	23	08.50	02 18 27	+56 55	L	2	14766	S	0	82DEC02	13:07:58 0007:00	EI189	402
HD14443A	23	00.00	02 18 27	+56 55	L	2	14766	L	0	82DEC02	13:17:50 0007:00	EI189	702
HD14443	23	08.40	02 18 27	+56 55	L	2	14767	S	0	82DEC02	14:05:05 0006:00	EI189	702
HD14443	23	08.40	02 18 27	+56 55	L	2	14767	L	0	82DEC02	14:15:02 0006:00	EI189	802
HD14443	23	08.40	02 18 27	+56 55	L	3	18706	L	0	82DEC02	14:24:22 0004:00	EI189	500
HD14520	29	09.20	02 19 10	+56 51	L	2	14768	S	0	82DEC02	15:10:51 0028:00	EI189	703
HD14520	29	09.20	02 19 10	+56 51	L	2	14768	L	0	82DEC02	15:43:48 0021:00	EI189	80
HD14520	29	09.20	02 19 10	+56 51	L	3	18707	L	0	82DEC02	16:09:18 0025:00	EI189	800
3C66B	86	13.00	02 20 02	+42 45	L	3	18698	L	0	82DEC01	11:40:28 0355:00	PS614	203
NGC1068	84	13.60	02 40 06	-00 13	L	2	14543	L	0	82NOV01	18:28:51 0064:00	EE255	303
NGC1068	84	13.70	02 40 07	-00 13	L	3	18508	L	0	82NOV08	19:22:15 0023:00	EE255	240
NULL	84	00.00	02 40 07	-00 13	L	2	14586	L	0	82NOV08	18:46:32 0023:00	EE255	
NGC1068	84	13.70	02 40 07	-00 13	L	1	01709	L	0	82NOV08	18:46:32 0023:00	EE255	342
HD17505	12	07.40	02 47 15	+60 12	L	3	18796	S	0	82DEC14	16:59:00 0002:00	EE214	400
HD17505	12	00.00	02 47 15	+60 12	L	3	18796	L	0	82DEC14	16:28:15 0001:00	EE214	
HD17505	12	07.40	02 47 15	+60 12	H	2	14835	L	0	82DEC14	15:15:03 0070:00	EE214	504
HD17505	12	07.40	02 47 15	+60 12	L	2	14836	L	0	82DEC14	17:04:23 0000:45	EE214	502
BD60/594	12	09.00	02 53 05	+61 12	H	2	14834	L	0	82DEC14	10:33:49 0180:00	EE214	404
HD18352	20	07.00	02 55 48	+61 05	H	3	18795	L	0	82DEC14	14:00:52 0060:00	EE214	500
TWHOR	50	05.60	03 11 17	-57 30	L	2	15115	L	0	83JAN26	10:56:34 0170:00	EC152	335
TW-HOR	50	05.60	03 11 17	-57 30	L	2	14940	L	0	82DEC28	15:06:31 0153:00	EC152	335
NGC1275	84	13.20	03 16 29	+41 19	L	2	14475	L	0	82OCT24	15:16:14 0150:00	EE255	344
NGC1276	84	00.00	03 16 29	+41 19	L	3	18384	L	0	82OCT24	17:52:30 0232:00	EE255	241
NGC1275	84	13.60	03 16 29	+41 19	L	3	18447	L	0	82NOV01	13:24:04 0145:00	EE255	331
NGC1275	84	13.50	03 16 29	+41 19	L	3	18488	L	0	82NOV06	12:57:13 0210:00	EE255	342
NGC1275	84	13.50	03 16 29	+41 19	L	3	18392	L	0	82OCT25	19:23:10 0142:00	EE255	331
HD21291	25	04.03	03 25 00	+59 46	L	3	18888	L	0	82DEC25	16:33:43 0006:00	STAN1	800
HD21291	25	04.05	03 25 00	+59 46	L	2	14907	S	0	82DEC25	16:42:38 0002:00	STAN1	
													802
HD21291	25	04.05	03 25 00	+59 46	L	2	14907	L	0	82DEC25	16:48:02 0002:34	STAN1	802
HD22928	24	03.00	03 39 21	+47 37	L	2	15103	L	0	83JAN25	11:39:42 0000:01	STAND	502
HD22928	24	02.66	03 39 21	+47 37	L	3	18889	L	0	82DEC25	17:28:43 0000:02	STAN1	501

OBJECT	CL	MAG	R.A.	DEC	D	C	IMAGE	A		DATE	EXPOSURE TIME		PRO	ECC
HD23432	22	05.80	03 42 55	+24 23	L	2	15137	S	0	83JAN28	11:52:12	0000:30	STAND	702
HD23432	22	05.80	03 42 55	+24 23	L	2	15137	L	0	83JAN28	11:46:01	0000:32	STAND	502
NGC1553	80	10.50	04 15 05	-55 54	L	3	18478	L	0	82NOV05	12:25:38	0441:00	EE098	204
N1553BACK	80	10.50	04 15 05	-55 54	L	2	14566	L	0	82NOV05	12:55:18	0037:00	EE098	002
HD28319	40	03.60	04 25 48	+15 45	L	3	18390	S	0	82OCT25	16:08:51	0000:40	STAN2	500
HD28319	40	03.60	04 25 48	+15 45	L	3	18390	L	0	82OCT25	16:01:39	0000:31	STAN2	700
HD28319	40	03.60	04 25 48	+15 45	L	2	14483	S	0	82OCT25	15:44:20	0000:10	STAN2	452
HD28319	40	03.60	04 25 48	+15 45	L	2	14483	L	0	82OCT25	15:34:07	0000:09	STAN2	702
NGC1667	81	13.70	04 46 10	-06 24	L	3	18771	L	0	82DEC10	11:57:17	0389:00	EE276	304
AB-AUR	34	07.00	04 52 34	+30 28	H	3	18987	L	0	83JAN11	09:39:55	0367:00	EA107	412
AB-AUR	34	07.00	04 52 34	+30 28	H	2	15038	L	0	83JAN11	08:51:38	0045:00	EA107	453
ABAUR	34	07.20	04 52 34	+30 28	H	2	14497	L	0	82OCT26	14:36:57	0045:00	EA100	453
ABAUR	34	07.20	04 52 34	+30 28	L	3	18405	L	0	82OCT26	16:46:33	0003:00	EA100	501
ABAUR	34	07.20	04 52 34	+30 28	L	3	18406	L	0	82OCT26	18:20:44	0003:00	EA100	501
ABAUR	34	07.20	04 52 34	+30 28	H	2	14498	L	0	82OCT26	15:57:29	0045:00	EA100	553
ABAUR	34	07.20	04 52 34	+30 28	H	2	14500	L	0	82OCT26	18:52:41	0045:00	EA100	453
ABAUR	34	07.20	04 52 34	+30 28	H	2	14501	L	0	82OCT26	20:14:55	0045:00	EA100	553
ABAUR	34	07.20	04 52 34	+30 28	L	3	18404	L	0	82OCT26	15:26:06	0003:00	EA100	501
ABAUR	34	07.20	04 52 34	+30 28	L	3	18408	L	0	82OCT26	21:03:58	0003:00	EA100	500
AB-AUR	34	07.00	04 52 34	+30 28	L	2	15039	L	0	83JAN11	10:08:55	0300:00	EA107	000
AB AUR	34	07.20	04 52 34	+30 28	H	2	14499	L	0	82OCT26	17:31:41	0045:00	EA100	554
ABAUR	34	07.20	04 52 34	+30 28	L	3	18407	L	0	82OCT26	19:42:01	0003:00	EA100	501
EPSAUR	40	03.60	04 58 22	+43 45	H	2	14646	L	0	82NOV16	16:05:23	0050:00	EI039	743
EPSAUR	40	03.60	04 58 22	+43 45	H	3	18571	L	0	82NOV16	16:59:21	0055:00	EI039	331
EPSAUR	40	03.60	04 58 22	+43 45	L	3	18570	S	0	82NOV16	15:49:04	0010:00	EI039	431
EPSAUR	40	03.60	04 58 22	+43 45	L	3	18570	L	0	82NOV16	15:04:17	0040:00	EI039	731
EPSAUR	40	03.60	04 58 22	+43 45	H	2	14645	L	0	82NOV16	14:42:42	0015:00	EI039	402
HD31964	33	03.65	04 58 22	+43 45	H	2	15127	L	0	83JAN27	13:04:06	0060:00	EM242	713
HD31964	33	04.00	04 58 22	+43 45	H	2	15128	L	0	83JAN27	15:20:49	0020:00	EM242	512
HD31964	33	04.00	04 58 22	+43 45	H	3	19098	L	0	83JAN27	14:07:19	0070:00	EM242	331
HD32630	21	03.30	05 03 00	+41 10	L	3	18721	L	0	82DEC03	17:24:11	0000:01	PHCAL	500
HD32630	21	03.30	05 03 00	+41 10	H	3	18720	L	0	82DEC03	16:57:37	0000:35	PHCAL	701
HD32630	21	03.30	05 03 00	+41 10	H	2	14778	L	0	82DEC03	16:43:12	0000:23	PHCAL	502
HD32630	21	03.30	05 03 00	+41 10	L	2	14777	L	0	82DEC03	16:14:35		PHCAL	502
AKN120	84	13.30	05 13 36	-00 12	L	3	18784	L	0	82DEC12	16:37:56	0070:00	EE252	341
AKN120	84	13.30	05 13 36	-00 12	L	2	14825	L	0	82DEC12	15:34:11	0060:00	EE252	453
AKN120	84	08.89	05 13 37	-00 12	L	2	15055	L	0	83JAN15	01:51:58	0100:00	SEYFE	002
AKN120	84	12.80	05 13 37	-00 12	L	2	14869	L	0	82DEC22	12:36:08	0070:00	SEYFE	441
AKN120	84	12.80	05 13 37	-00 12	L	3	18855	L	0	82DEC22	10:52:11	0100:00	SEYFE	350

OBJECT	CL	MAG	R.A.	DEC	D	C	IMAGE	A		DATE	EXPOSURE TIME		PRO	ECC
AKN120	84	12.50	05 13 37	+00 12	L	3	19004	L	0	83JAN15	13:53:02	0115:00	SEYFE	351
AKN120	84	12.80	05 13 39	-00 12	L	3	18856	S	0	82DEC22	13:50:36	0110:00	SEYFE	341
HD36521	10	12.30	05 26 47	-68 52	H	3	19059	L	0	83JAN22	10:06:46	0240:00	EM162	332
GSL1-12	13	12.60	05 26 57	-68 52	L	3	19060	S	0	83JAN22	15:25:30	0023:00	EM162	400
GSL1-12	13	12.60	05 26 57	-68 52	L	3	19060	L	0	83JAN22	14:48:42	0032:00	EM162	700
GSL1-12	13	12.60	05 26 57	-68 52	L	2	15090	L	0	83JAN22	14:15:08	0030:00	EM162	602
ANORI	58	11.80	05 30 47	-05 32	L	2	15013	L	0	83JAN07	08:45:48	0030:00	EC279	332
ANORI	58	11.80	05 30 47	-05 32	L	3	18962	L	0	83JAN07	08:22:58	0120:00	EC279	331
P1404	58	12.40	05 31 49	-05 38	L	3	18963	L	0	83JAN07	12:16:49	0190:00	EC279	231
P1404	58	12.41	05 31 49	-05 38	L	2	15014	L	0	83JAN07	11:43:20	0030:00	EC279	331
HD37043	14	02.80	05 32 59	-05 56	L	2	15102	L	0	83JAN25	10:24:11		STAND	502
HD37043	14	02.80	05 32 59	-05 56	L	3	19080	L	0	83JAN25	10:15:10		STAND	601
N63A	75	00.00	05 35 40	-66 03	H	3	18545	L	0	82NOV13	13:11:16	0045:00	EM126	121
N63A	75	00.00	05 35 40	-66 03	H	3	18546	L	0	82NOV13	14:16:48	0330:00	EM126	152
R127	510.1.00		05 36 54	-69 31	L	2	14713	S	0	82NOV24	19:35:37	0010:00	EI012	503
R127	510.1.00		05 36 54	-69 31	L	3	18649	L	0	82NOV24	19:04:49	0005:00	EI012	300
R 127	510.1.01		05 37 06	-69 32	H	2	14712	L	0	82NOV24	12:47:10	0372:22	EI012	508
R127	52	00.00	05 37 09	-69 31	L	2	14830	L	0	82DEC13	14:50:48	0005:30	EA025	501
R127	52	00.00	05 37 09	-69 31	L	2	14829	L	0	82DEC13	12:04:48	0010:00	EA025	701
R127	52	00.00	05 37 09	-69 31	H	3	18790	L	0	82DEC13	15:04:28	0163:00	EA025	303
R127	52	00.00	05 37 09	-69 31	L	3	18789	L	0	82DEC13	11:44:08	0015:00	EA025	501
MKN492	88	15.00	05 41 22	+23 22	L	3	18816	L	0	82DEC18	10:38:40	0429:00	EE251	103
CNORI	54	12.60	05 49 40	-05 25	L	2	14680	L	0	82NOV20	19:12:20	0020:00	EI079	401
CNORI	54	12.60	05 49 40	-05 25	L	3	18611	L	0	82NOV20	19:40:58	0007:00	EI079	301
OMET1969I	90	00.00	06 07 14	+26 22	L	3	18497	L	0	82NOV07	14:34:41	0015:00	ES284	000
OMET1969I	06	12.50	06 07 14	+26 22	L	2	14579	L	0	82NOV07	16:11:51	0040:00	ES284	222
OMET1969I	06	12.50	06 07 32	+26 22	L	3	18498	L	0	82NOV07	16:56:33	0007:30	ES284	030
SSAUR	54	11.40	06 09 35	+47 45	L	2	14679	L	0	82NOV20	17:05:00	0020:00	EI079	601
SSAUR	54	11.40	06 09 35	+47 45	L	3	18610	L	0	82NOV20	17:33:09	0026:00	EI079	701
HD46703	41	08.90	06 33 49	+53 33	L	3	18872	L	0	82DEC23	12:52:40	0040:00	EC067	201
HD46703	41	08.90	06 33 49	+53 33	L	2	14880	S	0	82DEC23	13:35:48	0010:00	EC067	302
HD46703	41	08.90	06 33 49	+53 33	L	2	14880	L	0	82DEC23	13:59:32	0015:00	EC067	402
HD47432	20	06.20	06 36 02	+01 39	L	2	15136	S	0	83JAN28	10:55:39	0000:18	STAND	502
HD47432	20	06.20	06 36 02	+01 39	L	2	15136	L	0	83JAN28	10:50:04	0000:20	STAND	502
HD47432	20	06.20	06 36 02	+01 39	L	3	19110	S	0	83JAN28	10:23:05	0001:00	STAND	701
HD47432	20	06.20	06 36 02	+01 39	L	3	19110	L	0	83JAN28	10:16:04	0000:51	STAND	501
HD48097	30	05.20	06 39 29	+17 41	H	3	18572	L	0	82NOV16	18:42:16	0018:00	EI039	500
HD48097	30	05.20	06 39 29	+17 41	H	2	14648	L	0	82NOV16	19:12:53	0013:00	EI039	502
HD48097	30	05.20	06 39 29	+17 41	L	2	14647	L	0	82NOV16	18:39:43	0000:12	EI039	502

OBJECT	CL	MAG	R.A.	DEC	D	C	IMAGE	A		DATE	EXPOSURE TIME	PRO	ECC
HD48097	30	05.20	06 39 29	+17 41	L	3	18573	L	0	82NOV16 19:38:01	0000:40	EI039	700
HD50896	11	06.90	06 52 08	-23 51	L	3	18835	S	0	82DEC20 11:35:00	0000:02	EA143	471
HD50896	11	06.90	06 52 08	-23 51	L	3	18835	L	0	82DEC20 11:33:34	0000:04	EA143	351
HD50896	11	06.90	06 52 08	-23 51	H	2	14855	L	0	82DEC20 11:06:12	0004:00	EA143	451
HD50896	11	06.90	06 52 08	-23 51	H	3	18836	L	0	82DEC20 12:30:29	0001:00	EA143	251
HD50896	11	06.90	06 52 08	-23 51	H	3	18834	L	0	82DEC20 10:39:01	0005:00	EA143	571
HD57061	13	04.40	07 16 37	-24 51	L	3	19079	S	0	83JAN25 08:50:45	0000:01	STAND	300
HD57061	13	04.40	07 16 37	-24 51	L	3	19079	L	0	83JAN25 08:50:45	0000:01	STAND	500
HD57061	13	04.40	07 16 37	-24 51	L	2	15101	L	0	83JAN25 08:58:09	0000:01	STAND	502
HD64414	26	05.00	07 31 30	-14 24	H	3	18980	L	0	83JAN10 11:42:24	0030:00	PHCAL	461
HD64414	26	05.00	07 31 30	-14 24	L	3	18979	S	0	83JAN10 10:12:35	0004:00	PHCAL	881
HD64414	26	05.00	07 31 30	-14 24	L	3	18979	L	0	83JAN10 10:08:27	0000:20	PHCAL	440
HD64414	26	05.00	07 31 30	-14 24	L	1	01765	L	0	83JAN10 12:17:44	0000:15	PHCAL	561
HD64414	26	05.00	07 31 30	-14 24	L	2	15030	L	0	83JAN10 09:59:57	0000:18	PHCAL	550
NULL	00	99.99	07 31 30	-14 24	H	2	15032	L	0	83JAN10		PHCAL	
HD64414	26	05.00	07 31 30	-14 24	H	2	15031	L	0	83JAN10 09:39:21	0020:00	PHCAL	220
HD64414	26	05.00	07 31 30	-14 24	H	3	18978	L	0	83JAN10 09:04:13	0030:00	PHCAL	220
HD64414	26	05.00	07 31 30	-14 24	H	1	01764	L	0	83JAN10 11:08:19	0020:00	PHCAL	572
HD60753	21	06.70	07 32 07	-50 28	L	1	01785	S	0	83JAN31 08:52:45	0000:18	PHCAL	402
HD60753	21	06.70	07 32 07	-50 28	L	1	01785	L	0	83JAN31 08:46:54	0000:06	PHCAL	602
HD60753	21	06.69	07 32 08	-50 28	H	1	01766	L	0	83JAN10 13:16:30	0010:00	PHCAL	503
HD60753	21	05.95	07 32 08	-50 28	L	3	18898	S	0	82DEC27 14:29:18	0000:30	PHCAL	601
HD60753	21	05.95	07 32 08	-50 28	L	3	18898	L	0	82DEC27 14:33:26	0000:40	PHCAL	501
NULL	00	00.00	07 32 08	-50 28	H	3	18717			82DEC03		PHCAL	
HD60753	21	06.70	07 32 08	-50 28	L	3	18714	S	0	82DEC03 11:53:42	0000:30	PHCAL	500
HD60753	21	06.70	07 32 08	-50 28	L	3	18714	L	0	82DEC03 11:49:53	0000:10	PHCAL	600
HD60753	21	06.70	07 32 08	-50 28	L	2	14775	L	0	82DEC03 11:18:46	0000:03	PHCAL	402
HD60753	21	06.70	07 32 08	-50 28	L	2	14774	S	0	82DEC03 10:46:52	0000:21	PHCAL	402
HD60753	21	06.70	07 32 08	-50 28	L	2	14774	L	0	82DEC03 10:40:59	0000:07	PHCAL	502
HD60753	21	06.70	07 32 08	-50 28	H	3	18716	L	0	82DEC03 12:52:38	0010:00	PHCAL	400
HD60753	21	06.70	07 32 08	-50 28	H	2	14776	L	0	82DEC03 12:25:54	0010:30	PHCAL	502
HD60753	21	05.95	07 32 08	-50 28	L	2	14934	S	0	82DEC27 14:39:49	0000:21	PHCAL	602
HD60753	21	05.95	07 32 08	-50 28	L	2	14934	L	0	82DEC27 14:43:57	0000:03	PHCAL	502
CALUV60%	00	00.00	07 32 08	-50 28	H	3	18718			82DEC03		PHCAL	
FLOOD100%	00	00.00	07 32 08	-50 28	H	3	18719			82DEC03		PHCAL	
HD60753	21	06.70	07 32 08	-50 28	L	3	18715	L	0	82DEC03 12:19:17	0000:04	PHCAL	500
L745-46A	41	300.00	07 38 00	-17 17	L	2	14719	L	0	82NOV25 13:11:43	0100:00	EA014	403
BD+75325	16	08.81	08 04 43	+75 06	L	2	14936	L	0	82DEC27 17:28:31	0000:24	PHCAL	502

OBJECT	CL	MAG	R.A.	DEC	D	C	IMAGE	A		DATE	EXPOSURE	TIME	PRO	ECC
BD+75325	16	08.83	08 04 43	+75 06	H	3	18883	L	0	82DEC24	17:32:11	0000:14	PHCAL	000
BD+75D325	16	9.50	08 04 43	+75 06	L	2	15153	L	0	83JAN30	12:20:05	0001:14	FA183	442
BD+75325	16	08.75	08 04 43	+75 06	L	3	18900	L	0	82DEC27	17:25:08	0000:14	PHCAL	500
BD+75325	16	08.82	08 04 43	+75 06	H	2	14890	L	0	82DEC24	17:29:41	0000:24	PHCAL	000
BD+75325	16	09.50	08 04 43	+75 06	L	3	19141	L	0	83JAN30	12:12:25	0000:43	FA183	440
HD67594	45	04.40	08 06 04	-02 50	L	2	15134	S	0	83JAN28	08:37:37	0001:30	STAND	402
HD67594	45	04.40	08 06 04	-02 50	L	2	15134	L	0	83JAN28	08:24:28	0000:25	STAND	302
HD67594	45	04.40	08 06 04	-02 50	L	2	15135	S	0	83JAN28	09:07:55	0002:00	STAND	502
HD67594	45	04.40	08 06 04	-02 50	L	2	15135	L	0	83JAN28	09:07:55	0002:00	STAND	702
NGC2537	82	12.00	08 09 41	+46 08	L	3	18927	L	0	83JAN01	09:22:15	0385:00	EE169	302
PD-481577	52	09.80	08 13 49	-49 04	H	2	14656	L	0	82NOV17	16:27:34	0150:00	EI075	605
PD-481577	52	09.80	08 13 49	-49 04	L	3	18580	L	0	82NOV17	19:00:49	0002:00	EI075	600
PD-481577	52	09.80	08 13 49	-49 04	L	2	14657	L	0	82NOV17	19:00:49	0002:00	EI075	502
PD-481577	52	09.80	08 13 49	-49 04	L	3	18578	L	0	82NOV17	12:51:31	0002:30	EI075	600
PD-481577	52	09.80	08 13 49	-49 04	H	3	18579	L	0	82NOV17	13:23:59	0180:00	EI075	602
PD-481577	52	09.80	08 13 49	-49 04	L	2	14655	L	0	82NOV17	12:57:15	0001:30	EI075	502
ZCAM	54	11.50	08 15 40	+73 16	L	2	14678	L	0	82NOV20	15:09:25	0019:00	EI079	501
ZCAM	54	11.50	08 15 40	+73 16	L	3	18608	L	0	82NOV20	14:52:10	0012:00	EI079	301
ZCAM	54	11.50	08 15 40	+73 16	L	3	18609	L	0	82NOV20	15:47:47	0040:00	EI079	501
CDS99	70	10.40	08 19 00	-36 03	L	2	15089	L	0	83JAN22	08:53:44	0015:00	EM162	112
CDS99	70	10.40	08 19 00	-36 03	L	3	19058	L	0	83JAN22	08:33:58	0015:00	EM162	110
TFLOOD	00	99.99	08 53 51	+33 06	H	3	19139	L	0	83JAN30			FA183	
TFLOOD	00	99.99	08 56 10	+33 08	H	2	15151	L	0	83JAN30			FA183	
MK392	37	15.20	08 56 10	+33 08	L	3	19140	L	0	83JAN30	09:44:02	0060:00	FA183	21
MK392	37	15.20	08 56 10	+33 08	L	2	15152	L	0	83JAN30	10:54:23	0024:00	FA183	331
HD77581	59	06.90	09 00 13	-40 21	L	2	14852	L	0	82DEC19	13:46:13	0000:40	EA087	502
HD77581	59	06.90	09 00 13	-40 21	H	3	18823	L	0	82DEC19	11:13:10	0150:00	EA087	501
IC2448	70	12.50	09 06 37	-69 44	H	2	15096	L	0	83JAN23	11:32:31	0230:00	EM162	235
IC2448	70	12.50	09 06 37	-69 44	H	3	19067	L	0	83JAN23	08:28:48	0180:00	EM162	271
IC2448	70	12.50	09 06 37	-69 44	L	3	19068	S	0	83JAN23	15:27:02	0020:00	EM162	330
GC2784BAC	80	11.50	09 10 05	-23 58	L	2	14561	L	0	82NOV04	14:35:48	0280:00	EE098	002
NGC2784	80	11.50	09 10 05	-23 58	L	3	18471	L	0	82NOV04	14:16:05	0331:00	EE098	103
HD80081	36	03.78	09 15 43	+37 01	L	3	18354	S	0	82OCT21	16:00:51	0000:45	EA115	700
HD80081	36	03.78	09 15 43	+37 01	L	3	18354	L	0	82OCT21	15:53:14	0000:15	EA115	700
HD80081	36	03.78	09 15 43	+37 01	L	3	18353	S	0	82OCT21	15:07:11	0000:35	EA115	501
HD80081	36	03.78	09 15 43	+37 01	L	3	18353	L	0	82OCT21	15:02:58	0000:06	EA115	501
HD80081	36	03.78	09 15 43	+37 01	L	2	14456	S	0	82OCT21	15:15:22	0000:05	EA115	602
HD80081	36	03.78	09 15 43	+37 01	L	2	14456	L	0	82OCT21	15:11:20	0000:05	EA115	402
HD80081	30	03.80	09 15 44	+37 05	H	3	19127	L	0	83JAN29	12:50:25	0006:20	FA179	501
HD80081	30	03.80	09 15 44	+37 05	H	2	15145	L	0	83JAN29	12:42:15	0004:30	FA179	602

OBJECT	CL	MAG	R.A.	DEC	D	C	IMAGE	A	DATE	EXPOSURE TIME	PRO	ECC
HD83754	21	04.34	09 37 54	-14 06	L	3	18884	S 0	82DEC25	10:47:30 0000:08	STAN1	601
HD83754	21	04.34	09 37 54	-14 06	L	3	18884	L 0	82DEC25	10:52:30 0000:09	STAN1	501
HD83754	21	04.33	09 37 54	-14 06	L	2	14903	S 0	82DEC25	10:58:42 0000:04	STAN1	502
HD83754	21	04.33	09 37 54	-14 06	L	2	14903	L 0	82DEC25	11:02:36 0000:05	STAN1	502
HD84937	40	08.20	09 46 12	+13 59	L	2	14881	S 0	82DEC23	16:12:02 0007:00	EC067	502
HD84937	40	08.20	09 46 12	+13 59	L	2	14881	L 0	82DEC23	15:55:16 0010:00	EC067	702
HD84937	40	07.78	09 46 12	+13 59	L	3	18873	L 0	82DEC23	15:12:01 0040:00	EC067	701
NULL	00	00.00	09 57 57	+56 08	L	2	14839	L 0	82DEC15		EE251	
Q0957+56	85	17.00	09 57 57	+56 08	L	1	01744	L 0	82DEC15	11:11:43 0390:00	EE251	342
ULL IMAGE	00	99.99	10 16 59	+20 06	L	2	15046		83JAN13		EE208	
UV1032+40	20	11.50	10 32 18	+40 36	H	3	18355	L 0	82OCT21	16:56:21 0130:00	EA115	402
UV1032+40	20	11.50	10 32 18	+40 36	L	3	18356	S 0	82OCT21	21:32:28 0003:00	EA115	400
UV1032+40	20	11.50	10 32 18	+40 36	L	3	18356	L 0	82OCT21	21:26:14 0001:40	EA115	400
UV1032+40	20	11.50	10 32 18	+40 36	H	2	14457	L 0	82OCT21	19:11:02 0130:00	EA115	304
NGC3351	81	2.5.00	10 41 19	+11 58	L	3	18628	L 0	82NOV22	15:03:00 0284:00	EE130	302
NGC3351	81	2.5.00	10 41 19	+11 58	L	2	14695	L 0	82NOV22	12:48:33 0130:00	EE130	306
HD93521	12	07.30	10 45 34	+37 50	L	1	01789	L 0	83JAN31	12:28:13 0000:11	PHCAL	242
HD93521	12	07.00	10 45 34	+37 50	L	1	01788	S 0	83JAN31	11:58:08 0000:09	PHCAL	502
HD93521	12	07.00	10 45 34	+37 50	L	1	01788	L 0	83JAN31	11:53:34 0000:03	PHCAL	602
NULL	99	00.00	10 50 23	+04 53	H	3	18806		82DEC16	10:25:20 0012:00	EE251	
1050+04	80	13.50	10 50 28	+04 53	L	3	18807	L 0	82DEC16	11:25:24 0382:00	EE251	413
1050+04	88	15.00	10 50 28	+04 53	L	1	01769	L 0	83JAN13	10:08:05 0333:00	EE208	405
HD94848	26	08.70	10 53 58	-60 07	L	2	14625	L 0	82NOV14	16:27:14 0003:01	EI203	502
CD-347151	58	10.40	10 59 30	-34 26	H	3	18967	L 0	83JAN08	09:02:58 0404:00	EC279	163
P1103-006	85	16.50	11 03 58	-00 36	L	3	19048	L 0	83JAN20	09:27:45 0380:00	EE044	343
HD96548	11	00.00	11 04 18	-65 14	L	2	14857	S 0	82DEC20	15:30:35 0000:45	EA143	551
HD96548	11	00.00	11 04 18	-65 14	L	2	14857	L 0	82DEC20	15:30:28 0000:20	EA143	551
HD96548	11	07.90	11 04 18	-65 14	H	3	18838	L 0	82DEC20	14:35:33 0033:00	EA143	451
HD96548	11	07.90	11 04 18	-65 14	H	2	14856	L 0	82DEC20	14:00:16 0025:00	EA143	441
HD96548	11	07.90	11 04 18	-65 14	H	3	18837	L 0	82DEC21	13:15:33 0040:00	EA143	451
HD96548	11	07.90	11 04 18	-15 14	H	3	18851	L 0	82DEC21	16:57:06 0050:00	EA143	471
HD96548	11	07.90	11 04 18	-65 14	H	3	18850	L 0	82DEC21	15:24:44 0040:00	EA143	451
HD96548	11	07.90	11 04 18	-65 14	H	2	14865	L 0	82DEC21	16:09:26 0030:00	EA143	452
HD98922	25	07.20	11 20 13	-53 05	L	2	14624	L 0	82NOV14	12:45:15 0001:00	EI203	602
HD98922	26	07.20	11 20 13	-53 05	H	3	18554	L 0	82NOV14	13:35:31 0120:00	EI203	541
HD98922	25	07.20	11 20 13	-53 05	L	3	18553	L 0	82NOV14	12:45:15 0003:00	EI203	550
NGC3690	82	12.00	11 25 41	+58 50	L	3	18935	L 0	83JAN02	08:57:33 0410:00	EE169	403
HD99946	66	07.10	11 27 25	+30 14	L	3	19031	L 0	83JAN18	14:47:30 0060:00	EI240	731
HD99946	66	07.10	11 27 25	+30 14	L	3	19030	L 0	83JAN18	12:53:02 0090:00	EI240	731

OBJECT	CL	MAG	R.A.			DEC		D	C	IMAGE	A		DATE	EXPOSURE	TIME	PRO	ECC
HD99946	66	07.10	11	27	25	+30	14	L	3	19028	L	0	83JAN18	09:00:00	0090:00	EI240	731
HD99946	66	07.10	11	27	25	+30	14	L	3	19029	L	0	83JAN18	10:59:00	0090:00	EI240	731
HD99946	66	07.30	11	27	26	+30	14	L	3	19011	L	0	83JAN16	14:18:22	0090:00	EI240	831
HD99946	66	07.10	11	27	26	+30	14	L	3	19008	L	0	83JAN16	08:32:30	0090:00	EI240	831
HD99946	66	07.30	11	27	26	+30	14	L	3	19010	L	0	83JAN16	12:22:48	0090:00	EI240	831
HD99946	66	07.30	11	27	26	+30	14	L	3	19009	L	0	83JAN16	10:28:14	0090:00	EI240	831
NGC3783	84	00.00	11	36	33	-37	27	L	2	14921	L	0	82DEC26	14:30:57	0090:00	EE252	464
NGC3783	84	00.00	11	36	33	-37	27	L	3	18894	L	0	82DEC26	16:05:53	0101:00	EE252	351
BHCEN	66	10.60	11	36	49	-63	08	L	2	14444	L	0	82OCT19	21:20:30	0006:00	EI073	502
BHCEN	66	10.70	11	36	49	-63	08	L	3	18332	L	0	82OCT19	20:43:16	0008:30	EI073	401
HD105058	36	08.80	12	03	11	+49	57	L	2	15147	L	0	83JAN29	15:25:14	0004:30	FA179	502
HD105058	36	08.80	12	03	11	+49	57	L	3	19129	L	0	83JAN29	15:34:21	0013:00	FA179	400
Q1206+459	85	15.80	12	06	26	+45	57	L	3	19074	L	0	83JAN24	09:17:27	0390:00	EE257	202
NGC4151	84	12.00	12	08	00	+39	41	L	2	14574	L	0	82NOV06	18:18:17	0040:00	EE255	563
NGC4151	84	12.00	12	08	00	+39	41	L	3	18490	L	0	82NOV06	19:02:06	0045:00	EE255	351
NGC4151	84	12.00	12	08	00	+39	41	L	3	18489	L	0	82NOV06	17:41:23	0025:00	EE255	350
NGC4151	84	12.00	12	08	00	+39	41	L	2	14573	L	0	82NOV06	17:07:53	0030:00	EE255	452
HZ21	17	14.20	12	11	25	+33	13	L	2	15154	L	0	83JAN30	14:24:04	0040:00	FA183	443
HZ21	17	14.20	12	11	25	+33	13	L	3	19142	L	0	83JAN30	13:52:52	0025:00	FA183	550
HZ21	00	10.67	12	11	25	+33	13	L	3	19143	L	0	83JAN30	15:10:35	0037:00	FA183	550
NGC4314	813.1.00		12	20	01	+30	10	L	2	14704	L	0	82NOV23	13:14:40	0120:00	EE130	305
NGC4314	813.1.00		12	20	01	+30	10	L	3	18637	L	0	82NOV23	15:19:47	0047:00	EE130	201
NGC4314	813.1.00		12	20	01	+30	10	L	2	14705	L	0	82NOV23	16:11:28	0213:00	EE130	307
HD108767	22	02.64	12	27	16	-16	14	L	2	14904	L	0	82DEC25	12:18:52	0000:02	STAN1	502
HD108767	22	02.62	12	27	16	-16	14	L	3	18885	L	0	82DEC25	12:11:50	0000:04	STAN1	500
HD110411	30	05.00	12	39	21	+10	30	L	2	15143	S	0	83JAN29	09:56:33	0000:13	FA179	502
HD110411	30	05.00	12	39	21	+10	30	L	2	15143	L	0	83JAN29	09:52:44	0000:05	FA179	502
HD110411	30	05.00	12	39	21	+10	30	L	3	19125	S	0	83JAN29	10:09:06	0000:35	FA179	600
HD110411	30	05.00	12	39	21	+10	30	L	3	19125	L	0	83JAN29	09:59:56	0000:13	FA179	500
HD11786	30	06.20	12	49	17	-26	28	L	3	19124	S	0	83JAN29	08:40:09	0005:00	FA179	700
06.20786	30	06.20	12	49	17	-26	28	L	3	19124	L	0	83JAN29	08:35:01	0001:25	FA179	500
06.20481	23	08.40	12	54	43	-49	30	H	3	18918	L	0	82DEC31	12:32:34	0195:00	EC004	601
HD111786	30	06.20	12	91	72	-26	28	L	2	15142	S	0	83JAN29	08:29:05	0001:00	FA179	562
HD111786	30	06.20	12	91	72	-26	28	L	2	15142	L	0	83JAN29	08:25:23	0000:20	FA179	452
OMET1982G	06	14.00	13	04	16	+32	54	L	3	18499	L	0	82NOV07	18:01:59	0015:00	ES284	030
06.2082G	90	00.00	13	04	16	+32	54	L	3	18500	L	0	82NOV07	19:27:38	0015:00	ES284	020
OMET1982G	06	14.00	13	04	16	+32	54	L	2	14580	L	0	82NOV07	18:28:46	0055:00	ES284	043
HD135421B	66	08.60	13	22	42	-37	30	L	3	19022	L	0	83JAN17	09:13:44	0394:00	EI240	303
MKN266	84	14.50	13	36	14	+48	31	L	3	18736	L	0	82DEC05	01:50:04	0418:00	EE189	342

OBJECT	CL	MAG	R.A.	DEC	D	C	IMAGE	A		DATE	EXPOSURE TIME		PRO	ECC
HD119069	23	08.40	13 38 53	-45 35	H	3	18919	L	0	82DEC31	16:26:56	0040:00	EC004	501
HD119069	23	08.40	13 38 53	-45 35	H	3	18917	L	0	82DEC31	10:54:52	0055:00	EC004	701
HD120315	21	01.48	13 45 34	+49 33	H	2	14889	L	0	82DEC24	16:12:31	0000:06	PHCAL	501
HD120315	16	01.47	13 45 34	+49 33	H	1	01751	L	0	82DEC24	15:21:51	0000:05	PHCAL	502
HD120315	21	01.48	13 45 34	+49 33	H	3	18882	L	0	82DEC24	16:18:21	0000:06	PHCAL	501
1350-00	80	15.00	13 50 10	+00 22	L	3	18997	L	0	83JAN14	10:18:37	0325:00	EE208	221
PG1351+64	85	14.80	13 51 46	+64 00	L	3	18457	L	0	82NOV02	17:07:13	0160:00	EE253	342
PG1351+64	85	14.80	13 51 46	+64 00	L	3	18975	L	0	83JAN09	08:53:50	0200:00	EE252	362
NGC5548	84	12.90	14 15 43	+25 22	L	3	18857	L	0	82DEC22	17:17:18	0030:00	SEYFE	330
NGC5548	84	13.20	14 15 43	+25 22	L	2	15025	L	0	83JAN09	12:47:14	0060:00	EE252	452
NGC5548	84	13.00	14 15 43	+25 22	L	3	18782	L	0	82DEC12	10:46:02	0030:00	EE252	330
NGC5548	84	00.00	14 15 43	+25 22	L	2	14920	L	0	82DEC26	11:46:21	0060:00	EE252	453
NGC5548	84	00.00	14 15 43	+25 22	L	3	18892	L	0	82DEC26	10:39:10	0060:00	EE252	351
NGC5548	84	00.00	14 15 43	+25 22	L	3	18893	S	0	82DEC26	12:51:06	0060:00	EE252	331
NGC5548	84	13.20	14 15 43	+25 22	L	3	18976	S	0	83JAN09	15:07:33	0040:00	EE252	23
NGC5548	84	13.20	14 15 43	+25 22	L	3	18976	L	0	83JAN09	13:52:34	0070:00	EE252	351
A1422+48	84	15.00	14 19 38	+48 01	L	1	01760	L	0	83JAN06	09:17:30	0150:00	EE266	331
A1422+48	84	15.00	14 19 38	+48 01	L	3	18951	L	0	83JAN05	08:55:09	0180:00	EE266	331
HD128167	40	04.33	14 32 30	+29 57	L	3	18874	S	0	82DEC23	17:27:08	0002:00	EC067	401
HD128167	40	04.33	14 32 30	+29 57	L	3	18874	L	0	82DEC23	17:23:30	0000:35	EC067	401
HD128167	40	04.32	14 32 30	+29 57	L	2	14882	S	0	82DEC23	17:34:02	0000:10	EC067	402
HD128167	40	04.32	14 32 30	+29 57	L	2	14882	L	0	82DEC23	17:31:33	0000:15	EC067	702
P1510-089	85	16.50	15 10 08	-08 54	L	3	19054	L	0	83JAN21	08:59:08	0408:00	EE044	232
S0141-455	84	13.50	15 16 57	-58 45	L	3	18455	L	0	82NOV02	12:56:40	0060:00	EE253	340
HD138749	26	04.20	15 30 54	+31 31	H	2	15125	L	0	83JAN27	10:21:51	0001:15	EA080	512
HD138749	26	04.20	15 30 54	+31 31	H	3	19095	L	0	83JAN27	09:50:26	0001:45	EA080	510
HD138749	26	04.20	15 30 54	+31 31	H	3	18824	L	0	82DEC19	14:48:42	0001:45	EA080	501
HD139195	46	61230	15 34 05	+10 10	L	2	15113	L	0	83JAN26	08:29:08	0006:00	EC152	512
AFETYREAD	99	00.00	15 56 38	+26 57	H	4	01174	L	0	82DEC14			EE214	
ECONDREAD	99	00.00	15 56 38	+26 57	H	4	01175	L	0	82DEC14			EE214	
HD147394	21	03.49	16 18 14	+46 25	L	3	18886	L	0	82DEC25	13:35:00	0000:03	STAN1	500
HD147394	21	03.64	16 18 14	+46 25	L	2	14905	L	0	82DEC25	13:41:28	0000:01	STAN1	502
HZ-HER	59	14.00	16 56 01	+35 25	L	3	18425	L	0	82OCT29	15:37:04	0075:00	EI020	331
HZHER	59	14.30	16 56 01	+35 25	L	3	18524	L	0	82NOV10	13:48:25	0040:00	EI020	200
HZ-HER	59	14.00	16 56 01	+35 25	L	3	18426	L	0	82OCT29	19:55:05	0075:00	EI020	331
HZ-HER	59	14.00	16 56 01	+35 25	L	2	14517	L	0	82OCT29	16:57:32	0174:00	EI020	335
HZ-HER	59	14.00	16 56 01	+35 25	L	2	14518	L	0	82OCT29	21:13:08	0030:00	EI020	303
HZHER	59	14.30	16 56 01	+35 25	L	3	18525	L	0	82NOV10	17:35:02	0075:00	EI020	201
HZHER	59	14.30	16 56 01	+35 25	L	3	18526	L	0	82NOV10	19:12:21	0035:00	EI020	200

OBJECT	CL	MAG	R.A.	DEC	D	C	IMAGE	A	DATE	EXPOSURE TIME		PRO	ECC
HZHER	59	14.30	16 56 01	+35 25	L	2	14598	L	0	82NOV10	14:34:54	0175:00	EI020	305
HD156074	50	07.50	17 11 56	+42 09	L	2	15114	L	0	83JAN26	09:31:16	0030:00	EC152	512
HD156074	50	07.60	17 11 56	+42 09	L	2	14938	L	0	82DEC28	10:34:10	0070:00	EC152	453
HD159561	31	02.20	17 32 36	+12 35	L	2	14482	L	0	82OCT25	14:28:19	0000:02	STAN2	452
HD162732	26	06.40	17 48 44	+48 24	H	3	18825	L	0	82DEC19	15:28:59	0025:00	EA080	501
HD162732	26	06.40	17 48 44	+48 24	H	3	19094	L	0	83JAN27	08:27:57	0025:00	EA080	511
HD162732	26	06.40	17 48 44	+48 24	H	2	15124	L	0	83JAN27	08:56:29	0022:00	EA080	513
NULL	00	00.00	18 31 32	-26 28	L	2	14529	L	0	82OCT31			PHCAL	
READUV160	00	09.80	18 31 33	-26 28	L	2	14538	L	0	82OCT31	19:26:52		PHCAL	
UV160	00	09.80	18 31 33	-26 28	L	2	14537	L	0	82OCT31	20:26:39	0005:01	PHCAL	
NVASGR82	55	09.80	18 31 33	-26 28	L	2	14531	L	0	82OCT31	16:51:42	0005:00	PHCAL	562
NULL	00	09.80	18 31 33	-26 28	L	2	14532	L	0	82OCT31			PHCAL	
UV60	00	09.80	18 31 33	-26 28	L	2	14533	L	0	82OCT31	17:15:46	0001:53	PHCAL	
V20	00	09.80	18 31 33	-26 28	L	2	14534	L	0	82OCT31	18:45:56	0038:00	PHCAL	
UV120	00	09.80	18 31 33	-26 28	L	2	14535	L	0	82OCT31	19:26:52	0003:46	PHCAL	
UV60	00	09.80	18 31 33	-26 28	L	2	14536	L	0	82OCT31	19:57:39	0001:53	PHCAL	
NVASGR82	55	09.80	18 31 33	-26 28	L	3	18439	L	0	82OCT31	15:08:06	0030:00	PHCAL	450
NVASGR82	55	09.80	18 31 33	-26 28	L	2	14530	L	0	82OCT31	15:42:26	0030:00	PHCAL	793
NVASGR82	55	09.80	18 31 33	-26 28	L	3	18440	L	0	82OCT31	16:16:40	0060:00	PHCAL	560
NOVAHONDA	55	09.50	18 31 33	-26 28	L	3	18330	L	0	82OCT19	16:25:23	0030:00	EI073	451
NOVAHONDA	55	09.50	18 31 33	-26 28	L	3	18329	L	0	82OCT19	15:10:14	0040:00	EI073	551
NOVAHONDA	55	09.50	18 31 33	-26 28	L	2	14442	L	0	82OCT19	16:58:36	0006:00	EI073	562
NOVAHONDA	55	09.50	18 31 33	-26 28	L	2	14441	L	0	82OCT19	15:57:15	0025:00	EI073	792
OMET-BOWE	06	14.50	19 10 51	-22 35	L	1	01719	L	0	82NOV12	13:35:39	0362:00	ES058	202
AFETYREAD	00	00.00	19 10 52	-22 33	L	2	14609			82NOV12			ES058	
SO141-G55	84	13.70	19 16 57	-58 45	L	1	01708	L	0	82NOV08	16:06:49	0050:00	EE255	452
SO141-G55	84	13.70	19 16 57	-58 45	L	3	18507	L	0	82NOV08	17:00:23	0050:00	EE255	341
HD181470	32	06.20	19 17 15	+37 21	L	2	15144	S	0	83JAN29	11:36:14	0000:40	FA179	602
HD181470	32	06.20	19 17 15	+37 21	L	2	15144	L	0	83JAN29	11:32:19	0000:15	FA179	502
HD181470	32	06.20	19 17 15	+37 21	L	3	19126	S	0	83JAN29	11:17:31	0001:40	FA179	700
HD181470	32	06.20	19 17 15	+37 21	L	3	19126	L	0	83JAN29	11:24:00	0000:30	FA179	500
HD181470	32	06.20	19 17 15	+37 21	H	2	15146	L	0	83JAN29	13:37:28	0025:00	FA179	503
HD181470	32	06.20	19 18 15	+37 21	H	3	19128	L	0	83JAN29	14:09:17	0030:00	FA179	501
NULL	00	00.00	19 45 35	+27 11	L	3	18587			82NOV18			EI075	
CALUV60%	00	00.00	19 45 35	+27 11	L	3	18588			82NOV18			EI075	
CALUV20%	00	00.00	19 45 35	+27 11	L	3	18589			82NOV18			EI075	
CALUV120%	00	00.00	19 45 35	+27 11	L	3	18590			82NOV18			EI075	
CALUV60%	00	00.00	19 45 35	+27 11	L	3	18591			82NOV18			EI075	
CALUV160%	00	00.00	19 45 35	+27 11	L	3	18592			82NOV18			EI075	

OBJECT	CL	MAG	R.A.	DEC	D	C	IMAGE	A		DATE	EXPOSURE	TIME	PRO	ECC
NULL	00	00.00	19 45 35	+27 11	L	3	18593			82NOV18			EI075	
NULL	00	00.00	19 45 35	+27 11	L	3	18594			82NOV18			EI075	
CKVUL	55	19.00	19 45 35	+27 11	L	3	18586	L	0	82NOV18	13:16:37	0160:00	EI075	002
NULL	00	00.00	19 45 35	+27 11	L	3	18595			82NOV18			EI075	
HD188728	36	05.23	19 53 52	+11 17	H	2	14449	L	0	82OCT20	14:24:52	0015:00	EA115	702
V1016CYG	51	0.8.00	19 55 19	+39 41	L	3	18668	S	0	82NOV27	12:54:33	0002:00	EA024	71
V1016CYG	51	0.8.00	19 55 19	+39 41	L	3	18668	L	0	82NOV27	12:59:17	0007:00	EA024	151
V1016CYG	57	10.80	19 55 19	+39 41	L	2	14736	L	0	82NOV27	19:35:02	0005:00	EA024	361
V1016CYG	51	0.8.00	19 55 19	+39 41	L	3	18669	L	0	82NOV27	13:58:41	0025:00	EA024	382
V1016CYG	51	0.8.00	19 55 19	+39 41	L	2	14733	S	0	82NOV27	13:20:46	0003:00	EA024	571
V1016CYG	51	0.8.00	19 55 19	+39 41	L	2	14733	L	0	82NOV27	13:28:29	0025:00	EA024	341
V1016CYG	57	10.80	19 55 19	+39 41	H	3	18671	L	0	82NOV27	17:00:34	0150:00	EA024	272
V1016CYG	57	10.80	19 55 19	+39 41	H	2	14735	L	0	82NOV27	15:30:56	0085:00	EA024	265
V1016CYG	57	10.80	19 55 19	+39 41	H	3	18670	L	0	82NOV27	15:00:29	0015:00	EA024	151
1016CYGNI	57	10.80	19 55 19	+39 41	H	2	14734	L	0	82NOV27	14:29:30	0025:00	EA024	052
NGC6853	70	00.00	19 57 24	+22 35	H	3	18340	L	0	82OCT20	15:05:37	0150:00	EA115	131
HD1921163	11	07.70	20 10 17	+38 12	H	2	14858	L	0	82DEC20	17:02:50	0020:00	EA143	451
HD192163	11	07.70	20 10 17	+38 12	L	2	14864	S	0	82DEC21	14:13:26	0000:25	EA143	462
HD192163	11	07.70	20 10 17	+38 12	L	2	14864	L	0	82DEC21	14:08:07	0000:25	EA143	352
HD192163	11	07.70	20 10 17	+38 12	H	2	14863	L	0	82DEC21	12:16:12	0030:00	EA143	452
HD192163	11	07.70	20 10 17	+38 12	H	2	14862	L	0	82DEC21	11:05:10	0020:00	EA143	352
HD192163	11	07.70	20 10 17	+38 12	L	3	18848	S	0	82DEC21	12:58:38	0000:30	EA143	481
HD192163	11	07.71	20 10 17	+38 12	L	3	18848	L	0	82DEC21	12:54:21	0000:50	EA143	361
HD192163	11	07.70	20 10 17	+38 12	H	3	18849	L	0	82DEC21	13:24:58	0020:00	EA143	360
HD192163	11	07.70	20 10 17	+38 12	H	3	18847	L	0	82DEC21	11:33:01	0040:00	EA143	471
HD192163	11	07.79	20 10 17	+38 12	H	3	18846	L	0	82DEC21	10:38:47	0020:00	EA143	350
HD192163	11	07.70	20 10 17	+38 12	H	3	18840	L	0	82DEC20	17:31:40	0015:00	EA143	351
HD192163	11	07.70	20 10 17	+38 12	H	3	18839	L	0	82DEC20	16:28:40	0020:00	EA143	361
HD193443	12	07.24	20 17 01	+38 07	H	3	18511	L	0	82NOV09	12:35:33	0115:00	EM236	401
NGC6905	70	15.00	20 20 09	+19 58	H	3	18366	L	0	82OCT22	14:39:15	0200:00	EA115	242
V1329CYG	51	2.5.00	20 49 02	+35 23	L	2	14725	L	0	82NOV26	16:53:51	0085:00	EA024	564
V1329CYG	51	2.5.00	20 49 02	+35 23	H	3	18660	L	0	82NOV26	13:48:46	0180:00	EA024	142
V1329CYG	51	2.5.00	20 49 02	+35 23	L	3	18659	L	0	82NOV26	12:39:51	0030:00	EA024	251
V1329CYG	51	2.5.00	20 49 02	+35 23	L	2	14724	L	0	82NOV26	13:13:21	0030:00	EA024	343
V1329CYG	57	00.00	20 49 02	+35 23	L	3	18661	L	0	82NOV26	18:22:53	0085:00	EA024	361
D200120	26	04.70	20 58 07	+47 19	L	3	18827	L	0	82DEC19	17:22:20	0000:01	EA080	500
HD200120	26	04.70	20 58 07	+47 19	H	3	19096	L	0	83JAN27	10:55:21	0001:30	EA080	511
HD200120	26	04.70	20 58 07	+47 19	H	2	15126	L	0	83JAN27	11:26:25	0001:30	EA080	512
HD200120	26	04.70	20 58 07	+47 19	H	3	18826	L	0	82DEC19	16:50:24	0001:30	EA080	501
HD200120	26	04.70	20 58 07	+47 19	H	2	14853	L	0	82DEC19	16:56:02	0001:30	EA080	602

OBJECT	CL	MAG	R.A.	DEC	D	C	IMAGE	A		DATE	EXPOSURE TIME		PRO	ECC
KS2135-14	85	15.50	21 35 01	-14 46	L	3	18741	L	0	82DEC06	12:28:59	0318:00	EE049	332
KS2135-14	85	15.50	21 35 01	-14 46	L	1	01739	L	0	82DEC07	11:49:58	0352:00	EE049	313
NULLIMAGE	00	00.00	21 40 20	-14 37		1	01738			82DEC07			EE049	
BD+284211	16	09.79	21 48 56	+28 37	L	2	14935	S	0	82DEC27	16:18:22	0003:00	PHCAL	602
BD+284211	16	09.79	21 48 56	+28 37	L	2	14935	L	0	82DEC27	16:14:23	0001:00	PHCAL	502
BD+284211	16	09.79	21 48 56	+28 37	L	2	14887	S	0	82DEC24	10:57:44	0003:00	PHCAL	700
BD+284211	16	09.79	21 48 56	+28 37	L	2	14887	L	0	82DEC24	10:53:47	0001:00	PHCAL	600
BD+284211	16	10.53	21 48 56	+28 37	H	1	01767	L	0	83JAN10	14:32:09	0068:00	PHCAL	501
BD+284211	16	09.79	21 48 56	+28 37	H	3	18880	L	0	82DEC24	11:03:48	0045:00	PHCAL	501
BD+284211	16	09.74	21 48 56	+28 37	L	1	01750	S	0	82DEC24	14:24:49	0002:30	PHCAL	501
BD+284211	16	09.74	21 48 56	+28 37	L	1	01750	L	0	82DEC24	14:41:49	0000:50	PHCAL	501
BD+284211	16	09.82	21 48 56	+28 37	H	1	01749	L	0	82DEC24	12:19:24	0065:00	PHCAL	503
BD+284211	16	09.80	21 48 56	+28 37	L	3	18881	S	0	82DEC24	13:31:46	0001:18	PHCAL	600
BD+284211	16	09.80	21 48 56	+28 37	L	3	18881	L	0	82DEC24	13:31:46	0000:26	PHCAL	500
BD+284211	16	09.79	21 48 56	+28 37	L	3	18899	S	0	82DEC27	16:10:40	0001:20	PHCAL	701
BD+284211	16	09.79	21 48 56	+28 37	L	3	18899	L	0	82DEC27	16:07:26	0000:26	PHCAL	501
HD209481	12	05.60	22 00 23	+57 45	H	3	19113	L	0	83JAN28	15:35:42	0006:00	STAND	501
HD209481	12	05.60	22 00 23	+57 45	L	2	15140	S	0	83JAN28	15:10:43	0000:06	STAND	502
HD209481	12	05.60	22 00 23	+57 45	L	2	15140	L	0	83JAN28	15:06:08	0000:08	STAND	502
HD209481	12	05.60	22 00 23	+57 45	L	3	19112	S	0	83JAN28	15:02:24	0000:14	STAND	660
HD209481	12	05.60	22 00 23	+57 45	L	3	19112	L	0	83JAN28	14:57:32	0000:18	STAND	550
HD210221	32	06.60	22 05 34	+53 03	L	3	18682	L	0	82NOV28	17:57:36	0004:00	STAND	300
HD210221	32	06.60	22 05 34	+53 03	L	3	18683	L	0	82NOV28	18:35:21	0012:00	STAND	500
HD210221	30	06.80	22 05 34	+53 03	L	3	18391	S	0	82OCT25	17:30:19	0000:33	STAN2	211
HD210221	30	06.80	22 05 34	+53 03	L	3	18391	L	0	82OCT25	17:35:08	0001:45	STAN2	111
HD210221	32	06.60	22 05 34	+53 03	L	2	14744	L	0	82NOV28	18:04:22	0004:02	STAND	702
HD210221	30	06.80	22 05 34	+53 03	L	2	14484	L	0	82OCT25	17:58:40	0000:51	STAN2	332
HD210221	32	06.60	22 05 34	+53 03	L	2	14745	L	0	82NOV28	19:05:21	0002:00	STAND	502
HD210839	15	07.60	22 09 48	+59 10	L	2	15139	S	0	83JAN28	13:50:17	0000:09	STAND	602
HD210839	15	07.60	22 09 48	+59 10	L	2	15139	L	0	83JAN28	13:45:07	0000:09	STAND	502
HD210839	15	07.60	22 09 48	+59 10	L	3	19111	S	0	83JAN28	13:40:44	0000:18	STAND	770
HD210839	15	07.60	22 09 48	+59 10	L	3	19111	L	0	83JAN28	13:35:23	0000:24	STAND	550
L119-34	43	14.40	22 16 10	-65 44	L	2	14743	L	0	82NOV28	13:08:14	0230:00	EA014	306
HD214680	13	04.90	22 37 00	+38 47	L	1	01786	L	0	83JAN31	10:20:55	0000:02	PHCAL	502
HD214680	13	04.90	22 37 01	+38 47	H	1	01787	L	0	83JAN31	11:05:52	0000:36	PHCAL	502
HD94878	26	08.70	22 44 53	+57 49	L	3	18555	L	0	82NOV14	16:50:24	0010:00	EI203	601
HD215835	26	08.60	22 44 54	+57 49	H	3	18556	L	0	82NOV14	17:58:17	0109:00	EI203	401
HD216598	66	08.80	22 51 22	+37 40	L	3	19035	L	0	83JAN19	08:45:51	0422:00	EI240	233
NGC7479	84	13.10	23 00 44	+08 36	L	2	14550	L	0	82NOV02	15:26:36	0030:00	EE253	343

OBJECT	CL	MAG	R.A.	DEC	D	C	IMAGE	A		DATE	EXPOSURE TIME		PRO	ECC
NGC7469	84	13.10	23 00 44	+08 36	L	3	18456	L	0	82NOV02	14:42:42	0040:00	EE253	330
NGC7469	84	13.00	23 00 44	+08 36	L	3	18783	L	0	82DEC12	13:06:29	0100:00	EE252	531
NGC7469	84	13.00	23 00 44	+08 36	L	2	14824	L	0	82DEC12	12:03:22	0060:00	EE252	453
CG-2-58-2	84	14.00	23 02 07	-08 57	L	3	18952	L	0	83JAN05	14:09:27	0098:00	EE266	350
CG2-58-22	84	14.00	23 02 07	-08 57	L	2	15001	L	0	83JAN05	12:32:15	0090:00	EE266	334
GC7590NUC	81	13.00	23 16 08	-42 30	L	3	18764	L	0	82DEC09	10:53:48	0413:00	EE276	304
NGC7590	80	13.50	23 16 08	-42 30	L	2	14821	L	0	82DEC11	10:49:39	0412:00	EE276	209
ZAND	57	10.30	23 31 15	+48 32	L	3	18601	S	0	82NOV19	13:16:59	0025:00	EI099	571
ZAND	57	10.30	23 31 15	+48 32	L	3	18601	L	0	82NOV19	12:33:01	0040:00	EI099	361
ZAND	57	10.30	23 31 15	+48 32	L	2	14669	L	0	82NOV19	13:41:31	0020:00	EI099	561
TXPSC	50	05.00	23 43 50	+03 12	L	2	15116	L	0	83JAN26	14:40:31	0065:00	EC152	333
TX-PSC	50	05.00	23 43 50	+03 12	L	2	14939	S	0	82DEC28	14:09:12	0010:00	EC152	102
TX-PSC	50	05.00	23 43 50	+03 12	L	2	14939	L	0	82DEC28	12:45:35	0080:00	EC152	342
SB939	28	10.40	23 57 48	-39 40	H	3	18367	L	0	82OCT22	20:36:43	0071:00	EA115	300

IAU Colloquium No. 81 on the "Local Interstellar Medium"

IAU Colloquium No. 81 on the "Local Interstellar Medium" will be held on 1984 June 4, 5 and 6 (Monday through Wednesday) at the University of Wisconsin, Madison, Wisconsin.

The Scientific Organizing Committee for this conference consists of A. Boksenberg, A. A. Boyarchuk, F. C. Bruhweiler (Co-Chairman), A. D. Code, M. Grewing, Y. Kondo (Chairman), W. Kraushaar, D. C. Morton, M. Oda, M. Peimbert and A. Vidal-Madjar.

The Local Organizing Committee comprises D. McCammon and B. D. Savage (Chairman).

Those interested in participating in this IAU Colloquium are invited to write Y. Kondo at Laboratory for Astronomy and Solar Physics, Goddard Space Flight Center, Greenbelt, MD 20771.

Third NASA IUE Symposium

The third NASA International Ultraviolet Explorer (IUE) Symposium, marking the completion of the first 6 years of the IUE guest observer program, will be held on 1984 April 3, 4 and 5 (Tuesday through Thursday) at Goddard Space Flight Center in Greenbelt, Maryland.

The Scientific Organizing Committee for this meeting consists of T. R. Ayres, R. D. Chapman (Co-Chairman), A. P. Cowley, R. Giacconi, Y. Kondo (Chairman), B. Margon, R. M. Nelson, J. B. Oke, J. C. Raymond, B. D. Savage, G. A. Wegner, and E. J. Weiler (ex-officio).

The Local Organizing Committee comprises S. R. Heap, J. N. Heckathorn, A. V. Holm, J. K. Kalinowski, J. M. Mead (Chairman) and R. J. Panek.

Further plans for this symposium will be announced in the IUE Newsletter. Those who do not currently receive the IUE Newsletter but are interested in participating in this meeting are invited to write R. D. Chapman at Laboratory for Astronomy and Solar Physics, Goddard Space Flight Center, Greenbelt, MD 20771.

Errors in Foregoing VILSPA Log

Please inform us by post of all errors or omissions in the log reproduced in this issue. Detach this page, fold and staple it leaving the mailing address (verso) visible.

CAMERA & IMAGE	DISPERSION	APERTURE	TARGET	DATE OF OBSERVATION	WRONG FIELD CONTENTS	CORRECT INFORMATION

Dr. A.W. Harris
UK Resident Astronomer
Villafranca Satellite Tracking Station
Apartado 54065
Madrid, Spain

QUESTIONNAIRE FOR NEWSLETTER CIRCULATION

☐ There is a misprint in my name/address on the present mailing label; the correct version appears below.

☐ Having become acquainted with the ESA IUE Newsletter through a colleague/library, I would like to be placed on the regular mailing list. My name and address, including the post code, are given below.

☐ Please delete my name and address (printed below) from the Newsletter distribution list.

NAME:

ADDRESS:

Now tear off this last page and return it to ESA, Paris, in the convenient posting format provided. Simply fold and staple leaving the mailing address (verso) visible.

Mrs. S. Babayan
European Space Agency
8-10 rue Mario-Nikis
75738 Paris Cedex 15
France